Traditional and Non-Traditional Inputs to the Vestibular System

By

Stephanie Eileen Wiitala

A dissertation submitted in partial fulfillment
of the requirements for the degree of
Doctor of Philosophy
(Biomedical Engineering)
in The University of Michigan
2018

Doctoral Committee:

Professor William Michael King, Chair
Assistant Professor Cynthia A. Chestek
Professor Susan E. Shore
Assistant Professor Kathleen H. Sienko

Stephanie E. Wiitala
hastepha@umich.edu
ORCID iD: 0000-0002-7160-0260

For two Elizabeths: Mary Elizabeth and Nancy Elizabeth,
and two Michaels: Michael Oliver and Michael Banning

Table of Contents

List of Figures

List of Tables

List of Acronyms

BIC	Bayesian information criterion
CCR	Cervico-collic reflex
CPG	Central pattern generator
COP	Center of pressure
COR	Cervical-ocular reflex
EPSP	Excitatory post- synaptic potentials
ES	Eye position sensitive
GVS	Galvanic vestibular stimulation
MLF	Medial longitudinal fasciculus
NIHL	Noise-induced hearing loss
OK	Optokinetic stimulation
OKR	Optokinetic reflex
PPEM	Pre-programmed eye movements
SCC	Semi-circular canals
VCR	Vestibulocollic reflex
VN	Vestibular nuclei
VO	Vestibular-only
VOR	Vestibular-ocular reflex

Abstract

One of the primary functions of the vestibular system is to provide stabilizing reflexes to the eye, head, and body. These reflexes are often coordinated with inputs from the visual and proprioceptive systems. More recently, research has shown that other, non-traditional, stimuli also affect the vestibular system, though the scope of this research has been limited. This thesis explores the effect of both traditional and non-traditional inputs on the vestibular system by characterizing their influence compensatory movements.

We begin by looking at the influence of the vestibular periphery and efference copy on compensatory eye movements (Chapter 2). While each of these has been described individually (as the vestibular-ocular reflex (VOR) and pre-programmed eye movements (PPEM) respectively), there is currently controversy in the field regarding 1) to what extent PPEM influence gaze stabilization in healthy animals, and 2) how these two inputs interact with each other. We propose a model of gaze stability in which VOR and PPEM work cooperatively, and compare model predictions to our data as well as data others have reported. We found that our model accurately predicted eye movements for all behavioral contexts tested. In Chapter 3, we describe the effect of single high-intensity noise exposure on the vestibular system. Currently, controversy surrounds whether, and to what extent, noise damages the semi-circular canals. We characterized changes to both ocular and head stability to better answer this question and found that after noise exposure there was loss of both ocular and head stability. However, the exact

nature of this deficit was not as expected and the influence of cervical pathways after vestibular lesion is discussed. Finally, in Chapter 4, we examine the effect of galvanic vestibular stimulation (GVS) and optokinetic stimulation on standing posture. We propose a model of postural stability inspired by the velocity storage model of ocular stability. While others have proposed more complex models that make similar predictions, those predictions have not been explicitly tested and, further, it's not clear if the added complexity is necessary. We found that, while simple, our model could correctly predict subjects' responses to both stimuli, suggesting that the body interprets and uses sensory information for postural stability in a manner similar to that for ocular stability.

Taken together these findings demonstrate that the influence of non-traditional inputs and pathways to vestibular system is substantial and should be considered both in laboratory and clinical settings. Specifically, we showed in Chapter 2 that PPEM are not merely an enhanced or adapted VOR, but part of a unique gaze stabilization system that merits independent consideration. In Chapter 3, we showed that a single noise exposure can cause significant functional damage to the vestibular system, suggesting that patients with noise-induced hearing loss should be tested for vestibular loss as well. Finally, in Chapter 4, we showed that GVS can be integrated like natural vestibular stimulation but only if it is properly conditioned first. This is of particular importance for vestibular prosthetic design, which uses GVS to substitute for lost vestibular input.

Chapter 1: Introduction

The focus of our research is on traditional and non-traditional inputs to the vestibular system and how these inputs effect compensatory movements. To introduce these ideas, we will first go over the main input of the vestibular system: the vestibular periphery. Next, we discuss the pathways related to traditional visual and vestibular inputs: the vestibular-ocular reflex (VOR), the optokinetic reflex (OKR) and the vestibulo-collic reflex (VCR). Finally, we will go over non-traditional inputs and how each are thought to effect ocular and postural stability. These include efference copy of head movement motor commands, galvanic vestibular stimulation (GVS), and sound.

1.1 The Vestibular Periphery

1.1.1 The Vestibular Organs

The vestibular organs are located in the inner ear, adjacent to the cochlea. They consist of three semi-circular canals: the anterior, posterior and horizontal (or lateral) canal, and two otoliths: the utricle and saccule. Together, they encode head rotations and translations respectively. Each is discussed in more detail below.

1.1.1.1 The Semi-Circular Canals

The semi-circular canals (SCC) are three fluid-filled interconnected tubes that are approximately orthogonal to each other (Figure 1.1, left panel) and are thus able to encode head movement in

three dimensions. In the guinea pig the anterior and posterior canals are both vertically aligned and perpendicular to each other while the lateral canal lies roughly in the earth-horizontal plane and is orthogonal to the other two (Vidal et al., 1986). Each canal has at its base an enlargement called the ampulla within which is the cupula, a gelatinous tissue which extends across the canal (Figure 1.1, right panel). When the head rotates the fluid that fills the canals, called endolymph, lags behind due to its inertia, causing the cupula to deflect. The deflection of the cupula can be modeled as a torsion pendulum, the dynamics of which allow the semi-circular canals to act as an angular velocity transducer for frequencies ranging from 0.025-25 Hz (Oman et al., 1987). As the bandwidth of typical head movements ranges from 0.5- 20 Hz, the deflection of the cupula is approximately proportional to head velocity for most physiological movements (MacDougall and Moore, 2005).

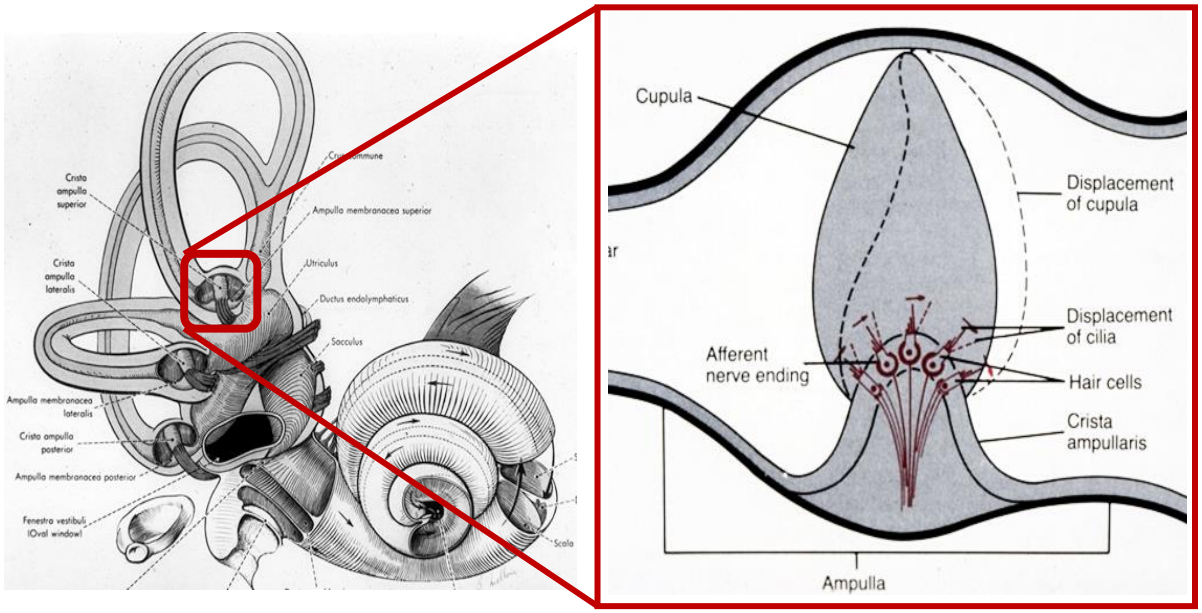

Figure 1.1 – Vestibule with detail of semi-circular canal ampulla

1.1.1.2 The Otoliths

Similar to how the semicircular canals respond to rotation, the otoliths respond to gravito-inertial force, which is the vector sum of linear acceleration and tilts with respect to gravity. The utricle and saccule, are approximately perpendicular to each other and are oriented in the guinea pig such that the utricle responds primarily to roll tilts and the saccule responds primarily to pitch tilts (Curthoys et al., 1999). However, the planes of both otoliths are curved, thus some saccular neurons respond to roll tilts and some utricular neurons respond to pitch tilts (Curthoys et al., 1999). The neuroepithelium of both organs, called the macula, consists the otolithic membrane, a gelatinous substrate within which are embedded small calcium carbonate crystals, called otoconia. Otoconia add weight to the otolithic membrane, causing it to deflect in response to linear acceleration, or tilts with respect to gravity.

1.1.2 Hair Cells

The deflection of the cupula and otolithic membrane is detected and encoded by hair cells. In the semi-circular canals (SCC), the bodies of the hair cells are located in the crista ampullaris at the base of the ampulla and the “hairs”, or stereocilia, extend into the cupula (Figure 1.1, right panel). In the otoliths, the hair cell bodies are imbedded in the macula, while the stereocilia extend into the otolithic membrane. The stereocilia are ordered from shortest to tallest with the tallest designated as the kinocilium. When the stereocilia are deflected towards the kinocilium, as seen in Figure 1.2, ion channels are opened which depolarize the hair cell and increase the firing rate of the afferent (Pickles et al., 1984). When the stereocilia are deflect away from the kinocilium these ion channels are closed, hyperpolarizing the cell and decreasing the firing rate of the afferent nerve.

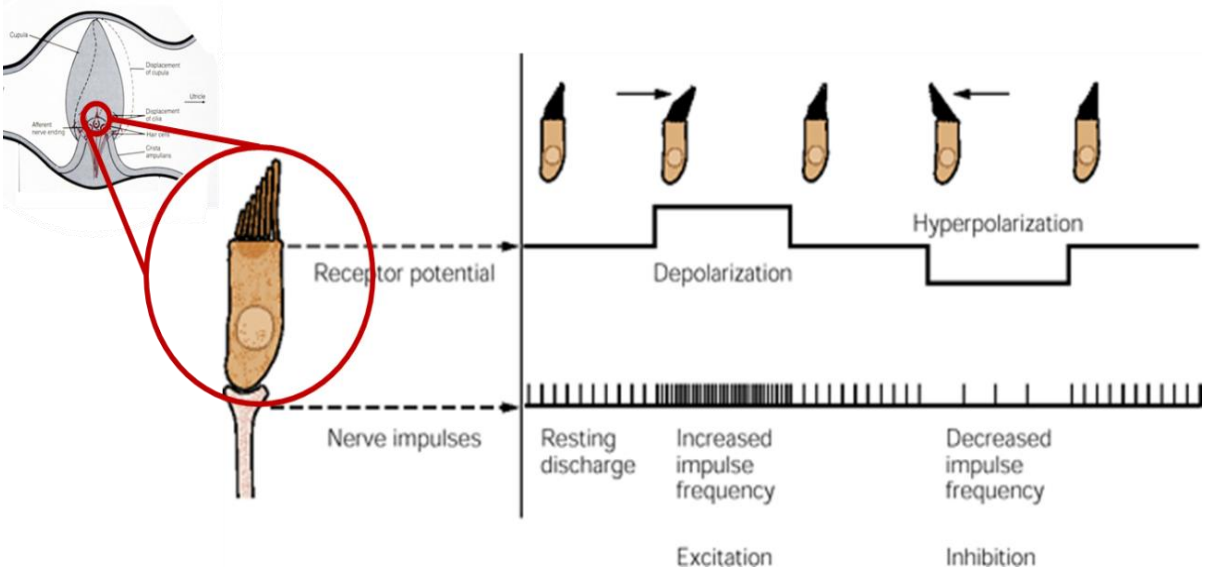

Figure 1.2 – Hair cell membrane potential and afferent firing rate in response to cupula deflection

1.1.3 Afferents

Primary vestibular afferents synapse onto hair cells from all five of the vestibular organs and travel to the vestibular nuclei via the vestibular portion of VIIIth cranial nerve. Early recordings from the vestibular nerve revealed two distinct afferent types based on firing patterns: regular afferents, which fire at regular intervals, and irregular afferents, which have variable firing rates (Fernandez et al., 1990). Over the years, it was discovered that differences between these two types of neurons also include firing dynamics, terminal morphology, and location in the neuroepithelium, each of which are discussed below.

As mentioned above, displacement of the cupula, and hair cell membrane potential, are approximately proportional to head velocity. However, this is not the case for primary afferents. While regular afferents tend to follow the dynamics of the cupula and display a relatively low, but steady, gain across most frequencies, irregular afferents tend to have higher gains and a more

phasic response (Figure 1.3; Baird et al., 1988). At frequencies above 2 Hz, irregular afferents deviate from cupula dynamics and show increased gains and increased phase leads (Goldberg and Fernandez, 1971a). As will be discussed in Section 1.2.3, this has important implications for the vestibular-collic reflex.

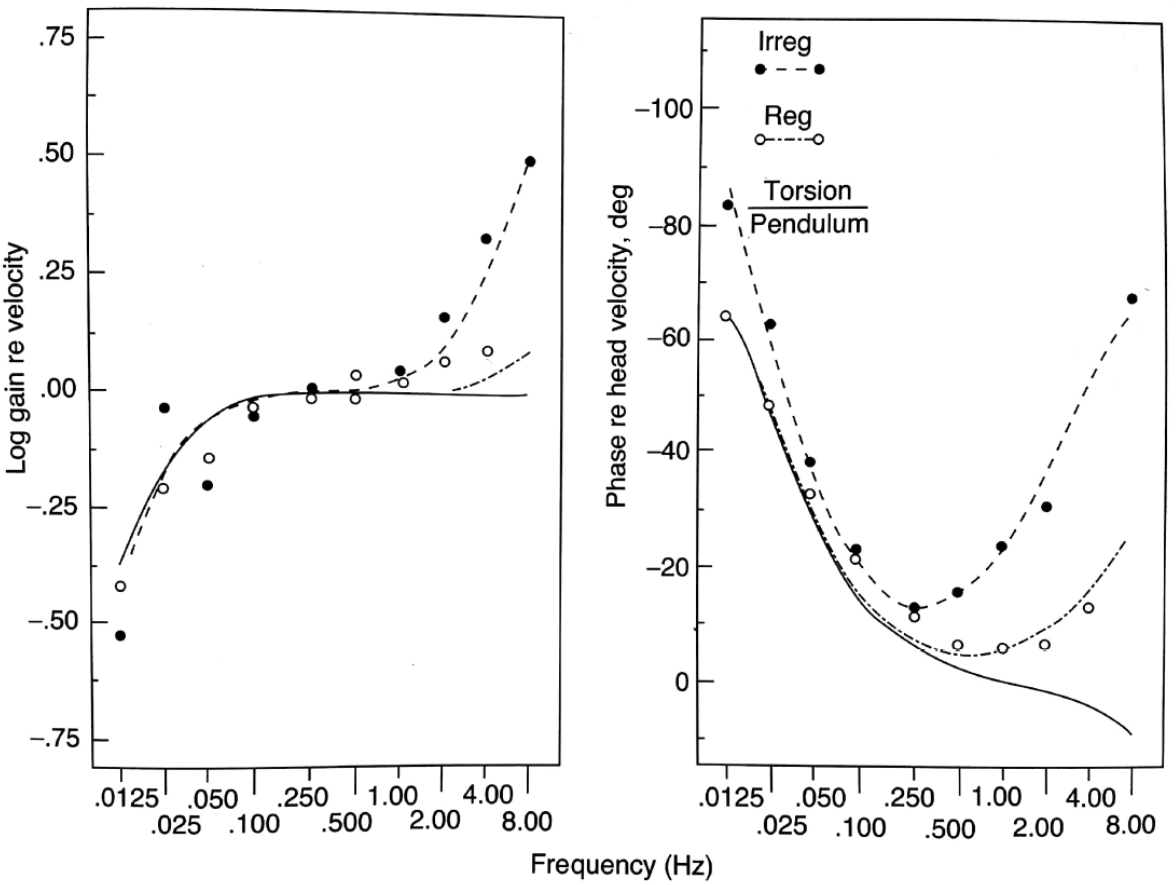

Figure 1.3 – Firing dynamics of regular and irregular afferents compared to torsion pendulum model of cupula dynamics

Along with physiological distinctions, such as firing pattern and dynamics, vestibular afferents can also be distinguished by anatomical differences such as terminal morphology and location within the sensory epithelium. Afferent terminations on hair cell are classified as either: calyx-only, bouton-only, or dimorphic (which form both calyx and bouton endings). Bouton-only

afferents terminate on hair cells that are located predominantly in the peripheral zone of canal epithelium or extrastriolar region of the otoliths and nearly always regular (Eatock et al., 2008). Calyx-only afferents predominantly innervate the central or striolar region and are irregular. These afferents have relatively low gains and baseline firing rates (Baird et al., 1988) and are particularly susceptible to noise damage (Stewart et al., 2017b) as will be discussed further in Chapter 4. While dimorphic afferents are found in both central and peripheral areas and are also predominately irregular (Eatock and Songer, 2011; Sadeghi et al., 2007).

Another important feature of all vestibular afferents, is that even when the head is at rest, they have a baseline firing rate, allowing them to encode both increases and decreases in angular velocity or gravito-inertial force (Figure 1.2). This information is then sent to the vestibular nuclei where afferents project onto secondary vestibular neurons.

1.1.4 Vestibular Nuclei

The vestibular nuclei (VN) are divided by cytoarchitecture into the superior, medial, lateral, and inferior vestibular nucleus. Neurons within the VN are differentiated by the signals they carry. While these secondary neurons have been extensively studied in the primate, in the guinea pig and mouse, cell populations are not as well-defined. Generally two cell types are reported: those that carry eye position signal and those that do not (Beraneck and Cullen, 2007; Ris et al., 1995a). Eye position sensitive (ES) cells are thought to be involved in the VOR pathway due to their similarity to known VOR interneurons in primate.

Non-ES cells display a firing behavior similar to vestibular-only (VO) neurons in primate (Beraneck and Cullen, 2007). Vestibular-only (VO) neurons are so called because they only encode head velocity and show no sensitivity to eye position or velocity. An important feature of this class of neurons is that they only encode head velocity that results from passive movements (Boyle et al., 1996; Mccrea et al., 1996; McCrea et al., 1999; Phillips et al., 1996; Roy and Cullen, 2001) allowing the body to distinguish self-motion from external movements (Cullen, 2012, 2014). Even when head velocity is the result of both passive and active head movements this class of neurons strictly encodes the passive component (Roy and Cullen, 2001). In the primate, these neurons send descending projections to the cervical spinal cord where they are thought to mediate the vestibular-colic reflex as well as ascending projections to the thalamus, cerebellum and cortex where they participate in spatial orientation.

1.2 Traditional Inputs and Pathways

As outlined above, the vestibular organs provide information about head orientation and movement. This information is then used to stabilize the eyes and head via the vestibular-ocular reflex (VOR) and the vestibulocollic reflex (VCR) respectively. We also discuss the optokinetic reflex (OKR), which is driven by visual inputs and supplements the VOR in stabilizing the eyes.

1.2.1 The Vestibular-Ocular Reflex (VOR)

To maintain visual acuity, the eyes must remain stable in space. During unexpected head movements, eye position is stabilized by the vestibular-ocular reflex. As seen in Figure 1.4, when the head rotates, the ipsilateral semi-circular canal sends an excitatory signal to the vestibular nuclei (Kasahara and Uchino, 1974; Precht and Shimazu, 1965). Secondary neurons in the

vestibular nuclei then project to the contralateral abducens (VI) nucleus, which activate the lateral rectus muscle (McCrea et al., 1987; Scudder and Fuchs, 1992) and send an excitatory signal to the ipsilateral oculomotor (III) nucleus, which activates the medial rectus muscle (McCrea et al., 1987). In addition, there are secondary VN neurons that project directly to the ipsilateral oculomotor (III) nucleus via the ascending tract of Deiters, which also activate the medial rectus muscle. Activation of these muscles causes a leftward rotation of both eyes thus compensating for the leftward rotation of the head and keeping the line of sight fixed in space.

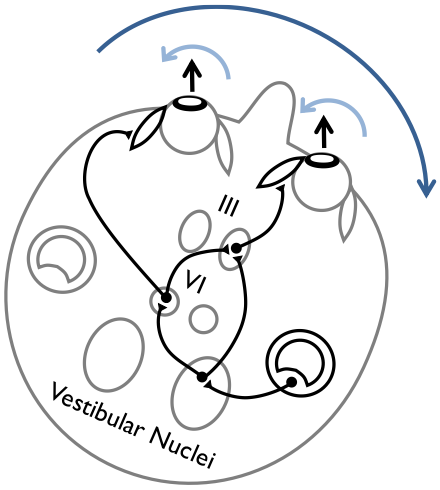

Figure 1.4 – Excitatory vestibular-ocular reflex pathway

1.2.1.1 VOR Testing and Clinical Applications

The vestibular-ocular reflex is often used to assess vestibular function by evaluating eye movements during prescribed head movements. A common diagnostic tool is a Barany Chair, which rotates the subject's whole body while eye movements are recorded either by video-equipped goggles or by search coil technique. VOR performance is quantified by the gain and latency of eye velocity with respect to head velocity. The gain is defined as the eye velocity divided by the head velocity. To ensure that the line of sight remains stable during head

movements the eyes must rotate equal and opposite to the head, thus the ideal gain is -1 or sometimes reported as 1. Likewise, it is ideal for the eyes to begin to move when the head begins to move and so the ideal latency is zero. In guinea pigs the gain of the VOR has been measured to be -0.6 (Escudero et al., 1993; Serafin et al., 1999; Shanidze et al., 2010a). In primates it is closer to -1 (Della Santina CC et al., 2002; Hoshowsky et al., 1994). In both animal populations, the latency is reported as between 5 and 7 milliseconds (Della Santina CC et al., 2002; Escudero et al., 1993; Schubert et al., 2008; Shanidze et al., 2010a; Sprenger et al., 2006). This latency corresponds to the minimum time for signal transduction in the VOR pathway (Huterer and Cullen, 2002) and as such is an unavoidable characteristic of the VOR.

For patients with vestibular pathologies it is not uncommon to have VOR gains that are less than ideal (Black RA et al., 2005; Della Santina CC et al., 2002; Halmagyi et al., 2003). When this is the case the eyes fail to counter-rotate sufficiently and the line of sight moves with the head instead of remaining still. This causes a loss in visual acuity called oscillopsia, which patients will often report as “blurry vision” (Herdman SJ et al., 2001; Tian et al., 2002). Researchers and clinicians have noted the recovery of the VOR in patients suffering from partial (for review see (Smith and Curthoys, 1989)) or even total vestibular loss (Atkin A and Bender MB, 1968; Kasai and Zee, 1978). Several strategies could be employed to improve VOR performance. Among those is the use of pre-programmed eye movements (discussed in Section 1.3.1.1).

1.2.2 The Optokinetic Reflex

While the vestibular-ocular reflex (VOR) is the primary means of stabilizing gaze during unexpected head movements, the body also integrates visual information. The optokinetic reflex

(OKR) responds to full-field visual flow, such as looking out the widow of a moving vehicle, and moves the eyes in order to stabilize the visual image on the retina (Cohen et al., 1977). This is because full-field visual flow was, until very recently in human history, usually the result of head movement. In addition, the dynamics of the semi-circular canals cause the VOR to have a very low gain in response low-frequency head movements (Goldberg and Fernandez, 1971a; Oman et al., 1987). These two facts taken together mean that low-frequency visual flow is usually interpreted as self-motion and, as such, there is a need to counter-rotate the eyes to maintain ocular stability. Thus, when presented with full-field visual flow, such as looking out the window of a moving vehicle, the eyes make a series of slow and fast movements: slow movements to track the visual flow due to the OKR, and fast movements to reset the eye in the orbit once it reaches the edge. In a laboratory setting, this can be replicated by sitting the subject inside a rotating drum (Figure 1.5, top).

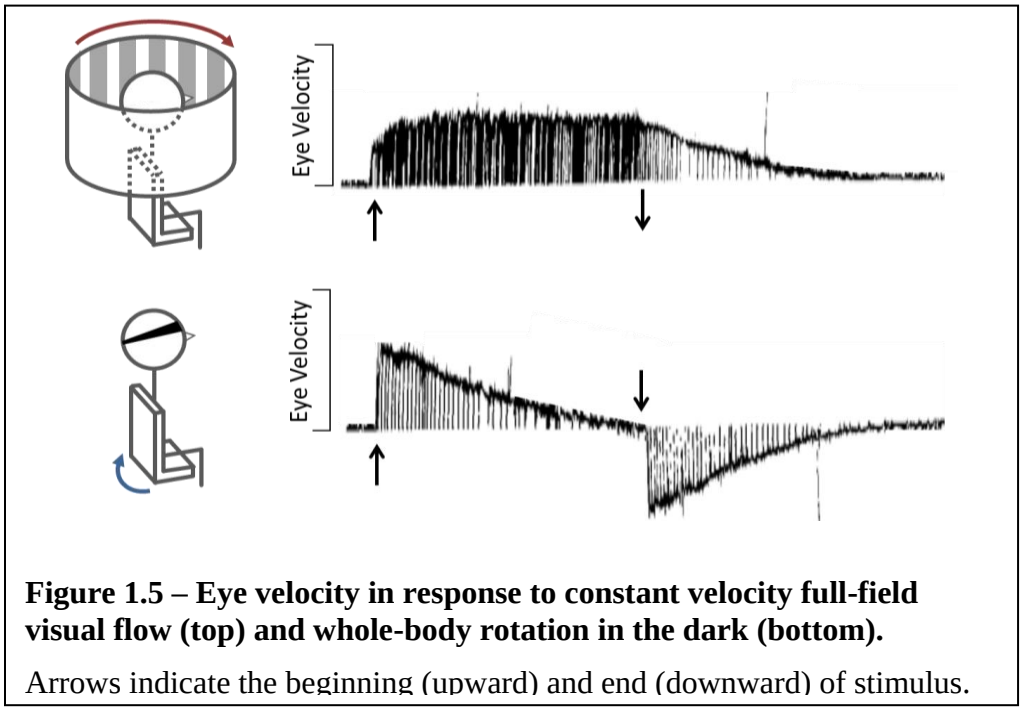

Figure 1.5 – Eye velocity in response to constant velocity full-field visual flow (top) and whole-body rotation in the dark (bottom).
Arrows indicate the beginning (upward) and end (downward) of stimulus.

1.2.2.1 Velocity Storage

Thus, information from both the vestibular and visual systems is used to estimate head movement and produce the necessary compensatory eye movements. How each contributes to gaze stabilization can be seen when they are tested individually. As seen in Figure 1.5 (bottom), eye movements in response to constant velocity (i.e. low frequency) whole body rotations in the dark are initially compensatory, then decay, and finally are reversed when the rotation stops (Cohen et al., 1977; Raphan et al., 1979). This behavior can in part be explained by the dynamics of the semi-circular canals, which are modeled as a dampened pendulum with a time constant of about seven seconds (Fernandez and Goldberg, 1971; Goldberg and Fernandez, 1971b). This means that in response to constant velocity, the cupula will initially deflect but will then return to upright after ~20 seconds (three times the time constant) even though the head is still moving. Consequently, when the head stops rotating, the cupula is then deflected in the opposite direction.

However, the decay of eye velocity in response to constant rotation is much slower than what would be expected, a phenomenon known as velocity storage (Cohen et al., 1981; Raphan et al., 1979). Further, in response to an optokinetic stimulus, eye velocity only gradually reaches drum velocity and when the lights are turned off eye velocity similarly only gradually decreases, a phenomenon which cannot be explain by the dynamics of the eye (Figure 1.5, top).

Ter Braak (1936) first suggested that the velocity storage seen after visual stimulation occurs to cancel the velocity storage of the semi-circular canals. Indeed, when both visual and vestibular systems are excited (i.e. whole-body rotation in the light) after-effects are eliminated. However,

this offered no explanation for why velocity storage should exist in the vestibular system. That is until Borah (1988) modeled these responses as the output of an optimal estimator. According to his model, velocity storage emerged as the result of relative noise in each sensor. This was an important development as now velocity storage had a functional interpretation, which could then be used to diagnosis dysfunction.

Indeed, abnormalities in eye movements during optokinetic and vestibular stimuli can be used to differentially diagnose oculomotor and vestibular dysfunction as well as central pathologies (Suzuki and Komatsuzaki, 1962; Zee et al., 1976). Responses are also given meaning when compared to model predictions. For example, a decrease in vestibular function can be modeled as an increase in vestibular noise. Given this condition, the model will predict a response with a decreased time constant which is in fact observed in certain vestibulopathic patient populations (Zee et al., 1976).

1.2.3 The Vestibulocollic Reflex (VCR)

Much like how the VOR works to stabilize the eyes in space, the vestibulocollic reflex (VCR) works to stabilize the head on the trunk (Goldberg and Cullen, 2011). For example, in response to a 57-degree rotation of the trunk (as seen in Figure 1.6) the passive dynamics of the head and neck (labeled 'Head Plant') will eventually bring the head back to its initial position on the trunk, but only after it has overshot its final position by almost 40% and oscillated for 1-2 seconds (Peng et al., 1996, 1999). One can imagine how disorienting this would be. Fortunately, in healthy subjects, the semi-circular canals detect head rotation and send both excitatory and inhibitory signals to the neck muscles, which then counter-rotate the head. Thus, the VCR

(labeled ‘Closed Loop VCR’ in Figure 1.6) increases head stability and by dampening oscillations and stiffening the neck, so that the head settles on its final position faster and with less deviation (Peng et al., 1996, 1999).

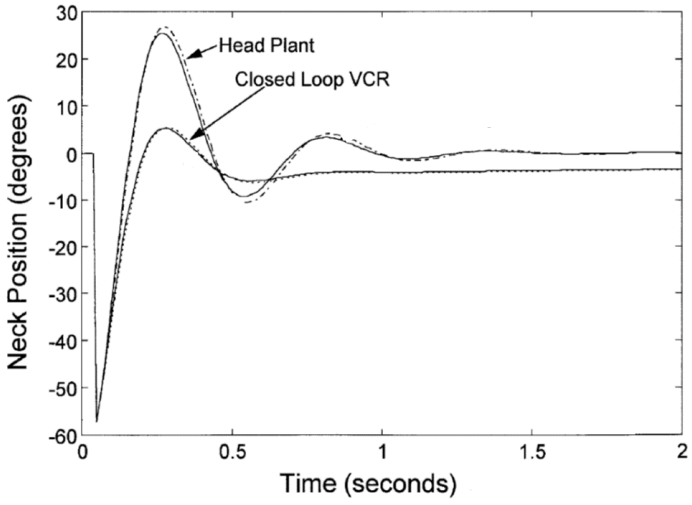

Figure 1.6 – Head response to body rotation with the VCR (Closed Loop VCR) and without the VCR (Head Plant)

There are a number of pathways mediating the VCR (Bilotto et al., 1982; Wilson et al., 1979) not all of which have been elucidated (Goldberg and Cullen, 2011). However, the most direct pathway is trisynaptic similar to the VOR (Shinoda et al., 1993; Wilson and Maeda, 1974; Wilson and Schor, 1999; Wilson and Yoshida, 1969). First, hair cells synapse onto primary afferents, next, afferents project onto VCR secondary neurons in vestibular nuclei (VN), and finally, VCR secondary neurons descend, primarily via the medial longitudinal fasciculus (MLF), to neck motoneurons. While this is the most direct pathway, both Bilotto (1982) and Wilson (1979) found that when the MLF was transected, there was very little change to VCR dynamics, indicating that other, less direct, pathways make a substantial contribution to the VCR. The VCR also has a considerably more complex motor output than the VOR. While the

exact nature of muscle activation in the VCR is beyond the scope of this dissertation, it is worth noting that while the eyes are controlled by three pairs of opposing muscles, the head is controlled by 30 muscles (Peterson et al., 2001).

The reason the VCR is of interest to this thesis is that, unlike the VOR, which has a net afferent input that is mostly regular, the VCR's net afferent input is predominantly irregular. This offers valuable insight into the effect of noise-overstimulation on the vestibular system, as irregular afferents are more susceptible to noise damage (Stewart et al., 2017b).

The hypothesis that the VCR is mediated by irregular afferents was first proposed based on the VCR's dynamics. Bilotto (1982) characterized the VCR over a broad frequency range (~0.2-4 Hz) and found that it behaved as a lead-lag system. As only irregular afferents offer a phase lead, the authors concluded that they must make a substantial contribution to the pathway. This was conclusion was complicated by the results of Boyle (Boyle et al., 1992) who recorded excitatory provoked synaptic potentials (EPSPs) in VCR secondary vestibular neurons (VN). They found that while the majority of afferent inputs to VCR neurons were irregular, about one-third were regular. The authors hypothesized that regular inputs might be cancelled by indirect polysynaptic pathways, rendering the net afferent input irregular. The result of Shanidze (2012) helped substantiate this hypothesis as they found that when irregular afferents were ablated using GVS, there was a substantial loss of head stability. This was especially true at higher frequencies as would be expected based on irregular afferent dynamics (see Section 1.1.3 for more details). Taken together these findings suggest that while the VCR does receive inputs from regular afferent, its functional dynamics are strongly influenced by irregular afferents.

1.3 Non-Traditional Inputs and Pathways

While the vestibular system primarily processes head movement signals from the peripheral organs and visual system as discussed above, it is also influenced by other stimuli such as efference copy, galvanic currents, and sound as will be discussed in more detail below.

1.3.1 Efference Copy

In 1867, Helmholtz noted that when one moves one's eye by pressing on it, the world appears to move. However, when one moves one's eye by simply looking around, the world appears stable. Despite both scenarios causing image motion across the retina, there is an important difference in perception. Helmholtz proposed an "effort of will" that the body uses to distinguish active versus passive movement (Helmholtz and Southall, 2005). Von Holst and Mittelstaedt (1950) formalized this hypothesis by proposing that during active movements when the body sends a motor command to the target muscles, a copy of that command, called an efference copy, is made. The efference copy is fed through an internal model that predicts the sensory feedback that will result. Equipped with this prediction the body can distinguish the sensory feedback that was a result of active movements, what they called reafference, and that which was a result of passive movements, or exafference (Holst and Mittelstaedt, 1950). As we will discuss below, when this prediction is of head movement, it can also be used to produce compensatory eye movement.

1.3.1.1 Pre-programmed Eye Movements

The contribution of preprogrammed eye movements to ocular stability was first discovered by Dichgans and colleagues (1973). They found that when vestibular input was eliminated, there

was an immediate drop in ocular stability. After a month, however, compensation produced recovery of 90%. To test the influence of central programming, the monkeys' heads were stopped unexpectedly during head rotations. In intact monkeys stopping the head also stopped the eye rotation (Bizzi et al., 1971). In labyrinthectomized monkeys, the eyes counter-rotated even though there was no head rotation for which to compensate. Thus, in the absence of visual and vestibular input, these animals still produced compensatory eye movements, leading the authors to conclude that these eye movements were centrally programmed. Others have found similar patterns of recovery in non-human primates after bilateral canal plugging (Newlands et al., 1999), unilateral labyrinthectomy (Newlands et al., 2001), and bilateral labyrinthectomy (Newlands et al., 2001; Sadeghi et al., 2012).

The results of Dichgans and others offered preprogramming as a potential explanation for the recovery seen in some vestibulopathic patients. Indeed when the VOR of vestibular patients is examined many have reported increased gains corresponding to active but not passive head movements (Black RA et al., 2005; Foster et al., 1997; Halmagyi et al., 2003). In healthy subjects, the results have not been as clear. Some have found that the VOR gain of healthy subjects is more accurate during active head movements (Collewijn et al., 1983; Hoshowsky et al., 1994; Jell et al., 1988; Tomlinson et al., 2009), while others have found no improvement (Foster et al., 1997). This might be because healthy subjects have a near-perfect VOR gain, even during passive perturbations, leaving little room for improvement. Indeed, Della-Santina found that while the gain of the VOR was not significantly different in healthy subjects during active rotations, there was a significant decrease in the latency (Della Santina CC et al., 2002). As the latency in a healthy adult corresponds to minimum time of signal transduction along the VOR

pathway (Huterer and Cullen, 2002) a decrease would be good evidence for pre-programming. It is also interesting to note that in recording from larval *Xenopus* frogs, Straka and colleges have shown that compensatory eye movements during locomotion are driven by an efference-copy that originates from a central pattern generator (CPG) in the spinal cord (Lambert et al., 2012). However, the use, or even existence, of CPGs in humans remains controversial.

1.3.2 Galvanic Vestibular Stimulation (GVS)

In the influence of galvanic (DC) currents on the vestibular system has been known for over two centuries when Alessandro Volta, in 1790, discovered that applying this stimulation across the head elicits a sensation of falling to the side of the cathode. Since then others have found that along with perceptual responses, galvanic vestibular stimulation (GVS) also produces stereotyped eye and body movement (MacDougall et al., 2003). Specifically, the eyes and body moved as though compensating for an actual head movement (Fitzpatrick and Day, 2004a; MacDougall et al., 2003). GVS has now become a common means of perturbing the vestibular input and is used extensively to explore the vestibular contribution to eye movements and standing posture (Fitzpatrick and Day, 2004a). In addition, because GVS bypasses the end organs and acts at the distal axon, it also beginning to be used as a tool to differentially diagnose a variety of vestibular pathologies (Dix and Hallpike, 1952; MacDougall et al., 2005).

As discussed in Section 1.1.3, the vestibular organs encode head movement by increasing or decreasing firing rate. GVS acts on primary afferents by increasing (cathodal current) or decreasing (anodal current) firing rate as well. However, GVS increases or decreases all afferents on one side, an arrangement that has no natural equivalent. Based on the orientation of each

organ, Fitzpatrick (2004) derived a vector of the equivalent rotation or linear translation/tilt that would produce the same afferent output. For example, a cathodal current applied to the afferents innervating the right horizontal canal, is equivalent to a rightward head rotation, as both would increase the firing rate of primary afferents. Combining all organs, Fitzpatrick could then predict the perception of movement based on any combination of GVS currents. For bilateral bipolar GVS, such as used in Chapter 4, where one side receives cathodal current and other side receives anodal current, the vector sum across all organs results in the perception of roll rotation towards the cathode, just as Volta described.

1.3.2.1 Posture

To maintain standing balance the body must keep the center of pressure within the limits of stability (Nashner et al., 1982, 1989a). This requires an accurate estimate of body position and motion (Peterka, 2002). The most salient input regarding center of pressure is from cutaneous sensors on the bottoms of the feet (Burgess and Perl, 1973; Kavounoudias et al., 2001). However, inputs for the visual and vestibular system provide important information regarding head orientation and velocity and the proprioceptive system provides information about joint position and movement (Winter et al., 2005). Together, visual, vestibular, somatosensory, and proprioceptive systems can all give information related to posture, however none is capable of providing accurate information at all times (Young, 2011a). Thus, the body must combine information from multiple sensors to produce the most accurate estimate. This estimate is then used to coordinated muscles in the neck, trunk, and leg to maintain upright posture (Keshner and Kenyon, 2000).

As demonstrated by several studies (Fitzpatrick et al., 2002a, 2006a; St George and Fitzpatrick, 2011; Wardman et al., 2003a) the body interprets GVS as an actual, unplanned, movement. Consequently, the body responds by tilting in the opposite direction. However, this response depends largely on the orientation of the head. Thus, bilateral bipolar GVS applied to a subject facing forward (as we used in Chapter 4) gives rise to the sensation of roll towards the cathode, which, in turn, causes a lateral tilt towards the anode. However, if the subject turns its head 90 degrees to the left or right, GVS causes a tilt in the anterior-posterior plane (Lund and Broberg, 1983). Postural responses to GVS also depend on the nature of the balance task. In free standing subjects, for example, GVS elicits muscle activity in the legs. However, this response is eliminated when the subject is seated, and the legs no longer contribute to postural stability (Britton et al., 1993; Fitzpatrick et al., 1994). Thus, it appears the body integrates the signals generated by GVS in a manner similar to that of natural vestibular stimulation, the extent to which this is true will be explicitly tested Chapter 4.

1.3.3 Sound

Vestibular responses to sound were first reported in the literature by Tulio in 1929, who drilled holes in the semi-circular canals of pigeons and found that they subsequently turned their head in response to loud sounds (Tullio, 1929). Since then, others have demonstrated that, even in healthy intact subjects, the vestibular system responds to air- and bone-conducted sound (for review see: Curthoys, 2010). Increased interest in these responses emerged when it was discovered that sound-evoked myogenic potentials could be measured in neck muscles, called cVEMP (Colebatch and Halrnagyi, 1992; Colebatch et al., 1994) and eye muscles, called

oVEMP (Jombík and Bahýl, 2005) and that these responses correlated with otolith function, allowing clinicians to test the saccule and utricle independent of the canals.

With increased interest in the clinical applications of cVEMP and oVEMP, there was an increased interest in understanding the mechanism underlying them. Most of the research into this topic has concluded that acoustic activation of the vestibular system is mediated predominantly by irregular afferents of the otoliths (Curthoys et al., 2006). However, recent findings have suggested that the semi-circular canals are also sound sensitive (Xu et al., 2009; Zhou et al., 2004) and is explored further in Chapter 3. Nonetheless, given that noise can activate the vestibular system, it makes sense, particularly from a clinical perspective, to ask the question: can noise damage the vestibular system?

1.3.3.1 Noise Damage in the Vestibular System

While chronic dizziness, vertigo, and even spontaneous nystagmus had been correlated with occupational noise-induced hearing loss (NIHL) for over a century (Habermann, 1890; Holmgren and Orembowsky, 1927), studies linking vestibular loss and hearing loss have been sporadic until recently (Girard et al., 2014; Manabe et al., 1995; Oosterveld et al., 1982; Picard et al., 2008; Shupak et al., 1994). Furthermore, studies looking into the anatomical changes that accompany vestibular loss are few and have conflicting reports, with some reporting no gross anatomical damage to the vestibular organs, but evidence of oxidative stress (Fetoni et al., 2009), damage only to the saccule (Akdogan et al., 2009), and damage to all, or nearly, all of the vestibular organs (Stewart et al., 2016).

The aforementioned discrepancies are likely exacerbated by the differences in noise exposure parameters (i.e. frequency bandwidth, length, and intensity) as well as the anatomical and histological changes that authors look for (i.e. hair cell loss, synaptopathy, oxidative stress, etc.). However, what can be concluded is that noise-overexposure has significant deleterious effects on vestibular function and that the otoliths appear to be particularly susceptible to noise damage, although the semi-circular canals are not immune.

1.4 Summary of Thesis

Taken together, the above discussion presents a strong case that non-traditional inputs have a significant effect on the vestibular system and its function. In the following chapters we will explore the use of efference copy in ocular stabilization (Chapter 2), the effect of noise-overstimulation on ocular and postural stability (Chapter 3), and the use of galvanic vestibular stimulation and velocity storage in postural control (Chapter 4). Additionally, we attempt to investigate the mechanism of each input's influence through the use of simple models. However, these studies are far from exhaustive, leaving open a number of possibilities for future directions, as discussed in Chapter 6.

Chapter 2: Interaction of Pre-Programmed Eye Movements with the Vestibular-Ocular Reflex

2.1 Abstract

The vestibular-ocular reflex (VOR) works to stabilize gaze during unexpected head movements. However, even subjects who lack a VOR (e.g. vestibulopathic patients) can achieve gaze stability during planned head movements by using pre-programmed eye movements (PPEM). The extent to which PPEM are used by healthy intact subjects and how they interact with the VOR is still unclear. We propose a model of gaze stabilization which makes several claims: 1) the VOR provides ocular stability during unexpected (i.e. passive) head movements; 2) PPEM are used by both healthy and vestibulopathic subjects during planned (i.e. active) head movements; and 3) when a passive perturbation interrupts an active head movement in intact animals (i.e. combined passive and active head movement) the VOR works with PPEM to provide compensation. First, we show how our model can reconcile some seemingly conflicting findings in earlier literature. We then test the above-mentioned predictions against data we collected from both healthy and vestibular-lesioned guinea pigs. We found that 1) vestibular-lesioned animals showed a dramatic decrease in compensatory eye movements during passive head movements, 2) both populations showed improved ocular compensation during active vs. passive head movements and 3) during combined active and passive head movements, eye movements compensated for both the active and passive component of head velocity. These results support our hypothesis that while the VOR provides compensation during passive head

movements, PPEM are used by both intact and lesioned subjects during active movements and, further, that PPEM work together with the VOR to achieve gaze stability.

2.2 Introduction

Maintaining a stable line of sight in the midst of head movement is essential to normal function. Indeed, those who suffer from oscillopsia, an inability to stabilize the visual world, can be severely disabled and even incapacitated by their condition (Chambers et al., 1985; Crawford, 1964). During unexpected, or passive, head movements, it is the vestibular-ocular reflex (VOR) that works to stabilize gaze by producing compensatory eye movements. However, only recently has the question of how gaze is stabilized during planned, or active, head movement been raised.

One of the first to study this question was Dichgans et al. (1973) when they investigated what drove gaze stabilization at the end of self-generated eye-head gaze shifts. They systematically eliminated sensory feedback and found that after bilateral vestibular lesions, there was a dramatic decrease in compensatory eye movement. However, they also noted that after a few weeks there was a nearly complete recovery of compensation during planned head movements. Moreover, these compensatory eye movements occurred even when the head movement was unexpectedly blocked, suggesting that they were pre-programmed. The authors hypothesized that during an active head movement, the body can predict how the head will move and thus, pre-program the necessary compensatory eye movements. Yet healthy intact animals did not exhibit this pattern: when head movements were prevented in these subjects, so were the compensatory eye movements. This led to the conclusion that PPEM were an adaptive strategy only developed with the loss of vestibular input, and that in healthy animals, it was the VOR that was primarily

responsible for gaze stabilization even during planned head movements. This is in line with what clinicians have observed in vestibulopathic patients. Namely, that while compensatory eye movements during passive perturbations remain insufficient, patients can partially recover gaze stability during active head movements (Black RA et al., 2005; Foster et al., 1997; Halmagyi et al., 2003; Herdman SJ et al., 2001; Tian et al., 2002).

However, improved compensation during active, as compared to passive, head movements has also been documented in healthy human and non-human subjects both in terms of increased gain (Collewijn et al., 1983; Hoshowsky et al., 1994; Jell et al., 1988; Steen and Collewijn, 1984; Tomlinson et al., 2009) and decreased latency (Della Santina CC et al., 2002; Shanidze et al., 2010b). As the latency in a healthy subject corresponds to minimum signal transduction time along the VOR pathway (Huterer and Cullen, 2002), a decrease in latency would be evidence for pre-programming. An important difference between these studies and that of Dichgans et al., is how each identified PPEM. Dichgans defined PPEM as compensatory eye movements, which occurred even when the planned head movement was prevented. Other authors defined PPEM as eye movements that exhibited improved compensation as measured by gain and latency.

We have developed a model, that unifies these seemingly conflicting findings. It suggests that PPEM are indeed a part of normal gaze stabilization resulting in improved compensation during active head movements, similar to what clinicians have observed. It also predicts that if the gains of PPEM and VOR are similar (as is the case for non-human primates and humans), PPEM would not be observed in healthy subjects when planned head movements are prevented, as described by Dichgans et al.

Our model also predicts that while PPEM are the primary means of gaze stability during active head movements, the VOR remains online to compensate for any unexpected passive perturbations. This claim, that the VOR remains operational during voluntary movements, harkens back to an older, but still on-going controversy regarding gaze shifts. Briefly, gaze shifts require the eyes and head move in the same direction; thus, the VOR would seem counterproductive. This has led many to argue that the during gaze shifts, the VOR is suppressed (Cullen et al., 2004; Laurutis and Robinson, 1986; Tabak et al., 1996). Others, however, have found that the VOR remains online and continues to compensate for passive perturbations (Blakemore and Donaghy, 1980; Freedman et al., 1998; Guitton and Volle, 1987; Guitton et al., 1984; Morasso et al., 1973).

Similarly, our hypothesis that PPEM stabilize gaze during active head movements would seem to render the VOR counterproductive as it would interfere with the ongoing PPEM. Thus, VOR suppression (which we will refer to as the "Suppression Model") presents itself as a plausible mechanism for preventing this interference. However, as will be described in more detail below, our model allows the VOR to compensate for unexpected perturbations while preventing it from interfering with PPEM. We refer to this as the "Cooperative Model" and it is precisely this cooperation between PPEM and the VOR, which allows us to reconcile conflicting findings in earlier literature as previously described.

Consequently, our model makes three claims: 1) the VOR provides ocular stability during passive head movements; 2) PPEM are used by both healthy and vestibulopathic subjects during

active head movements; 3) during active head movements, the VOR is not suppressed but continues to provide compensation. To test our model, we first compare compensatory eye movements in healthy and lesioned animals during active and passive head movements to confirm the necessity of the VOR during passive head movements and the presence of PPEM during active movements in both populations. We then examine compensatory eye movements that occur when a passive perturbation interrupts an ongoing active head movement. If the VOR is suppressed, we expect these eye movements to reflect only the active component; if the VOR is intact, eye movements should compensate for the total head velocity.

2.3 Model

Our hypothesis is that while the VOR pathway provides gaze stabilization during passive head movements, pre-programmed eye movements (PPEM) are used during active head movements. Thus, our model (Figure 2.1) is composed of two parallel pathways, which we denote as "Active" (top) and "Passive" (bottom). We have also included a gaze command input (bottom right) to simulate previous studies, which used gaze shifts. During gaze stabilization, however, the gaze command is always zero and can effectively be ignored.

The passive pathway represents the traditional understanding of gaze stabilization. The head is moved by either an external force or a self-generated motor command. In either case, the resulting head velocity ($\dot{H}$) is detected and processed by the VOR pathway to produce a compensatory eye movement which can be described by $\dot{E} = p\dot{H}(t - t_{d,p})$ where p is the passive gain and $t_{d,p}$ is the passive time delay associated with the VOR pathway, usually 5-7ms (Huterer and Cullen, 2002; Shanidze et al., 2010b).

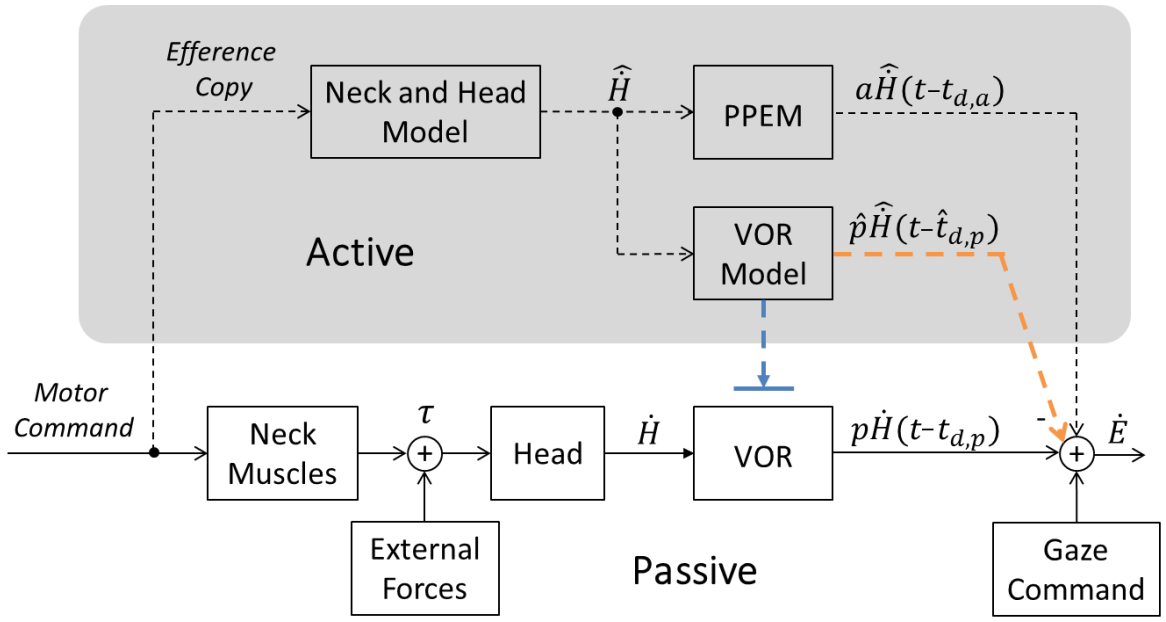

Figure 2.1 – Proposed Model of Gaze Stabilization

Bottom portion represents traditional pathways (i.e. the VOR and Gaze Command). Top portion (in grey, labeled "Active") includes a pathway that estimates head velocity ("Neck and Head Model") and necessary pre-programmed eye movements ("PPEM") and two alternative pathways that interact with the VOR. The Suppression Model, in blue, that turns off the VOR and the Cooperative Model, in orange, that estimates the VOR's response ("VOR Model") and subtracts it from the total eye movement.

We propose that in addition to the passive pathway there is an active pathway that provides enhanced compensation during planned head movements. By taking a copy of the motor command, called an efference copy (Holst and Mittelstaedt, 1950) and feeding it into an internal model of the head and neck muscles, the body can predict how the head will move ($\hat{\dot{H}}$). Based on this prediction, it can pre-program the necessary eye movements which can be described by $\dot{E} = a\dot{H}(t - t_{d,a})$ where a is the gain of the PPEM, or the active gain, and $t_{d,a}$ is the active delay.

As the vestibular system detects all head movements, including active ones (Cullen and Minor, 2002), the VOR could produce eye movements that would interfere with PPEM. We propose that to prevent this interference, the active pathway selectively cancels the VOR. To do this, the same prediction of head movement ($\widehat{\dot{H}}$) used to produce PPEM is also sent to an internal model of the VOR. This model predicts the eye movements the VOR will produce according to the formula $\dot{E} = \hat{p}\widehat{\dot{H}}(t - \hat{t}_{d,p})$, where $\hat{p}$ is the estimate of the passive gain and $\hat{t}_{d,p}$ is the estimate of passive delay (Figure 2.1, orange pathway). This prediction is then subtracted from the actual output of the VOR. Thus, the VOR is prevented from interfering with PPEM but can still provide compensation for unexpected passive perturbations. We refer to this model as the Cooperative Model. However, as discussed previously, an alternative mechanism for preventing VOR interference is simply to suppress the VOR altogether during active movements (Figure 2.1, blue pathway), which we refer to as the Suppression Model.

In this paper, we will evaluate eye movements during three types of head movements: 1) passive-only, 2) active-only, and 3) combined active and passive, where a passive perturbation interrupts an active movement. Below are the predictions made by each model.

1) During a passive-only movement, when $\widehat{\dot{H}} = 0$, both models predict

$$\dot{E} = p * \dot{H}(t - t_{d,p}) \quad (1)$$

2) During an active-only movement, when $\dot{H} = \widehat{\dot{H}}$, the Cooperative model predicts

$$\dot{E} = p * \dot{H}\left(t - t_{d,p}\right) - \hat{p} * \dot{H}\left(t - \hat{t}_{d,p}\right) + a * \dot{H}(t - t_{d,a}) \quad (2)$$

For animals that can correctly estimate their VOR dynamics (i.e. $\hat{p} = p, \hat{t}_{d,p} = t_{d,p}$), this reduces to the following formula:

$$\dot{E} = a * \dot{H}(t - t_{d,a}) \quad (3)$$

According to the Cooperative Model, we use equation (3) for healthy intact animals. However, for animals that have recently undergone a change in VOR dynamics (such as a vestibular lesion) equation (2) is more appropriate as it can take time for the internal model to update its estimate of the VOR dynamics and thus $\hat{p} \neq p$ and $\hat{t}_{d,p} \neq t_{d,p}$.

3) During a combined head movement, the Cooperative Model predicts

$$\dot{E} = p * \dot{H}\left(t - t_{d,p}\right) - \hat{p} * \widehat{\dot{H}}\left(t - \hat{t}_{d,p}\right) + a * \widehat{\dot{H}}(t - t_{d,a}) \quad (4)$$

However, in our analysis, we often refer to the "active" and "passive" component of head movement rather than the actual ($\dot{H}$) and predicted ($\widehat{\dot{H}}$) head movement. To make these ideas clearer, we reformulate equation (4) in those terms. We can think of the predicted head movement ($\widehat{\dot{H}}$) as the active component of head movement, as it is the head movement expected to result from the active motor command. We will thus denote $\widehat{\dot{H}}$ as $\dot{H}_a$. The total head velocity ($\dot{H}$) can be thought of as the sum of the active and passive component ($\dot{H}_a + \dot{H}_p$). Making these substitutions and rearranging, we find that in a healthy intact animal ($\hat{p} = p, \hat{t}_{d,p} = t_{d,p}$), equation (4) becomes

$$\dot{E} = p * \dot{H}_p(t - t_{d,p}) + a * \dot{H}_a(t - t_{d,a}) \quad (5)$$

Alternatively, the Suppression Model predicts:

$$\dot{E} = a * \dot{H}_a(t - t_{d,a}) \quad (6)$$

Note, the distinguishing feature of Suppression Model is that eye movements reflect only the active component of head movement ($\dot{H}_a$).

To simulate results from Dichgans and others (Dichgans et al., 1973; Newlands et al., 1999; Sadeghi et al., 2012) we used the following parameters. Intended head velocity ($\widehat{\dot{H}}$) was always set to a decaying exponential waveform, designed to emulate the head movement reported by Dichgans et al. Actual head velocity was set equal to the intended head velocity (i.e. $\dot{H} = \widehat{\dot{H}}$) when the head was free to move and set to zero when head movement was prevented. For PPEM, we used an active gain (a) of -1.0 and a latency ($t_{d,a}$) of 0ms to simulate ideal compensation. For the VOR, we used a passive gain (p) of -1.0 for healthy animals (Dichgans et al., 1973; Huterer and Cullen, 2002; Newlands et al., 1999, 2001) and 0.0 for lesioned animals (Dichgans et al., 1973; Newlands et al., 1999; Sadeghi et al., 2012) and latency ($t_{d,p}$) of 5ms (Huterer and Cullen, 2002). For the VOR Model, we assume that in a healthy adult animal, the VOR dynamics are stable and can be accurately estimated. We, therefore, set the estimated passive gain and latency ($\hat{p}, \hat{t}_{d,p}$) equal to the actual passive gain and latency. After a labyrinthectomy, we assume that the VOR Model initially maintains its original dynamics, but with time, these change to reflect the animal's new state. What this new state is depends on a number of factors including the severity of the lesion and compensation from other systems. In Dichgans' study, the authors found that

while the passive VOR gain was effectively zero after lesion, the cervical-ocular reflex (COR) provided about 30% of ocular compensation. Given the lack of the COR before lesioning, we assume that the COR is interpreted as the passive VOR and therefore set estimated passive VOR gain to -0.3. For animals that also underwent cervical deafferentation, and therefore had no VOR or COR, we set the estimated passive gain to 0.0.

2.4 Experimental Methods

2.4.1 Surgical Preparation

All procedures were approved by the University of Michigan's University Committee on Use and Care of Laboratory Animals and were in accordance with the National Institutes of Health Guide for the Care and Use of Laboratory Animals. Seven male pigmented guinea pigs were used for this study. All animals underwent an initial surgery during which a head bolt and eye coil were implanted. Briefly, animals were sedated using a combination of ketamine and xylazine. A midline incision was made to expose the skull and a head post was attached using bone cement and dental acrylic. Next, an eye coil was implanted below the conjunctiva of the right eye. Animals were allowed to recover for 7-14 days before data was collected.

In addition, 3 animals underwent bilateral vestibular lesions after control data was collected. Lesions were performed by filling the inner ear cavity with streptomycin. Lesions were performed one at a time. That is, each animal first underwent a unilateral lesion and, after approximately one month, underwent the same procedure on the contralateral side.

2.4.2 Test Procedure

Animals were comfortably restrained to a turn table, such that their bodies were fixed to the turn table but their heads were free to move (for details, Shanidze et al., 2010b). Eye movements were recorded via a scleral eye coil (see Surgical Preparation for details). Head movements were recorded via two orthogonal coils imbedded in a light-weight plastic ball which attached to the head post. All procedures were performed in the dark.

Passive stimuli consisted of transient velocity steps of 60 deg/s generated by the turntable. Using a Gaussian acceleration profile, maximum step velocity was reached after 90ms, lasted for approximately 400ms, and then decelerated in a similar manner. Each testing session consisted of at least 100 steps and active movements were encouraged throughout testing by placing food in eccentric locations. Control animals were tested between 5-9 times while lesioned animals were tested 14-20 times.

2.4.3 Data Analysis

Orientation data from eye and head coils was differentiated and low-pass filtered at 40Hz to obtain gaze ($\dot{G}$) and head ($\dot{H}$) velocity in space. Eye ($\dot{E}$) velocity in the head was defined as $\dot{E} = \dot{G} - \dot{H}$. The velocity feedback signal from the turntable was defined as body velocity ($\dot{B}$) and head-on-body ($\dot{HoB}$) velocity was defined as $\dot{HoB} = \dot{H} - \dot{B}$.

Active-only movement was defined as head velocity that surpassed 10 deg/s for at least 200ms in the absence of any turntable movement. In total, there were 225 minutes of active movement from control animals and 220 minutes from lesioned animals that were included in the analysis.

Passive-only movements were defined as head movements that occurred in response to velocity steps in the absence of any additional active head movement. When a velocity step interrupted an on-going active movement, the head movement was defined as a combination of active and passive. In these cases, we defined the passive component ($\dot{H}_p$) as the averaged passive-only response for that day, while the active component ($\dot{H}_a$) was defined as the total head velocity ($\dot{H}$) minus the averaged response (Brooks and Cullen, 2014). For both control and lesioned animals, there were approximately 3500 passive-only steps and 600 combined active and passive steps.

As other dynamics and reflex pathways can contribute to eye movement, we restricted our analysis to the first 65ms of head movement in all conditions defined above. All fits were performed using least-squares regression. To determine the gain and latency for active- and passive-only movements, we used the following fit (Huterer and Cullen, 2002):

$$\dot{E} = offset + g * \dot{H}(t - t_d) \quad (7)$$

Similar to equations (1) and (3), where g is either the active (a) or passive (p) gain, $\dot{H}$ is the total head velocity, and t_d is either the active ($t_{d,a}$) or passive ($t_{d,p}$) latency. The only exception to this was for lesioned animals during active-only movements where the assumptions that $\hat{p} = p$ and $\hat{t}_{d,p} = t_{d,p}$ do not hold. Thus, these movements were fit according to equation (2):

$$\dot{E} = offset + p * \dot{H}(t - t_{d,p}) - \hat{p} * \dot{H}\left(t - \hat{t}_{d,p}\right) + a * \dot{H}(t - t_{d,a}) \quad (8)$$

Parameters fit to passive-only and active-only data (i.e $p, t_{d,p}, a, t_{d,a}, \hat{p}, \hat{t}_{d,p}$) were used for fits to combined active and passive movements. For these movements, the Cooperative Model predicted eye movements described by equation (5) for healthy animals and equation (4) for lesioned animals, thus we used equations (9) and (10) respectively:

$$\dot{E} = offset + p * \dot{H}_p(t - t_{d,p}) + a * \dot{H}_a(t - t_{d,a}) \quad (9)$$

$$\dot{E} = offset + p * \dot{H}_p(t - t_{d,p}) + p * \dot{H}_a(t - t_{d,p}) - \hat{p} * \dot{H}_a\left(t - \hat{t}_{d,p}\right) + a * \dot{H}_a(t - t_{d,a}) \quad (10)$$

While the Suppression Model predictions were described by equation (6) for both populations;

$$\dot{E} = offset + a * \dot{H}_a(t - t_{d,a}) \quad (11)$$

To compare these two models, we first used the coefficient of determination (R^2). However, as the two models have different number of parameters, we also used the Bayesian Information Criterion (BIC) which is considered one of the most conservative model selection criterion (Posada et al., 2004; Schwarz, 1978a) and is defined as:

$$BIC = n * \ln(SSE/n) + k * \ln(n)$$

Where n is the number of observations, SSE is the sum-squared errors, and k is the number of parameters. A lower BIC indicates a better fit.

Statistical significance was assessed using a paired t-test with alpha=0.05.

2.5 Results

In Dichgan's original paper, PPEM were defined as compensatory eye movements seen when a planned head movement was unexpectedly prevented. They found that while PPEM were observed in animals within a few days of vestibular lesion, they were not observed in healthy subjects, leading them to conclude that PPEM were strictly an adaptive phenomenon. We believe our model can account for these findings despite our inclusion of PPEM as a part of normal gaze stabilization.

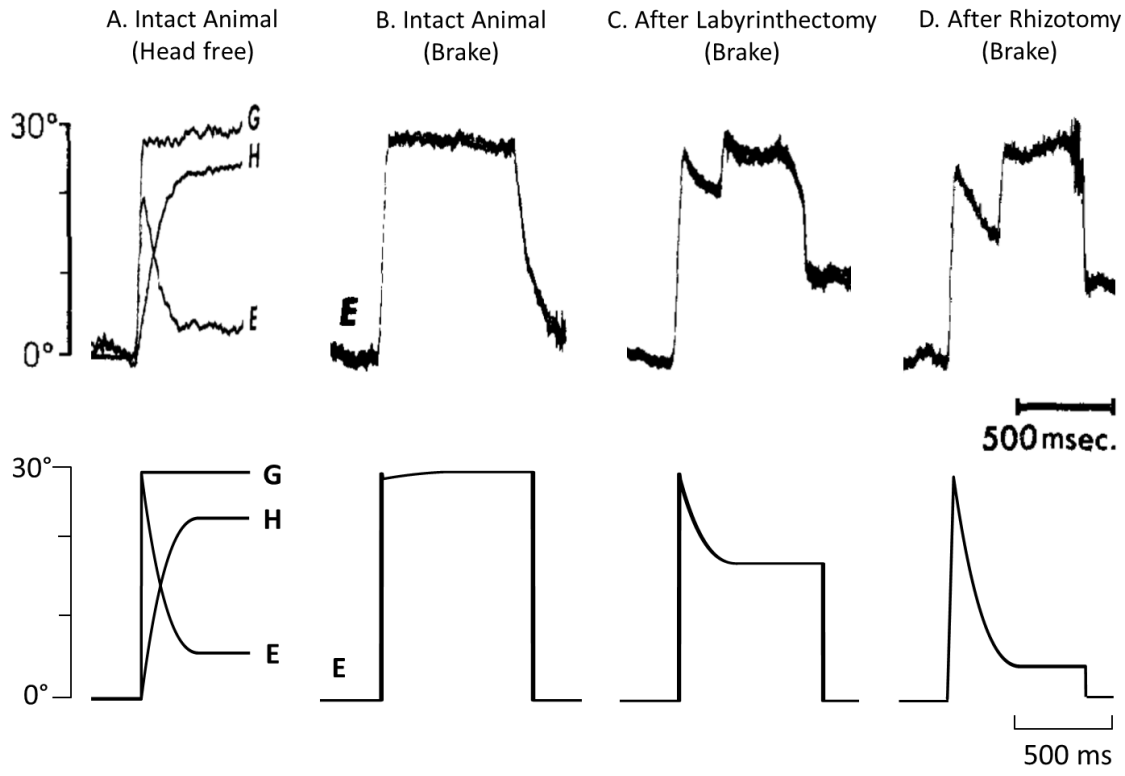

Figure 2.2 - Model Simulations Compared to Dichgans' Data

(Top) Data from Dischgans (1973) and (bottom) model simulations. A) Gaze (G), head (H) and eye (E) position traces from an intact animal during a voluntary head rotation. B) Eye position from an intact animal when a voluntary head rotation is unexpectedly stopped via head brake. C) Eye position from a vestibular-lesion animal when a voluntary head rotation is unexpectedly stopped.

In Figure 2.2, we present four results from Dichgans et al. 1973 paper (top) along with predictions from our model (bottom). Starting on the far left (A) we present gaze (G), head (H) and eye (E) position traces for a healthy animal during a planned head rotation. As can be seen, the eye counter-rotates with respect to the head to stabilize gaze in both experimental data and model simulations. When a head rotation is unexpectedly stopped using a head brake, as seen in B, there is no counter-rotation of the eye. However, when this same paradigm is used with a vestibular lesioned animal, as seen in C, the eye begins to counter-rotate despite there being no head rotation. Additionally, in an animal that has undergone both a labyrinthectomy and cervical deafferentation (D), there is an even greater counter-rotation of the eye. In all four examples, the model was able to predict the experimental data using PPEM as part of normal gaze stabilization.

To further test our model, we collected head and eye movement data from both healthy and vestibular lesioned guinea pigs in order to characterize compensatory eye movements during passive, active, and combined active and passive head movements. Figure 2.3 presents exemplary data from healthy intact animals. During a passive head rotation (left panel) the guinea pig produces compensatory eye movements that are delayed and diminished with respect to the head (see inset for detail). However, during active head movements (middle panel), eye movements show an increase in gain and decrease in latency, in line with the hypothesis that these are PPEM. When a passive perturbation interrupts an active movement (i.e. combined movement, right panel) the eye appears to compensate for the total head velocity as is expected by our model. To further demonstrate this point, we present in this figure predictions from our model (‘Cooperative Model’ in orange), which allows the VOR to continue to compensate during active head movements; as well as the alternative hypothesis (‘Suppression Model’ in

blue) in which the VOR is suppressed during active head movements. During passive-only and active-only head movements these two models make the same predictions. However, during combined active and passive head movements these two models clearly differentiate themselves with the Cooperative Model more closely aligned with the actual eye movement.

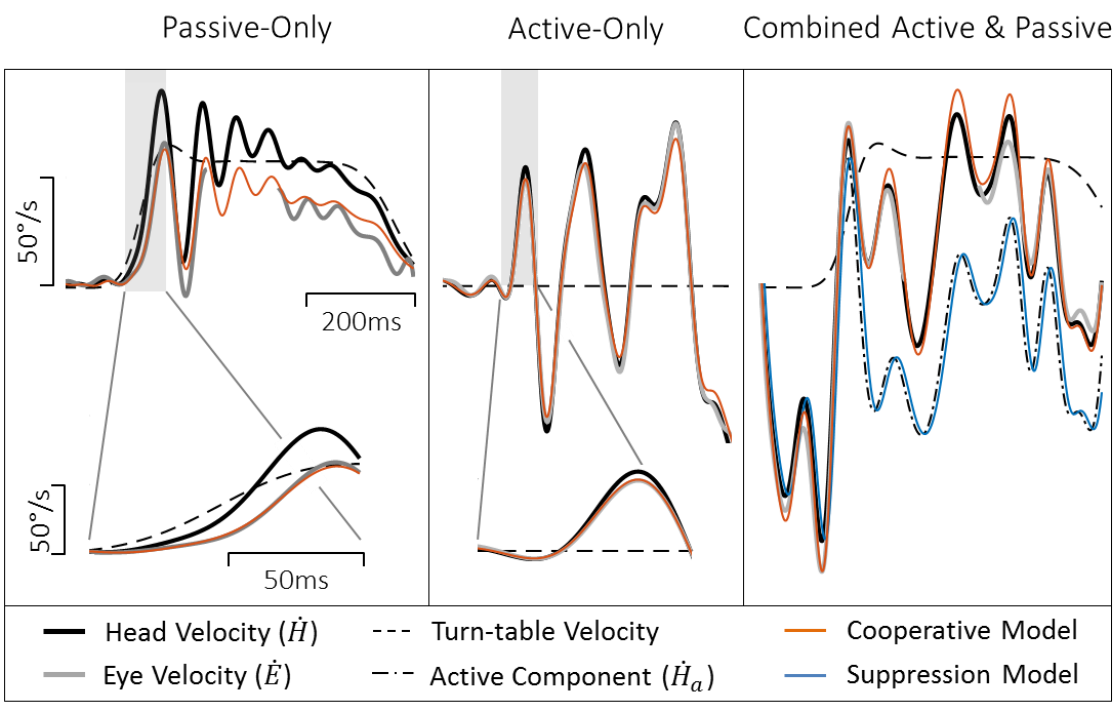

Figure 2.3 – Exemplary data from healthy guinea pigs

Data from healthy guinea pigs during passive (left), active (middle) and combined (right) head movements. Details show difference in gain and latency of eye movements during passive and active head movements. Model predictions are identical for passive- and active-only movements, but can be distinguished during combined movements.

To quantify these findings, we regressed eye velocity against the total head velocity (equation (7)) for passive-only, active-only and combined head movements (Figure 2.4, black bars). For combined head movements, we also regressed eye velocity against the passive and active component of head velocity independently (equation (9)) to determine how each component was

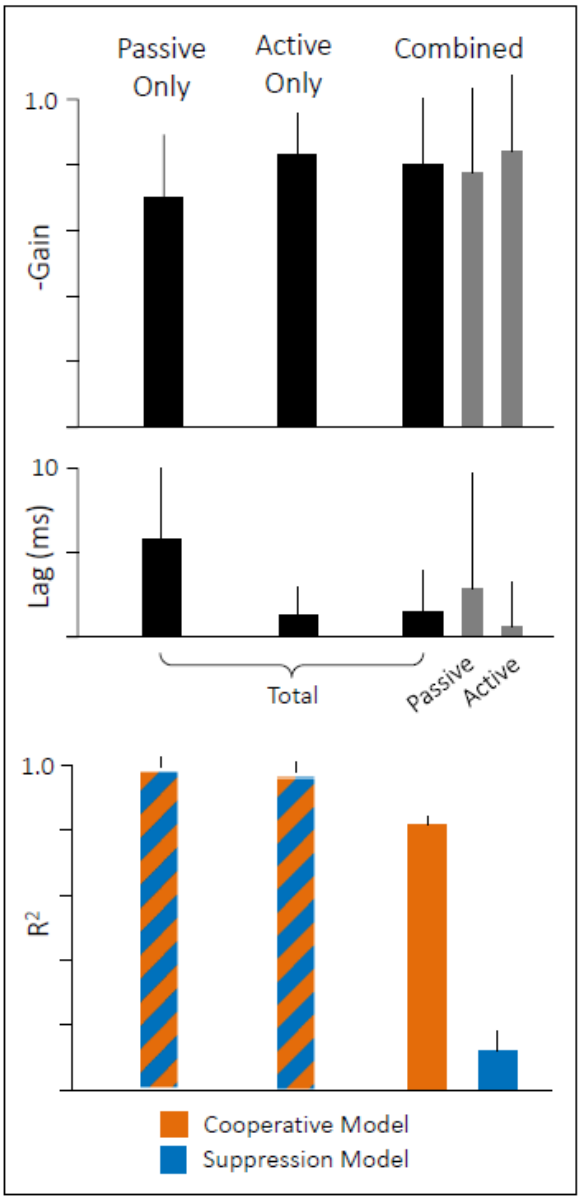

Figure 2.4 –Aggregate VOR, PPEM, and model performance from healthy animals

(Top and middle) Gain and latency of eye movements during passive, active, and combined head movements. Regressions were performed against total head velocity (black bars, eqn. 6) and against passive and active components of head velocity independently (grey bars, eqn. 7). (Bottom) Goodness of fit for each model.

being used (Figure 2.4, grey bars). During passive-only movements we found the VOR had a gain of -0.70 (±0.19) and latency of 5.8ms (± 4.2). Both values are in line with what has been previously reported for this species (Escudero et al., 1993; Serafin et al., 1999; Shanidze et al., 2010a). We also found that despite a relatively low gain, eye movements show a strong correlation to head movement, as demonstrated by a high R^2 (0.98 ± 0.03). During active-only movements, compensatory eye movements had significantly higher gain (-0.83 ± 0.13; $p<0.001$) and shorter latency (1.3ms ± 1.6; $p<0.001$) as would be expected with PPEM and as previously noted by others (Della Santina CC et al., 2002; Shanidze et al., 2010b).

During combined active and passive movements, we found that when eye movements were regressed against total head velocity they had a gain of -0.80 (± 0.20) and latency of 1.4ms (± 2.6). We also regressed eye movements against the active and passive component to quantify the gain and latency associated with each. We found the passive gain was -0.78 (± 0.26) while the active gain was -0.84 (± 0.23). In addition, the latency associated with the passive component was 2.9ms (± 7.0) and 0.7ms (± 2.6) for the active component. These results mirror those seen during passive- and active-only head movements, namely, that the active component has a higher gain and shorter latency than that of the passive component.

These results would suggest that during active head movements the VOR does continue to compensate for passive perturbations. To explicitly test this theory, we compared our model ('Cooperative') against the alternative ('Suppressive'), which proposes that the VOR is suppressed during planned movements. We first examined the goodness of fit of each model (Figure 2.4, bottom panel) and found that the R^2 was higher for the Cooperative model (0.81 ± 0.13) compared to the Suppressive model (0.12 ± 0.41). Next, we calculated the Bayesian Information Criteria (BIC), which takes into account the number of parameters in a model (see Methods for more detail). According to this metric a lower score indicates a better fit to the data. We found that the BIC for the Suppression model was (555 ± 101), greater than that of the Cooperative model (420 ± 87) indicating that the Cooperative model provides a much better description of the data.

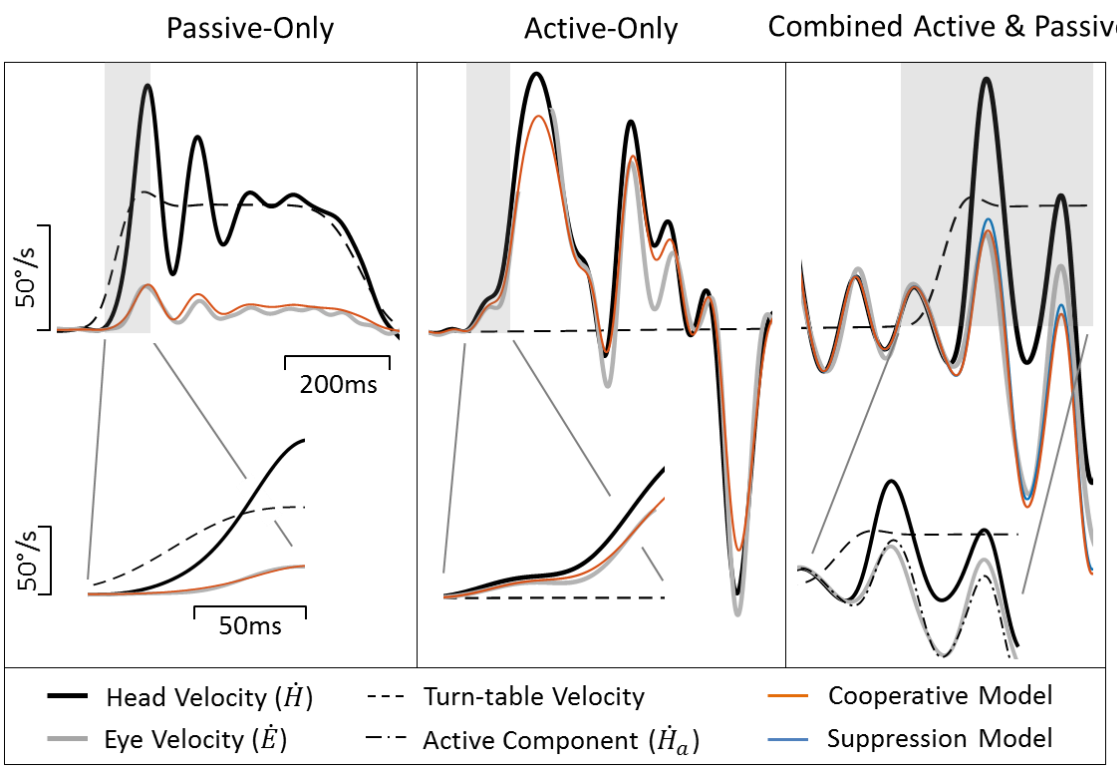

Figure 2.5 – Exemplary data from lesioned animals

Data from lesioned guinea pigs during passive (left), active (middle) and combined (right) head movements. Details show difference in gain and latency of eye movements during passive and active head movements. Model predictions are identical for passive- and active-only movements, but can be distinguished during combined movements.

We also performed this analysis on lesioned animals to test two further predictions of our model. First, that despite no longer having a functional VOR, PPEM would still be present during active head movements. Second, that given the lack of a VOR in these subjects, the two models would do equally well in predicting eye movements.

Figure 2.5 shows exemplary data from lesioned animal during passive, active, and combined head movements. As would be expected from a lesioned animal, there is limited ocular compensation during a passive perturbation (left panel). However, during active head

movements (middle panel), there is a robust counter-rotation of the eye, similar to that seen in intact animals (Figure 2.3, middle panel). When a passive perturbation interrupts an ongoing active movement (right panel), we see a very different pattern of eye movement than that seen in healthy animals. In lesioned animals, the eye appears to primarily follow the active component, as can be seen in the inset, and fails to compensate for the passive perturbation. This can also be seen in how closely the two models align. The Suppression Model, despite only taking into account the active component of head velocity, makes a similarly accurate prediction of eye velocity as does the Cooperative Model, which takes into account both the active and passive component, indicating that the eye is only compensating for the active component.

To quantify these findings, we performed a similar analysis as described above for intact animals. We found that during passive-only head movements, lesioned animals have a VOR gain of -0.24 (± 0.19) and latency 7.4ms (± 8.6). Thus, there was still some amount of ocular compensation (as can be seen in Figure 2.5, left panel); however, it was greatly reduced from the pre-lesion VOR gain of -0.7. We also found that these eye movements have a high correlation to head movement 0.92 (± 0.1) despite their low gain. During active-only head movement, lesioned animals produce compensatory eye movements with a gain of -0.55 (± 0.24) and latency 3.7ms (± 2.5) with a similarly high correlation to head movement (0.92 ± 0.06). This is consistent with the pattern seen in intact animals, namely, that compensatory eye movements during active head movements have a higher gain and shorter latency, in line with the theory that these eye movements are pre-programmed. For combined active and passive head movements, we found that the passive gain was -0.44 (± 0.24) while active gain was -0.61 (± 0.28) and passive lag was 3.1ms ± 8.1 while active lag was 1.7ms ± 4.2. Again, mirroring the pattern seen in intact animals

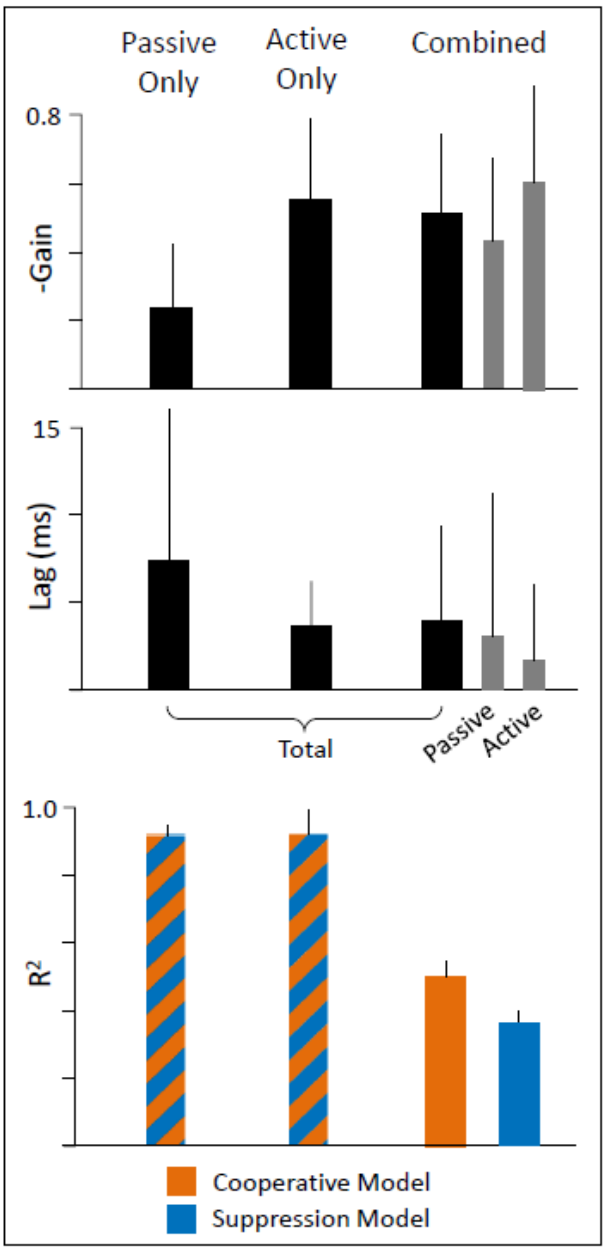

Figure 2.6 - Aggregate VOR, PPEM, and model performance from healthy animals

(Top and middle) Gain and latency of eye movements during passive, active, and combined head movements. Regressions were performed against total head velocity (black bars, eqn. 6) and against passive and active components of head velocity independently (grey bars, eqn. 7). (Bottom) Goodness of fit for each model.

of having a higher gain and shorter latency associated with the active, compared to the passive, component.

To determine which model of VOR and PPEM integration performed better, we again focus on combined active and passive head movements. We found that like intact animals, the Cooperative model was a better fit to the data than the Suppression model as demonstrated by a higher R^2 (0.50 ± 0.3 vs. 0.36 ± 0.3) and a lower BIC (435 ± 85 vs 490 ± 117). However, as will be discussed in more detail below, the differences in performance between these two models is greatly diminished in lesioned animals.

2.6 Discussion

The role of PPEM as an adaptive mechanism has been explored in a number of species (human: Black RA et al., 2005; Della Santina CC et al., 2002; Foster et al., 1997; Halmagyi et al., 2003; Herdman SJ et al., 2001; Kasai and Zee, 1978; Tian et al., 2002; non-human primate: Newlands et al., 1999, 2001; Sadeghi et al., 2012; rodent: Shanidze et al., 2010a) since it was first reported in primates by Dichgans et al. in 1973. These studies note the occurrence of compensatory eye movements in vestibular deficient subjects during active, but not passive, head movements. Recently, some studies have also noted improved compensation (i.e. increased gain and decreased latency) of eye movements during active head movements in healthy animals as well, suggesting the use of PPEM (human: Collewijn et al., 1983; Hoshowsky et al., 1994; Jell et al., 1988; Tomlinson et al., 2009; Della Santina CC et al., 2002; rodent: Shanidze et al., 2010a; Steen and Collewijn, 1984). If PPEM are a part of normal gaze stabilization, two questions naturally arise, which this paper seeks to address: first, why didn't Dichgans et al. make the same observation, and second, what happens to the VOR during active movements.

If the VOR remains fully functional it would inevitably produce its own compensatory eye movements, which would interfere with the PPEM. We hypothesized that the efference copy signal used to drive PPEM could also be used to predict the VOR. This prediction could then be used to negate the eye movements the VOR would produce in response the planned head movement (Figure 2.1, "Cooperation Model"). This would prevent the VOR from interfering with PPEM but allow it to compensate for unexpected head movements. However, it is also possible, and perhaps a simpler explanation, that during active head movements, the VOR is completely suppressed ("Suppression Model").

To test these two possibilities, we collected data from seven healthy animals and three lesioned animals. Both models use the VOR for passive-only movements and PPEM for active-only head movement; they differentiate themselves when a passive perturbation interrupts an active movement (what we call a "combined movement"). In the Suppression Model, the VOR is completely suppressed and thus, cannot offer compensation. Whereas the Cooperation Model only cancels the VOR with respect to the intended head movement and so can offer compensation for unexpected perturbations. As such, we hypothesized that the Cooperation Model would offer a superior fit to the data in healthy animals but in lesioned animals, which lack a VOR, the two models would make similar predictions.

As can be seen in Figure 2.3 (left and middle panel), compensatory eye movements in healthy animals have a higher gain and shorter latency during active compared to passive head movements, confirming earlier reports of the use of PPEM in healthy animals. These results are summarized in Figure 2.4. When a passive perturbation interrupted an active movement, we found that the eye followed the total head velocity rather than just the active component (Figure 2.3, right panel) as predicted by the Cooperative Model. To quantify this observation, we compared the goodness of fit (R2) as well as the Bayesian Information Criterion (BIC) for each model. We found that the Cooperative Model had both a higher R2 (0.81 vs 0.12) as well as a lower BIC (420 vs 555) indicating a superior fit to the data.

For lesioned animals, we found very little compensation during passive movements (Figure 2.5, left panel) as would be expected, but robust compensation during active head movements (Figure

2.5, middle panel; summarized in Figure 2.6). While PPEM were intact after lesion, there was a noticeable decrease in gain (-0.55 vs. -0.83). To investigate this finding, we examined the gain of PPEM over the course of several months (Figure 2.7) and found that the gain gradually increased as Dichgans found in primates. Thus, while the gain of PPEM eventually returns to its original value, taking an average of all data over the post-lesion recovery would result in an overall lower mean gain.

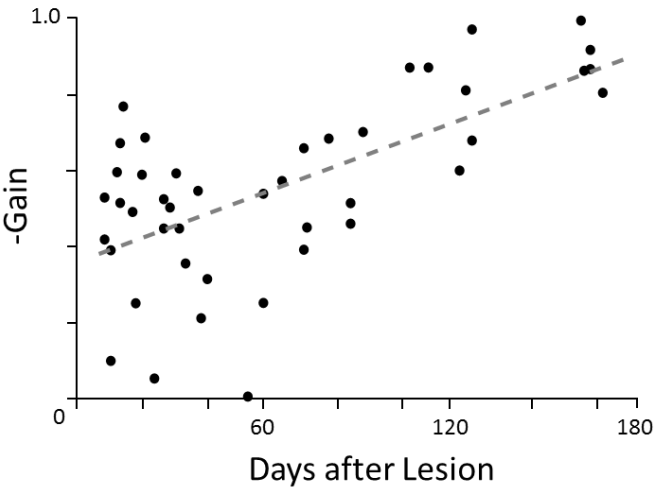

Figure 2.7 – Gain of pre-programmed eye movements as a function of time after lesion.

Finally, we found that during combined head movements, eye movements in lesioned animals predominately follow the active component of head velocity; thus both models offer similar fits (Figure 2.5, right panel). When we compare the goodness of fit of these two models, we found that while the Cooperative Model still has a higher R2 (0.50 vs 0.36) and lower BIC (435 vs 490), the difference between the two models was much lower. We suspect the Cooperation Model is still a superior fit in our lesioned animals because there was some residual vestibular function, as evidenced by a non-zero VOR gain (Figure 2.6). As can be seen in Equations 5 and

6, the difference between the two models is a function of the passive gain and they are only equivalent when the gain is zero. Nonetheless, it is interesting to note that the passive gain in lesioned animals decreased by a little more than half of that in healthy animals (-0.7 vs -0.24), and the difference in performance between the two models was also decreased by about half (R2: 85% vs. 30% difference; BIC: 32% vs 13% difference), in agreement with model predictions.

We were also interested in resolving conflicting reports in the literature as to whether or not PPEM were a part of normal gaze stabilization. Those who reported that PPEM were only found in lesioned animals did so because when the head was unexpectedly stopped, lesioned animals produced compensatory eye movements as though the head had moved, whereas healthy animals did not. However, we found that our Cooperative Model was able to produce both the PPEM observed in lesioned animals as well as the "lack" of such eye movements in healthy animals despite including PPEM for both populations (Figure 2.2). Two key features of our model that allow for this reconciliation are: 1) that the VOR is selectively cancelled such that it will only provide compensation to unexpected head movements, and 2) what the body expects from the VOR is based on an estimated passive gain ($\hat{p}$) which can be updated. According to this understanding, the eye movement produced during a voluntary head movement is defined as:

$$\dot{E} = p * \dot{H} + (a - \hat{p}) * \widehat{\dot{H}}$$

Using Dichgans' methodology, the actual head velocity would be zero ($\dot{H} = 0$) and if the active gain is ideal ($a = -1$), then the gain of the PPEM reduces to:

$$PPEM = (-1 - \hat{p}).$$

We assume a healthy animal accurately estimates its passive gain ($\hat{p} = -1$), thus the gain of the PPEM would be zero, that is, no eye movement would be produced, just as described by Dichgans (Figure 2.2b). In a vestibular lesioned animal, we assume the estimated passive gain would initially be the pre-lesion value ($\hat{p} = -1$) but with time would decrease to match the new passive gain, resulting in a gradual increase in PPEM gain (Figure 2.8). This fits well with Dichgans' finding that the amplitude of PPEM increased with time. They also report that after cervical deafferentation, the PPEM gain further increased. There are two potential explanations for this: 1) cervical deafferentation always occurred after labyrinthectomy, thus the increase in PPEM gain was simply the continued decrease in estimated passive gain; or 2) the COR gain, which in healthy animals is effectively zero but in lesioned animals was -0.3, could have been interpreted as the passive VOR gain, causing the estimated passive gain to settle at a non-zero

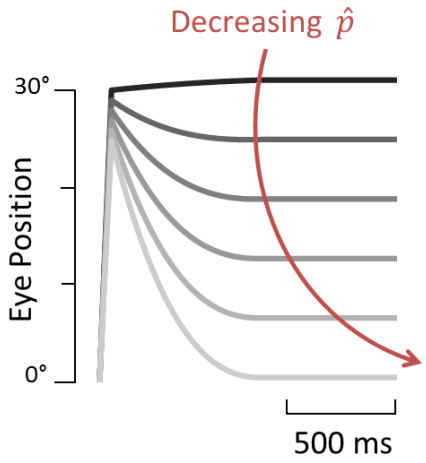

Figure 2.8 – Simulation of pre-programmed eye movements as a function of $\hat{p}$.

Darker traces are simulation with higher value of $\hat{p}$ and result in very little compensation, whereas lighter traces, with lower values of $\hat{p}$ show large pre-programmed eye movements

value. After cervical deafferentation, the COR disappears and thus the estimated passive gain decreases to zero. We based our simulations on this latter interpretation and found that model predictions matched well with the experimental data reported by Dichgans (Figure 2.2c and d).

As mentioned in the Introduction, the idea of the VOR being selectively cancelled finds its origins in Bizzi's linear summation theory which he proposed to account for the lack of VOR counter-rotation during eye-head gaze shifts. This theory has found support in Bizzi's own studies (Morasso et al., 1973) as well as those of others (Blakemore and Donaghy, 1980; Freedman et al., 1998; Guitton and Volle, 1987; Guitton et al., 1984). In addition, there is research to support a neural mechanism for this phenomenon. Recordings performed by Cullen and colleagues have shown that VO neurons will encode head velocity only during passive head movements (Roy and Cullen, 1998, 2001), despite receiving the entire head velocity signal from primary afferents (Cullen and Minor, 2002). Furthermore, when an active movement occurs in the midst of passive movement, VO neurons encode only the passive component (Cullen et al., 2011) suggesting a selective cancellation. They have proposed a model that is structurally similar to ours, namely, that during active movement, the body can predict the resulting sensory feedback and subtract this from the total head velocity signal from the periphery, leaving only the passive component. They have even reported a signal coming from the cerebellum which corresponds to this prediction (Brooks and Cullen, 2013).

However, there is also evidence, both in eye movements and in single unit recordings, that the VOR is suppressed during active movements. In response to Bizzi's original paper, several studies have shown that when the subject' head is perturbed during the gaze shift, there is no

compensation, indicating that the VOR has been turned off (Cullen et al., 2004; Laurutis and Robinson, 1986; Tabak et al., 1996). Yet, this methodology has produced mixed results with some reporting only partial suppression or none at all (Blakemore and Donaghy, 1980; Freedman et al., 1998; Guitton and Volle, 1987; Guitton et al., 1984; Morasso et al., 1973). In recording from larval *Xenopus* frogs, Straka and colleges have shown that compensatory eye movements during locomotion originate from a central pattern generator (CPG) in the spinal cord (Lambert et al., 2012) and not from the vestibular periphery. Further, they have found that the gain of the incoming vestibular signal is significantly decreased during locomotion (Chagnaud et al., 2015). To what extent CPGs are used in higher-level animals, if at all, remains controversial. While there is evidence that they are used for more rhythmic movements like locomotion (Brandt et al., 1999; Jahn et al., 2000), it is unlikely that they are used for the spontaneous unstructured head movements we have described here.

There are several limitations to this study. First, our lesioned animals appeared to have residual vestibular function (i.e. non-zero VOR gain). This may account for why the Cooperative Model still out-performed the Suppression Model despite our prediction that both would produce similar fits. Second, this was a relatively small study with only seven control and three lesioned animals, only two of which were we able to follow for more than two months after lesion. More animals followed for longer amounts of time would have allowed us to better characterize the process of recovery. Finally, our model was extremely simple, lacking dynamics as well as other known inputs to the vestibular system, including proprioception. The latter is of particular importance given the role the COR has been found to play in primates after labyrinthectomy. While we believe the COR most likely plays a similar role in the guinea pig, our goal in this paper was to

simply address the contribution of PPEM to ocular stability. Further studies would need to be done to assess the COR's role in gaze stabilization in this species.

Despite these limitations, our results suggest that not only are PPEM a part of normal gaze stabilization, but that they work cooperatively with the VOR. This is achieved by selectively cancelling the VOR during active head movements in a manner similar to Bizzi's linear summation theory. Further, it is precisely this selective cancellation that allows us to reconcile the conflicting reports in earlier literature as to whether PPEM are a part of normal gaze stabilization. Finally, it is interesting to note that while the gaze shifts Bizzi sought to explain are unique to foveate animals, we have found a similar phenomenon in an afoveate species during gaze stabilization, perhaps indicating that this system is a more primitive version of what is used in higher-order animals.

Chapter 3: Effects of a Single Noise Exposure on Ocular and Postural Stability in the Guinea Pig

3.1 Abstract

Previous research into the effects of high-intensity noise on the vestibular system has largely focused on the otoliths. Those that have looked at the semi-circular canals have relied on the vestibular ocular reflex (VOR) as a metric of functional damage. However, the VOR is primarily influenced by regular afferents while noise appears to effect primarily irregular afferents. Fortunately, the vestibulocollic reflex (VCR) receives predominantly irregular input and a model characterizing its role in head stability has been developed. We use this model to predict the effect of a diminished VCR on head stability and compare model predictions to animal responses before and after noise exposure. We first characterized the VOR and VCR in healthy guinea pigs using a step input. We then exposed animals to a single session of high-intensity noise and characterized head and eye stability to determine what, if any, vestibular loss occurred. We found that percent overshoot increased, and natural frequency decreased as would be expected from a diminished VCR. In addition, there were significant decreases in VOR performance. However, we also found increased dampening in head response, against model predictions. We conclude that even a single exposure to noise can cause damage to irregular afferents and that this damage has functional implications for both ocular and head stability. We also hypothesize that in response to vestibular loss there is an increased contribution from neck proprioceptive driven reflexes such as the cervico-collic reflex and cervico-ocular reflex.

3.2 Introduction

While there is a growing consensus that noise-overstimulation can damage the vestibular organs, the exact nature and extent of damage is not well understood. Part of the difficulty of establishing a consensus is the multifaceted nature of the vestibular system itself, which receives multi-sensory integration at the very earliest stages of processing, is subject to central adaptation, and produces output measures that include evoked potentials, eye movements, balance, and subjective perception. Given such a comprehensive repertoire of inputs, processing, and outputs, it is not surprising there are often conflicting reports regarding the effects of noise overstimulation on the vestibular system

To investigate the peripheral mechanism of noise damage, many have looked to the otoliths (Akdogan et al., 2009; Hsu et al., 2008; Zuniga et al., 2012). And for good reason, they are the most proximate to the oval window, where sound pressure enters the labyrinth, and have an evolutionary legacy of once being hearing organs (Fay and Popper, 2000). Indeed, it has been demonstrated that even in higher-order animals, afferents from the otoliths are still sensitive to clicks, although their threshold is high (about 60 dB SL; (Curthoys et al., 2006)). Indeed, many have shown that the otoliths are particularly susceptible to noise overstimulation. These studies have assessed damage by looking at histology (Akdogan et al., 2009; Hsu et al., 2008; Stewart et al., 2016, 2017b) or by outputs such as VsEP and VEMPs (Akin et al., 2012; Hsu et al., 2008; Kumar et al., 2010; Perez et al., 2002; Stewart et al., 2017b).

However, the semi-circular canals have also been shown to be click-sensitive above 80 dB SPL (Xu et al., 2009; Zhou et al., 2004) as well as susceptible to noise damage (Fetoni et al., 2009;

Stewart et al., 2016). While there have been studies looking at canal-driven eye movements, such as the vestibular ocular reflex (VOR), results from these studies are conflicting, with some showing a decrease in VOR gain and others showing no change (Fetoni et al., 2009; Golz et al., 2001; Manabe et al., 1995; Oosterveld et al., 1982; Shupak et al., 1994; Stewart et al., 2016; Ylikoski et al., 1988). Further, the VOR pathway is thought to be predominately influenced by regular afferents (Minor and Goldberg, 1991). Those that have studied sound sensitivity in the vestibular organs have found that irregular afferents are overwhelmingly more sensitive to sound (Curthoys et al., 2006) and more susceptible to noise damage (Stewart et al., 2017b). Thus, the VOR does not offer the best metric for noise-induced dysfunction in the semi-circular canals. However, the vestibulocollic reflex (VCR) is thought to be predominately mediated by irregular afferents (Bilotto et al., 1982; Boyle et al., 1992; Shanidze et al., 2012) and consequently offers a means of assessing the function of the irregular afferent pathway.

Briefly, the vestibulocollic reflex (VCR) is a closed loop reflex that works to stabilize the head during body movements. Like the VOR, it is driven primarily by the canals and the most direct pathway is comprised of only three neurons (Bilotto et al., 1982; Wilson et al., 1979), making it an excellent counterpart to the VOR when investigating irregular afferents. Peng et al. (1996, 1999) developed a model of head stability and found that without the VCR the head responds as an under damped second order system. That is, the head oscillates, with decreasing amplitude, about its final value (Figure 3.1). However, with the VCR, these oscillations are greatly diminished, and the head response is dampened. Specifically, the percent overshoot is decreased, the frequency of oscillations is increased, the damping coefficient is increased, and the settling

time is shortened. Thus, one can evaluate the function of the VCR by measuring these four metrics, similar to the gain and latency of the VOR.

The claim that the VOR and VCR performance correspond to regular and irregular afferent function is not without nuance. The strongest evidence for both claims comes from how each reflex responds to galvanic vestibular stimulation (GVS) which functionally ablates irregular afferents (Kim and Curthoys, 2004; Minor and Goldberg, 1991). In primates, GVS has no effect on VOR performance, indicating that it is almost entirely driven by regular afferents (Minor and Goldberg, 1991). However, in the guinea pig, Shanidze et al. found that there was a 30% decrease in VOR during GVS, suggesting a less homogenous afferent input in this species (Shanidze et al., 2012). Nonetheless, the authors also found that GVS caused a substantial loss of head stability, supporting the hypothesis that the VCR is mediated by irregular afferents. Controversy arises when comparing these results to those of Boyle et al. (1992) who investigated the relative contribution of regular and irregular afferents to secondary vestibular neurons. They found that while the net afferent profile to the VOR and VCR was regular and irregular respectively, secondary relay neurons mediating them received mixed inputs from both afferent types. Taken together, these findings demonstrate the need to assess both the VOR and VCR to fully capture potential damage to the irregular afferents.

3.3 Methods

3.3.1 Surgical Preparation

All procedures were approved by the University of Michigan's University Committee on Use and Care of Laboratory Animals and were in accordance with the National Institutes of Health

Guide for the Care and Use of Laboratory Animals. Six male pigmented guinea pigs were used for this study. All animals underwent an initial surgery during which a head bolt and eye coil were implanted. Briefly, animals were sedated using a combination of ketamine and xylazine. A midline incision was made to expose the skull and a head post was attached using bone cement and dental acrylic. Finally, an eye coil was implanted below the conjunctiva of the right eye.

3.3.2 Noise Exposure

Six guinea pigs were used for this study. Before noise exposure, each animal's hearing was tested using Auditory Brainstem Response (ABR). Animals were then exposed Six awake and alert guinea pigs were exposed to 120dB SPL octave band noise centered at 1.5kHz for five hours free field (Kappalite 3012H0, Eminence Speaker LLC, Eminence, KY, USA) in a double walled sound exposure booth while awake and alert. Acoustic output was measured using an FFT analyzer (SRS760 Stanford Research Systems, Sunnyvale, CA, USA) as well as Bruel & Kjaer type 4136 microphone, type 2619 preamplifier, and type 2804 power supply (Bruel & Kjaer Sound and Vibration Measurement, Naerum, Denmark).

3.3.3 Data Collection

Animals were comfortably restrained to a turn table, such that their bodies were fixed to the turn table but their heads were free to move (for details, Shanidze et al., 2010). Eye and head movements were recorded via search coils. The eye coil was surgically implanted into the sclera (as described above) and two orthogonal head coils were imbedded in a lightweight plastic ball, which attached to the head post. All measurements were performed in the dark.

Passive body movements consisted of transient velocity steps of 30, 60 and 90 degrees per second (°/s) generated by the turntable. Using a Gaussian acceleration profile, maximum step velocity was reached after 90ms, lasted for approximately 400ms, and then decelerated in a similar manner. Each testing session consisted of approximately 100 steps of each speed. Each animal was tested 3-4 times before and after noise exposure, post-exposure testing was all done within three weeks of exposure.

3.3.4 Data Analysis

Orientation data from eye and head coils was differentiated and low-pass filtered at 20Hz to obtain gaze ($\dot{G}$) and head ($\dot{H}$) velocity in space. Eye ($\dot{E}$) velocity in the head was defined as $\dot{E} = \dot{G} - \dot{H}$. Saccades were identified using an acceleration threshold and automatically removed. The velocity feedback signal from the turntable was defined as body velocity ($\dot{B}$). For a trial to be included in the analysis, there had to be an absence of active head movement. In total, there were over 4300 pre-lesion trials and 4500 post-lesion trials (approximately 1500 for each step size).

To evaluate VCR performance we calculated percent overshoot, frequency of oscillations, damping ratio and settling time. Percent overshoot was calculated from the first peak in head velocity with respect to the turntable velocity. To calculated damping ratio, we first fit an exponential of the form

$$y = a * \exp(b * t)$$

to the peaks of the head oscillations (see Figure 3.1). We then used the time constant of the fit to extract the damping ratio according to the formula:

$$\frac{\dot{H}(t+T_d)}{\dot{H}(t)} = e^{-2\pi\zeta/\sqrt{1-\zeta^2}}$$

Where $\dot{H}(t)$ is head velocity at time t, T_d is the period of damped oscillations and ζ is the damping ratio. MATLAB's fast Fourier transform ('fft') function was used to find the damped natural frequency (ω_d). Using ω_d and ζ, the undamped natural frequency was calculated using:

$$\omega_n = \frac{\omega_d}{\sqrt{1-\zeta^2}}$$

Settling time was defined as the time at which head velocity was no greater than (or less than) 10% of the final value (see dashed lines in Figure 3.1). Finally, to evaluate variability in the VCR, we used standard deviation of percent overshoot across all steps for each day and animal.

VOR performance was characterized using gain and latency. Gain was defined as the ratio of peak eye velocity to peak head velocity. Latency was defined as the time between the onset of head velocity and the onset of eye velocity. To evaluate the variability in the VOR pathway, standard deviation of the VOR gain across all steps for each day and animal was used.

3.3.5 Statistics

For each animal and each day, the above metrics were averaged for all trails of the same step size. Outliers were defined as values that exceeded the mean plus or minus three times the standard deviation. This occurred in less than 3% of values. Statistical significance was assessed using a linear mixed model with step size and noise exposure as fixed variables and animal and test day as random variables and alpha set to 0.05. As test day was not significant for any metric, all pre-exposure days were combined as were all post-exposure days.

3.3.6 Histology

After cardiac perfusion, ears were fixed locally by opening the oval window, perforating the apical end of the cochlea, and gently perfusing 4% paraformaldehyde for 2 hours. Vestibular organs were isolated rinsed with PBS followed by permeabilization with 0.3% Triton X-100 in PBS. Primary antibodies were incubated for 1 hour at room temperature: mouse anti-neurofilament (1:100, Sigma), rabbit anti-myosin VIIa (1:100, Proteus Biosciences, Ramona, CA no. 25-6790). Organs were incubated with Alexa Fluor 488 and Alexa Fluor 595 conjugated secondary antibodies (Invitrogen) for 45 minutes at room temperature before being washed, mounted and imaged on a Leica DMRB microscope.

3.4 Results

Mean and standard deviations for all metrics for each step size before and after noise exposure are listed in Table 3.1, along with p-values associated with step size and exposure. Each metric is discussed in more detail below.

	Pre-Exposure						Post-Exposure						P-Values	
	30°/s		60°/s		90°/s		30°/s		60°/s		90°/s		Step Size	Expsosure
	mean	st.dev.	mean	st.dev.	mean	st.dev.	mean	st.dev.	mean	st.dev.	mean	st.dev.		
% Overshoot	40.7	8.8	44.3	8.6	35.4	14.4	48.1	9.4	44.7	7.2	47.0	11.2	0.66	**0.00**
Natural Freq.	13.9	2.1	12.6	1.3	11.7	1.2	13.9	1.0	12.3	1.2	11.2	1.5	**0.00**	**0.02**
Damping Coef.	0.05	0.02	0.08	0.02	0.07	0.01	0.06	0.02	0.07	0.02	0.10	0.03	**0.00**	**0.04**
Settling Time	232	26	241	36	252	24	249	46	219	35	227	19	1.00	0.85
-VOR gain	0.49	0.13	0.49	0.13	0.49	0.16	0.40	0.12	0.41	0.16	0.38	0.17	0.06	**0.03**
VOR latency	18.1	5.2	15.9	4.3	12.9	3.4	21.6	6.2	17.6	7.9	16.3	4.6	**0.03**	**0.04**
% COR Trials	4.3	8.9	6.7	9.9	7.8	5.0	9.4	12.9	14.3	12.1	17.0	9.7	**0.00**	**0.00**
VCR Variability	25.3	12.0	34.4	12.5	40.3	9.2	29.8	11.8	45.4	15.3	50.7	15.4	**0.00**	**0.00**
VOR Variability	0.19	0.07	0.22	0.07	0.25	0.08	0.21	0.08	0.32	0.17	0.33	0.14	0.87	0.06

Table 3.1 – Mean, standard deviation, and p-value for each metric.
P-values with grey shading are those that reached significance

To characterize VCR performance, we examined head responses to velocity step rotations of the body. In Figure 3.1, we show multiple trials collected from an animal before (grey) and after (blue) noise exposure in response to 60 °/s velocity steps. In response to steps in body rotation, the head produces a classic under damped second-order response with exponentially decaying head oscillations. This response is seen both before and after noise exposure. However, after noise exposure the overshoot (peak head velocity) is both greater and shows increased variability. Further, the frequency of head oscillations noticeably decreases. One can also see that head oscillations decay faster after noise exposure, indicative of an increase in dampening ratio but that the settling time is comparable.

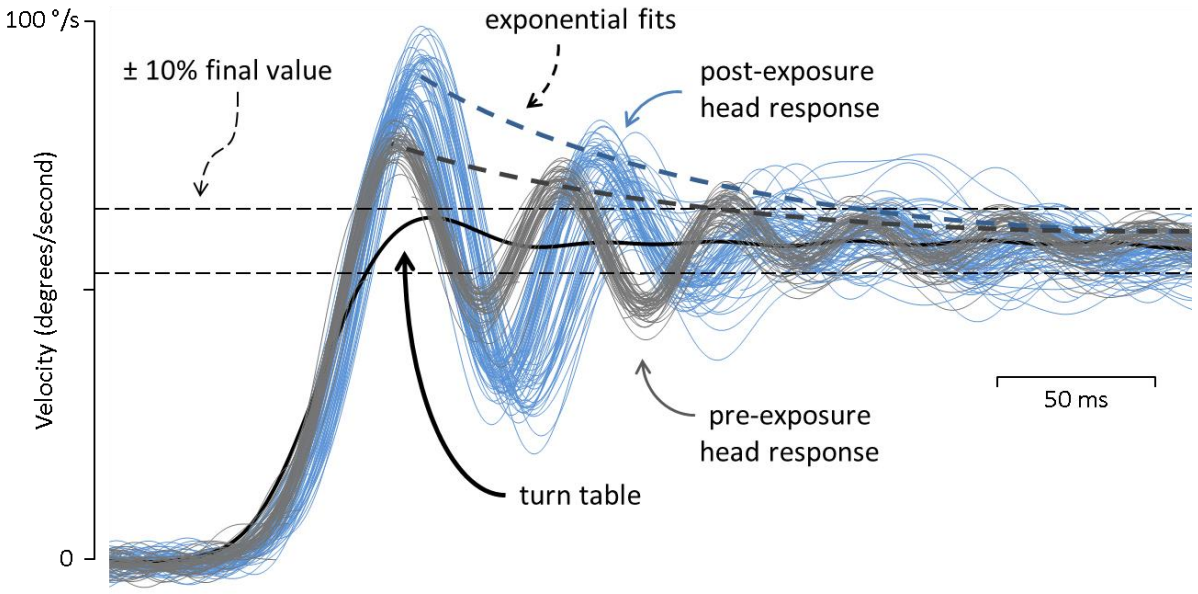

Figure 3.1 – Example head velocity responses before and after noise exposure

Animals are rotated on a turn table which produces a step in velocity (black trace). The head response as a second-order system both before (grey) and after (blue) noise exposure. However, after noise exposure, percent overshoot increases and becomes more variable. There is also a noticeable decrease in frequency of ringing.

As mentioned in the introduction, Peng and colleagues found that without a VCR there was decreased damping of the head in response to body rotations (Peng et al., 1996). This presented as increased overshoot, decreased frequency of oscillations, decreased damping coefficient, and increased settling time. In accord with Peng's model, we found that percent overshoot significantly increased from 43% to 48% (p=0.001) and frequency of head oscillations significantly decreased from 13.1Hz to 12.4Hz (p=0.002). However, we also found that the damping coefficient significantly increased from 0.07 to 0.08 (p=0.02) and that settling time showed no significant change (p=0.78).

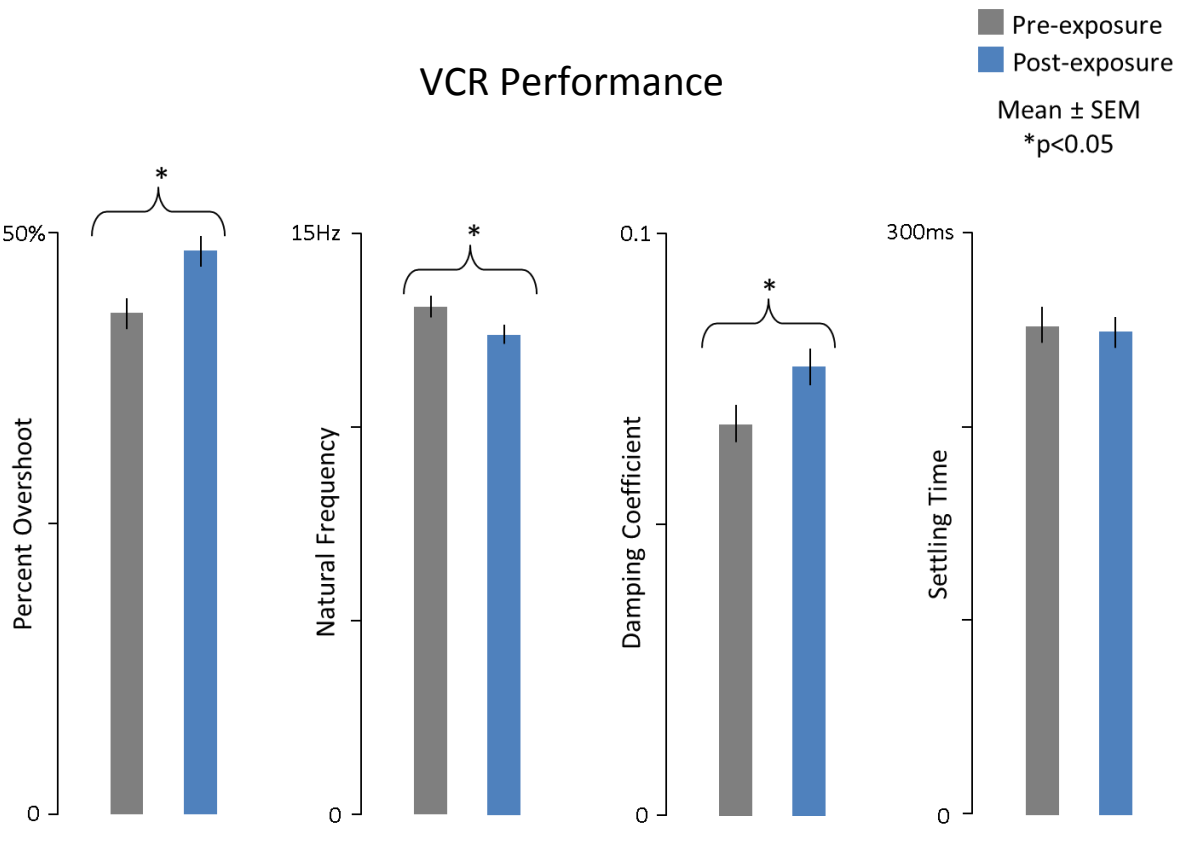

Figure 3.2 – Vestibulocollic reflex performance before and after noise exposure

Vestibulocollic Reflex was assessed before and after noise exposure. We found a significant increase in percent overshoot, significant decrease in natural frequency, and significant increase in damping after noise exposure. However, no change in settling time was observed.

To characterize, VOR performance we compared eye velocity to head velocity during passive body rotations. In Figure 3.3, we present head and eye velocity data from multiple trials of all three step sizes. Each point is the peak head and eye velocity for a single trial. We also include a linear fit to both the pre- and post-exposure data, the slope of which is an approximation of VOR gain. Before noise exposure (grey) the VOR gain for this animal is approximately -0.63 which then drops to -0.11 after noise exposure (blue). There is also a noticeable increase in variability of eye velocity after noise exposure.

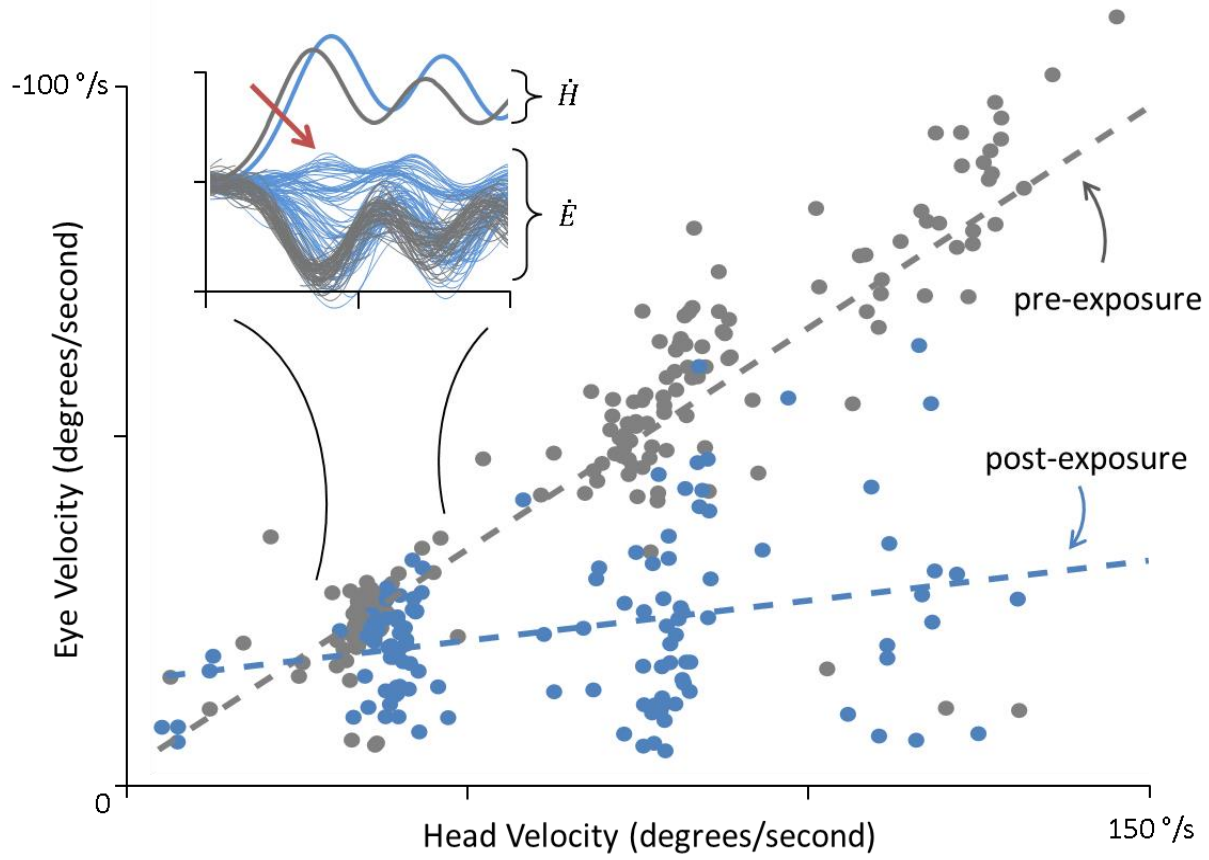

Figure 3.3 – Example vestibular-ocular reflex data before and after noise exposure

A perfect VOR would produce eye movements equal to head movements and thus a slope of 1.0. This animal has a VOR of 0.63 before exposure (grey) which drops to 0.11 after noise exposure (blue). There is also a noticeable increase in variability after noise exposure. Detail is of head velocity (***Ḣ***) and eye velocity (***Ė***), the red arrow points out trials where eye movement was anti-compensatory

As shown in Figure 3.4, we found that across all animals, the gain decreased from -0.56 to -0.50 (p=0.003) and latency increased from 13.7 to 16.3ms (p=0.003). An increase in latency may be due to several factors. The most obvious is an increase in detection threshold such that head velocity must reach a higher value before the eye begins to move. However, we also note that along with an increased latency there is the occasional anti-compensatory eye movement (i.e. the eye moves in the same direction as the head) as pointed out in the inset of Figure 3.3. As the VOR cannot produce anti-compensatory eye movements, we believe they are the result of the

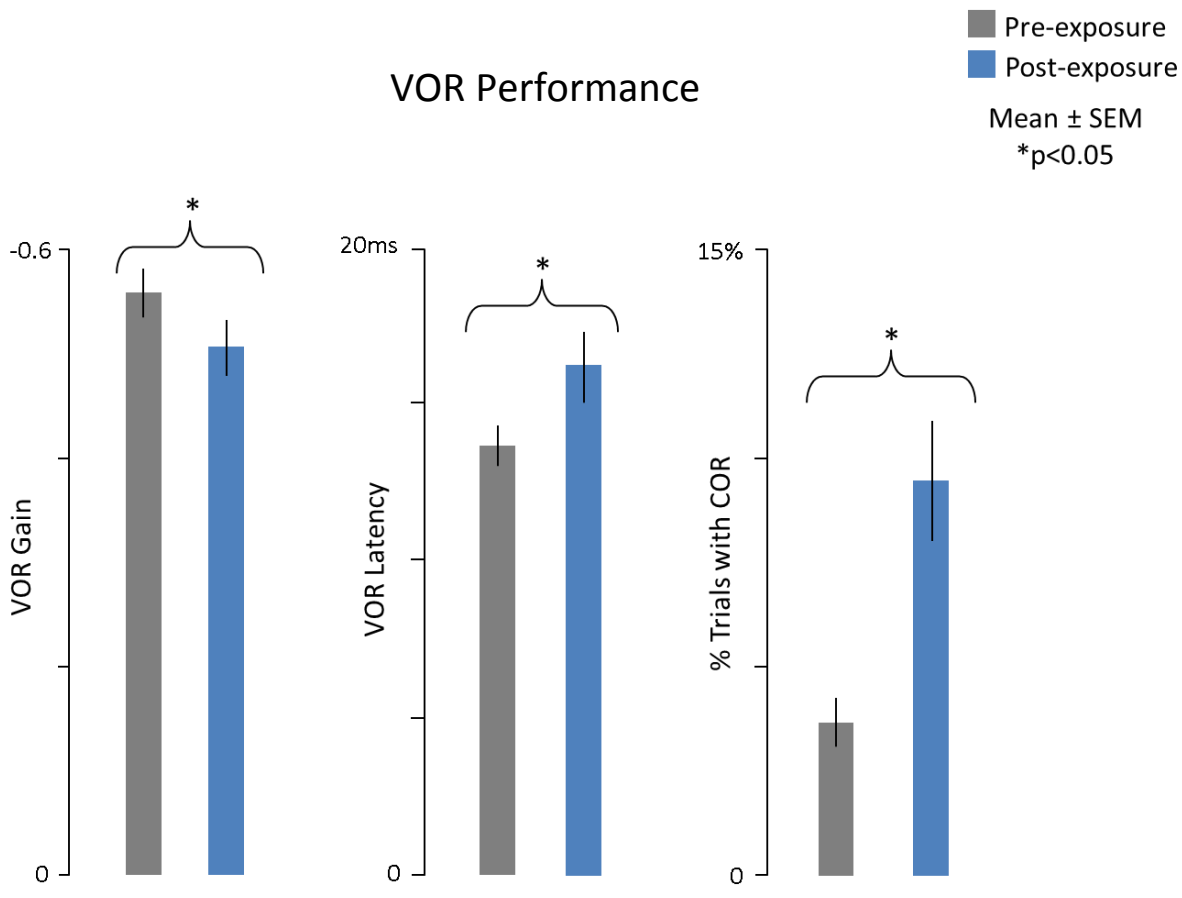

Figure 3.4 – Vestibular-ocular reflex performance before and after noise exposure

We measure ocular stability before (grey) and after (blue) noise exposure. After noise exposure (blue) there was a significant decrease in VOR gain, significant increase in VOR latency, and significant increase in trials with a COR

cervico-ocular reflex COR. To quantify the COR's influence, we calculated the number of trials during which gaze velocity (i.e. eye in space velocity) exceeded head velocity as this could only occur if there were an anti-compensatory eye movement. We found the percent of trials where this was observed significantly increased from 3.6% to 9.5% ($p<0.001$) as seen in Figure 3.4.

As mentioned above, while characterizing the VOR and VCR, we noticed that along with decreased performance, there was an increase in variability. Previous studies of vestibular loss have also noted increased variability of responses in addition to reduced sensitivity (Cousins et

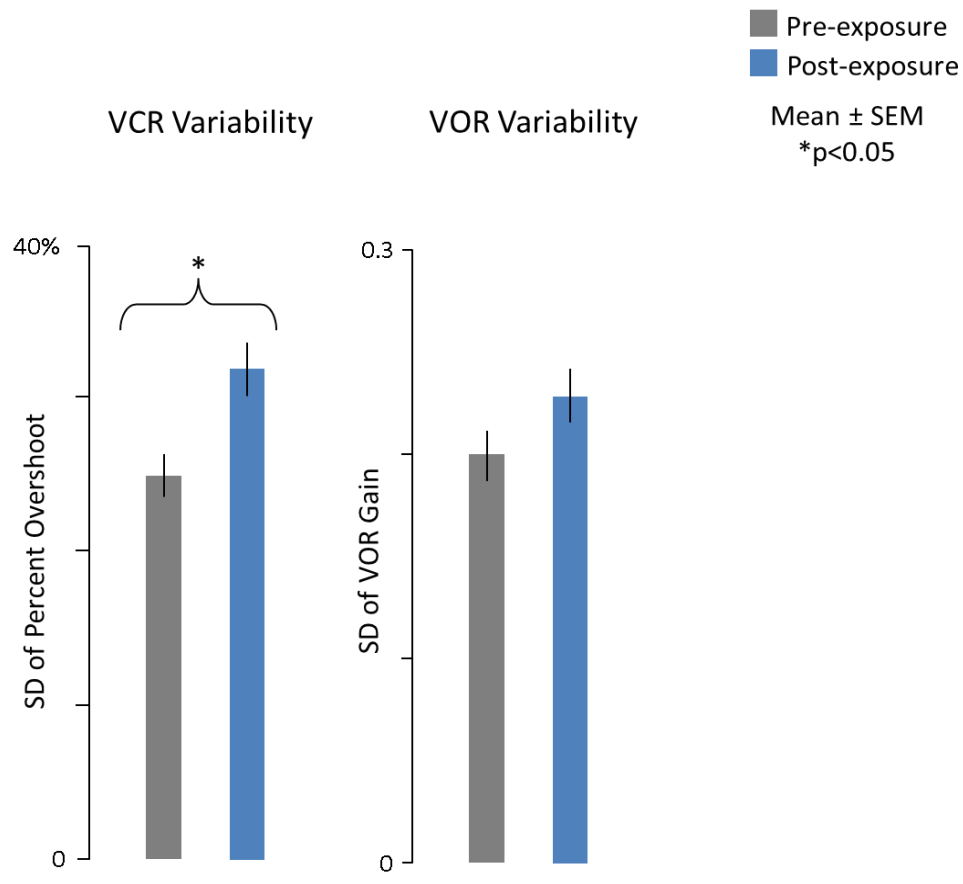

Figure 3.5 – Variability in the vestibular-ocular and vestibulocollic reflexes

Variability in both reflexes was measured before (grey) and after (blue) noise exposure. We found a significant increase in variability in the VCR pathway and a nearly significant ($p=0.062$) increase in the VOR pathway.

al., 2013; Jamali et al., 2014). Thus, we sought to quantify variability in each pathway before and after noise exposure. For the VCR pathway, we used the standard deviation of head velocity peak for each animal, each day, and found that it increased from 25% to 32% ($p<0.001$). In the VOR pathway, we used standard deviation of gain and found that variability increased after noise exposure from 0.2 to 0.23, although this did not reach statistical significance ($p=0.062$).

3.5 Discussion

The goal of this study was to investigate the effect a single high-intensity noise exposure on the semi-circular canals. To do this, we examined two of the major canal-driven reflexes: the vestibular-ocular reflex (VOR) and the vestibulocollic reflex (VCR). We suspected that the VCR would show greater deficits as it is thought to be predominately mediated by irregular afferents, which are more susceptible to noise damage (Stewart et al., 2017b), while the VOR is thought to be primarily mediated by regular afferents. However, as there is evidence that in the guinea pig the VOR is also influenced by irregular afferents, we examined reflex performance and response variability of both pathways (Shanidze et al., 2012).

We found that the gain of the VOR in healthy, pre-exposed animals was -0.55 in agreement with previous reports for this species (Ris et al., 1995b; Shanidze et al., 2010a) and the latency was 13.7 ms similar to what others have found using this technique (Della Santina CC et al., 2002). For the VCR, the damping ratio was 0.07 which is considerably lower than that found in humans and cats (0.3-0.8; Guitton et al., 1986; Peng et al., 1996). However, this value is still within the range of under damped systems, which is the dominant feature of head and neck dynamics across all three species. The natural frequency in guinea pig was considerably higher than that of

humans (13 Hz vs. 2-3Hz; Keshner and Peterson, 1995; Peng et al., 1996). However, Shanidze et al. (2010) found resonance-like behavior in guinea pig at roughly 10Hz, suggesting that the head dynamics of this species might simply give rise to a relatively high natural frequency.

To describe the relative contributions that the head plant and VCR make to head stability, Peng used several time- and frequency-domain parameters (Peng et al., 1996). The parameters which showed the greatest change in the absence of the VCR were: increased percent overshoot, decreased natural frequency, decreased damping ratio, and increased settling time. We found a similar increase in the percent overshoot and decrease in natural frequency after noise exposure. However, we also found a significant increase, not decrease, in the damping ratio. Further, this increase in damping appears to have negated the effect of the increased overshoot resulting in no significant difference in settling time. The increase in damping may be due to a heightened cervico-collic reflex (CCR). According to Peng's model, the CCR's main contribution to head stability is an increase in damping. Without testing the cervical pathway directly, we can't say for certain if this is the case, however, an increased contribution of neck proprioceptive pathways has a precedent in ocular stability, as will be discussed below.

To characterize the VOR we used gain and latency. After noise exposure, the gain of the VOR decreased roughly 10% (from -0.56 to -0.5), which, while small, was significant. This conflicts with much of the previous research, which has found that 1) the VOR pathway is primarily mediated by regular afferents and 2) that noise primarily damages irregular afferents. If both of these assertions are true, one would suspect that noise overstimulation would have no effect on the VOR. However, there is supporting evidence that, at least in the guinea pig, the VOR

pathway might be less homogenous than previously reported. Shanidze et al. (2012) found that during GVS, which silences irregular afferents, the VOR decreased by roughly 30%, suggesting that a substantial proportion of the VOR pathway in guinea pig is made of up of irregular afferents or that irregular afferents have a proportionately greater influence on the reflex.

We also found that noise exposure led to a significantly increased latency in the VOR. When we examined data more carefully, we hypothesized that this increase in latency was a result of the cervical-ocular reflex (COR) interfering with the VOR. Briefly, the COR works to stabilize gaze by producing eye movements that are in the opposite direction of neck rotation (Bronstein and Derrick Hood, 1986). During most head movements, the head and neck rotate in the same direction so that the COR and VOR work together. However, in our paradigm, the body is rotated under the head and, due to its inertia, the head initially lags behind the body, causing a neck rotation in the opposite direction of head rotation. To illustrate this point, consider when the turntable rotates to the right. The head will initially remain still in space, thus the neck is stretched to the left and the COR produces a right-ward eye movement. When the head does begin to move, it rotates to the right and the VOR produces a left-ward eye movement opposing the COR. Many who have investigated the COR have found that in healthy animals, the gain is very low compared to the VOR but that after vestibular lesion it is enhanced (Bronstein and Derrick Hood, 1986; Dichgans et al., 1973; Sadeghi et al., 2012). Thus, in our pre-exposure animals, the VOR dynamics are still dominant. However, after noise exposure the decrease in VOR gain and presumptive increase in COR gain would allow the COR to briefly cancel or even overpower the VOR such that eye movements might appeared delayed or anti-compensatory as seen in the inset of Figure 3.3. Indeed, we found that the number of trials in which gaze velocity

exceeded head velocity, which could only occur if there were an anti-compensatory eye movement, almost tripled after noise exposure (Figure 3.4), suggesting that the COR is enhanced after noise exposure, similar to other vestibular lesions.

Finally, we characterized the variability of each reflex before and after noise exposure. Previous research in has shown that there is an overall increase in detection thresholds in vestibulopathic subjects (Cousins et al., 2013; Jamali et al., 2014). This manifests as decreased sensitivity as well as increased variability, even if only irregular afferents are lost (Sultemeier and Hoffman, 2017). We found that along with decreased performances in the VOR and VCR, there was an increase in variability. This further suggests that high-intensity noise exposure affects the vestibular system in ways consistent with more traditional lesions.

There are several limitations to this study. First, histology was not performed until after animals had received five noise exposures (four additional exposures after the one used for this study) over the course two and a half months. Although we found no obvious loss of hair cells, it's possible that over the time course of the study, damage to hair cells may have recovered. Additionally, we did not test for synapse loss. Thus, we cannot say with certainty what the mechanism of vestibular loss was in these animals. However, Stewart (2017) reported in rats that after a similar high-intensity noise exposure there was a significant decrease in the proportion of calyx-only irregular afferents, although no significant loss of hair cells. They also found a concomitant decrease in head stability (Stewart et al., 2017a), similar to what we saw in our study. Thus, there is a precedent for vestibular synaptopathy as a pathology following noise over-exposure, which is also associated with loss of head stability.

Second, an equally important function of vestibular irregular afferents, that was not tested here, is their contribution to VOR compensation and adaptation via the "phasic pathway". The phasic pathway, while making little contribution to the VOR in healthy subjects, becomes critical after lesion (Cullen et al., 2009; Lasker et al., 2000; Minor and Lasker, 2009). This means that damage to irregular afferents, such as that done by noise, causes a two-fold injury to the VOR: diminishing its performance and then limiting its ability to adapt to this dysfunction. On the other hand, Sadeghi et al. (2007) found that in response to labyrinthectomy, there was an increase in the proportion of irregular afferents, potentially aiding adaptation. As adaptation is a critical component of the vestibular system, these findings emphasize the need to examine if, and how, noise damage affects this process. However, for this study we only recorded from animals for up to two weeks after exposure and did not explicitly test VOR adaptation, thus the effect of noise damage on VOR adaptation remains an open question.

Despite these limitations, the current study provides evidence that a single high-intensity noise exposure can cause significant functional damage to the semi-circular canals. After noise exposure, there is a decrease in performance and increased variability in the VOR and VCR pathways. Further, we present evidence suggesting that in response to vestibular loss, neck proprioceptive pathways (i.e. COR and CCR) are enhanced to compensate for deficits in the VOR and VCR respectively. Taken together, these findings demonstrate not only that noise overstimulation damages the semi-circular canals, but that this damage is functionally similar to other, more traditional, types of vestibular loss.

Chapter 4: A Shared Neural Integrator for Human Posture Control

4.1 Abstract

Control of standing posture requires fusion of multiple inputs including visual, vestibular, somatosensory, and other sensors, each having distinct dynamics. The semicircular canals, for example, have a unique high-pass filter response to angular velocity, quickly sensing a step change in head rotational velocity followed by decay. To stabilize gaze direction despite this decay, the central nervous system supplies a neural "velocity storage" integrator, a filter that extends the angular velocity signal. Similar filtering might contribute temporal dynamics to posture control, as suggested by some state estimation models. However, such filtering has not been tested explicitly. We propose that posture control indeed entails a neural integrator for sensory inputs, and test its behavior with classic sensory perturbations: a rotating optokinetic stimulus to the visual system and a galvanic vestibular stimulus to the vestibular system. A simple model illustrates how these two inputs and body tilt sensors might produce a postural tilt response in the frontal plane. The model integrates these signals through a direct weighted sum of inputs, with or without an indirect pathway containing a neural integrator. Comparison with experimental data from healthy adult subjects (N=16) reveals that the direct weighting model alone is insufficient to explain resulting postural transients, as measured by lateral tilt of the trunk. In contrast, the neural integrator, shared by sensory signals, produces the dynamics of both optokinetic and galvanic vestibular responses. These results suggest that posture control may

involve both direct and indirect pathways, which filter sensory signals and make them compatible for sensory fusion.

4.2 Introduction

Human posture control relies on a combination of visual, vestibular, somatosensory, and other sensory information (Young 1984). The combination of multiple inputs makes posture relatively robust to sensory and physical perturbations. For example, when a standing person is presented with a visual field (optokinetic stimulus) that rotates about the roll (naso-occipital) axis, they will usually begin to lean in the direction of rotation but stop short of falling over (Keshner and Kenyon, 2000; Tanahashi et al., 2007). Other sensors provide additional references for body tilt that fuse with, and in part contradict, the visual input, so that the steady-state tilt appears to be a compromise between the various inputs. Another feature of the response is that it is gradual rather than immediate. A step change in the angular velocity of visual input initiates a change in body pose, which only reaches steady-state after ten or more seconds (Dichgans and Brandt, 1978). This resembles a low-pass filter response, suggesting that the central nervous system (CNS) may filter incoming sensory signals. It is unknown, however, what form this filter might take, and whether it is even necessary to explain the behavior. Perhaps the dynamics of the sensors themselves are sufficient to explain the behavior without invoking a higher-order process. To resolve this question, we propose two models of sensory integration, with and without a filter. We compare model predictions to experimental data to determine whether filtering can explain how humans combine sensory information.

Evidence of CNS filtering is also observed in postural responses to a vestibular stimulus. Galvanic vestibular stimulation refers to a direct current applied to the mastoid processes that affects the vestibular nerve (Fitzpatrick and Day, 2004b; e.g., Nashner and Wolfson, 1974). A step change in current produces a postural response somewhat complementary to that of optokinetic stimulus, such that the body immediately tilts to the side. If the step is prolonged, this is followed by a gradual return to upright stance (Figure 4.1), again taking some tens of seconds (Fransson et al., 2003; e.g., Séverac Cauquil et al., 1998), reminiscent of the optokinetic response. This cannot be explained by the step stimulus, which is immediate, nor by the

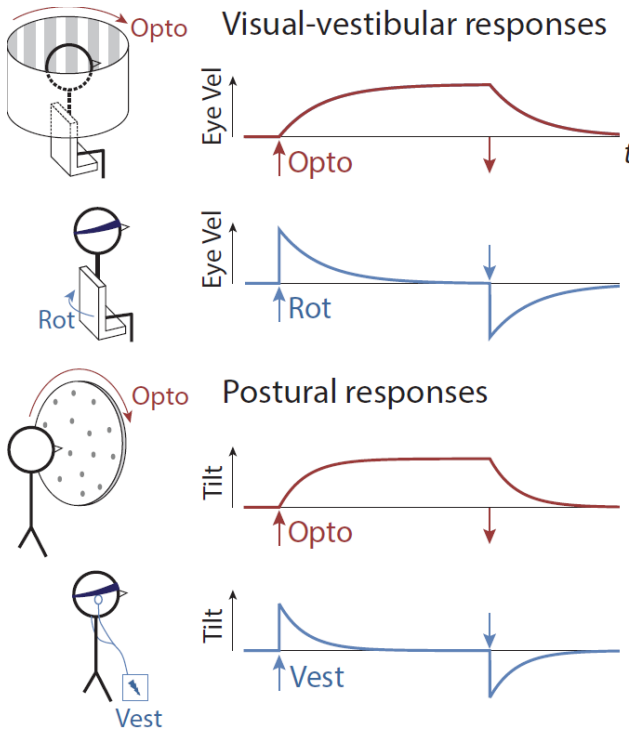

Figure 4.1 Conceptual comparison of ocular and postural responses

Ocular and postural responses to two types of sensory perturbations: optokinetic and vestibular Visual- stimulus is a step in angular velocity applied optokinetically (Opto) with a rotating visual field. Vestibular stimulus is either physical, with a rotating (Rot) chair,or a step in direct current of galvanic vestibular stimulus (Vest). Response is compensatory eye movements or trunk tilt

dynamics of vision and the somatosensors, which also have relatively faster dynamics and time delays (Young 1981, 1984). The semicircular canals do have slower, high-pass filter characteristics, where a step change in angular velocity causes a sudden response that decays with a time constant of about 7 seconds (Cohen et al., 1981; Robinson, 1981). However, galvanic vestibular stimulation appears to act on the vestibular nerve rather than the canals, (Goldberg et al., 1984), suggesting that the slow return here is attributable to the CNS rather than the dynamics of the semicircular canals.

Similar concepts of CNS filtering have long been applied to the stabilization of gaze (Figure 4.1, visual-vestibular responses). Head rotations normally produce feedback from both visual and vestibular systems, which then drive compensatory eye movements. A step in rotational velocity of the visual field alone (optokinetic stimulus without head rotation) produces eye movements that only gradually match the stimulus velocity, similar to a low-pass filter with a time constant of approximately 20 seconds (Robinson, 1981). A complementary behavior occurs in response to a step change in angular velocity of the head, without visual input (e.g., vestibular stimulus alone). The compensatory eye movements resemble a decaying exponential, similar to a high-pass filter with the same time constant as the optokinetic response (Raphan et al., 1979). Both responses are explained by a single model, where the eye velocity command is produced by visual and vestibular signals feeding through a direct pathway, which directly sums the signals, as well as an indirect pathway into a shared neural integrator, or velocity storage unit (Cohen et al., 1981). Both pathways converge to act as a filter (Robinson, 1981), such that vestibular signals, especially sensitive to high-frequency information, are high-pass filtered, whereas visual

signals are low-pass filtered. In the veridical case where both inputs are present, the two complementary responses sum to an almost immediate, step-like compensatory eye movement.

A number of theoretical frameworks predict such neural integration by the CNS. Velocity storage for gaze stabilization is predicted by optimal state estimation models, where an internal model of head and sensor dynamics is used to estimate head tilt and rotation with minimum error (Borah et al., 1988b; Merfeld et al., 1999; Ormsby and Young, 1977), subject to assumed noise distributions. These have since been extended to broader approaches such as Bayesian estimation (Green and Angelaki, 2010), as well as computational approaches such as particle filters (Karmali and Merfeld, 2012; Laurens and Droulez, 2007; Paulin, 2005) for arbitrary probability distributions. These may be considered generalizations of state estimation theory that can predict an even greater variety of behaviors.

It is conceivable that posture control could incorporate neural integration similar to visual-vestibular responses (Figure 4.1, Postural responses). Similar models of control and estimation (Goodworth and Peterka, 2012; Kiemel et al., 2011; Kuo, 1995, 2005) have long been applied to posture, and the associated CNS filtering suggests a need for neural integration analogous to the velocity storage integrator. However, postural responses have not typically been characterized in terms of simple time constants, and the models have yet to be tested in terms of such simple perturbations and responses. For posture control, only visual input is directly amenable to experimental perturbations (Keshner and Kenyon, 2000; Nashner et al., 1989b; Tarr and Warren, 2002). Vestibular inputs may be perturbed with galvanic vestibular stimulation (Goldberg et al., 1984), and somatosensory inputs with vibration (Kavounoudias et al., 2001; Lee et al., 2012,

2013a, 2013b), but the physiological interpretation of such inputs is less certain. Further insight may require more complex inputs (e.g., a combination of inputs with sway-referencing). As a result, there is little evidence of neural integration in posture, in contrast to the well-documented velocity storage phenomenon observed in eye movements (Cannon and Robinson, 1987; Mcfarland and Fuchs, 1992; Yokota et al., 1992).

The present study examines the fusion of sensory information for posture control, with and without a hypothesized neural integrator circuit. The simplest means of fusion would be to form a direct weighted sum of the inputs from the sensory systems to produce a body tilt response without filtering. This is contrasted with an indirect pathway through a shared integrator, which affords the ability to perform low- and high-pass filtering, not unlike the integrator for gaze stabilization. Here we compare these alternatives, using simple models of the sensory system dynamics, including vision, the semicircular canals, and combined tilt information from somatosensors, otoliths, and other modalities. To test the model, we perform an experiment where stimuli are applied to the visual and vestibular systems, and the resulting body tilt responses are examined. We thus seek to test whether posture control shows evidence for shared neural integration analogous to that long observed in visual-vestibular responses.

4.3 Model

We propose two alternative models for CNS processing of sensory information (Figure 4.2): A *Neural Integrator model* and a *Direct Weighting model*. The first feeds the afferent signals through two pathways, termed direct and indirect, each forming a weighted sum (linear combination) of inputs, but with the latter also passing through a neural integrator. Both

pathways converge and add together to produce the tilt estimate. The Direct Weighting is a simpler alternative, dispensing with the indirect pathway and integrator. Both models receive input from three sensory modalities—vision, semicircular canals, and body tilt sensors—each modeled with very simple dynamics (Figure 4.2), so that sensor and CNS processing together determine the overall behavior. We examine these behaviors in the context of two types of

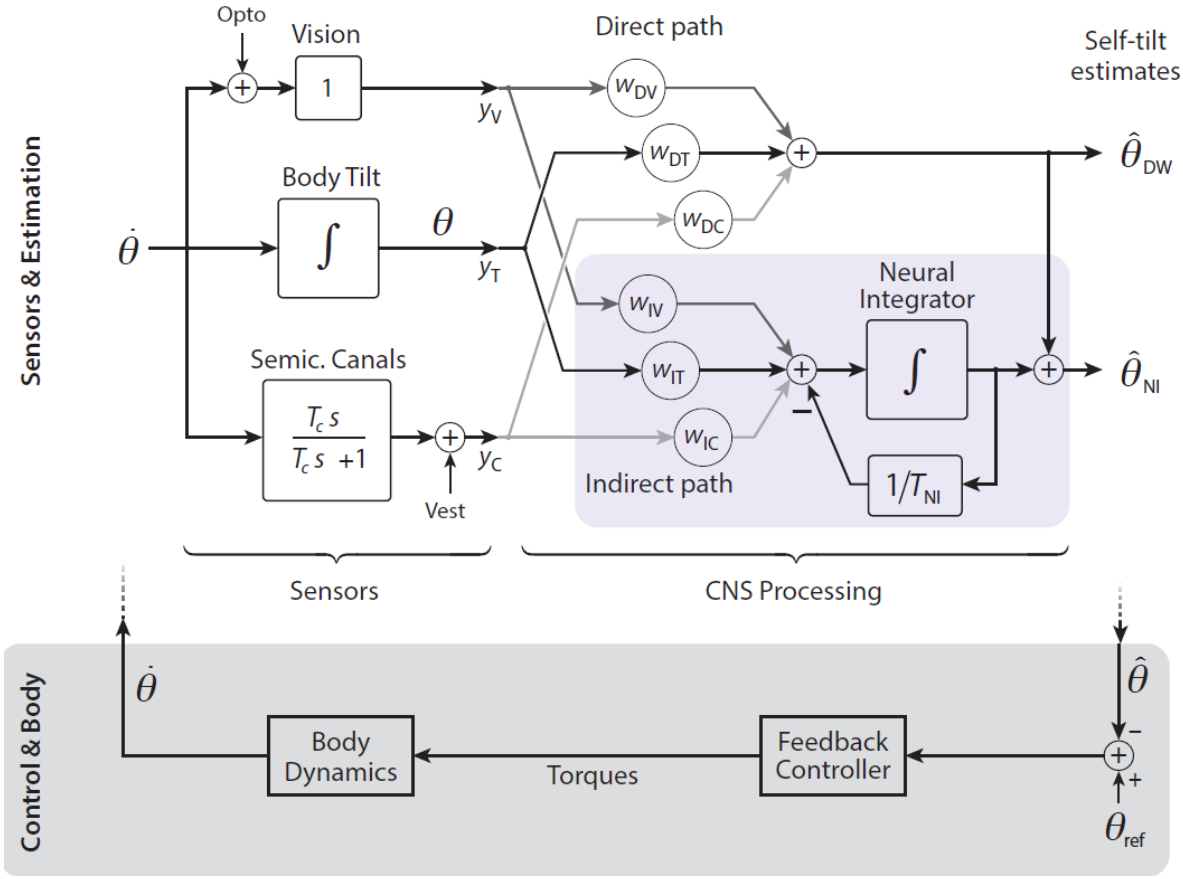

Figure 4.2 Simple model of sensors and sensory processing for posture control.

Angular velocity $\dot{\theta}$ of the body is transduced by vision, body tilt sensors (somatosensors, otoliths) and semicircular canals. Sensory processing is modeled with two pathways, Direct and Indirect. The Direct path is a weighted sum of the sensory data, whereas the Indirect path (shaded area) augments a weighted sum with a Neural Integrator using negative feedback. The tilt estimate $\hat{\theta}_{\mathrm{NI}}$ is produced from the sum of both direct and indirect paths. A simpler alternative Direct Weighting model uses only the Direct path $\hat{\theta}_{\mathrm{DW}}$. Vision and canals are subject to external perturbations, Opto and Vest, respectively.

stimuli, optokinetic and galvanic vestibular stimulation. The two models are used to determine the simplest possible system that can explain the observed postural behaviors.

We model the sensors with linearized dynamics. We treat vision as having proportional sensitivity to the angular velocity of the visual field (Dichgans et al. 1972; Cohen et al. 1981; Young 1984), and the semicircular canals as having first-order high-pass filter characteristics with time constant approximately $T_c = 7$ s (Cohen et al., 1981; Robinson, 1981). Tilt refers to sensors such as somatosensors and otoliths, which contribute sensitivity to the vertical through reference to ground or gravity (e.g., Burgess and Perl, 1973; Peterka and Benolken, 1995). We treat the dynamics of such sensors as much faster than the observed postural response (Agarwal and Gottlieb, 1984; Young and Meiry, 1968), and therefore lump them into a composite tilt sensor with constant gain.

The sensory outputs feed into the CNS processing model to produce a tilt estimate. This refers to a hypothesized internal CNS representation $\hat{\theta}$ of the body's tilt, which is not directly measurable but rather indirectly revealed by the body's actual tilt θ, in an attempt to align the body with vertical. The actual body motion results from CNS control (not modeled explicitly; see Figure 4.2, bottom shaded area), acting on the internal tilt estimate. For simplicity, we ignore the closed-loop control dynamics, with the reasoning that the body can be controlled at much higher bandwidth than the postural responses resulting from the relatively slow dynamics of the semi-circular canals and sensory processing. This is analogous to the approach for eye movements, which often treat the control and eye dynamics as fast, relative to these same sensory/processing dynamics (e.g., Raphan et al., 1979; Robinson, 1981). (As a simple indication of body

bandwidth, we asked subjects to actively sway their bodies quickly from side to side, and observed a closed-loop natural frequency of 0.85 ± 0.38 Hz (mean ± s.d., N = 16), at least 20 times faster than the sensory processing bandwidth examined here.) We also presume that control actions feed an efference copy into the sensory processing system, so that self-generated movements do not themselves cause self-opposing postural responses. Another simplification is that we define a sign convention such that the angular motion of the visual field (e.g., clockwise direction), the internal estimate of body tilt (e.g., counter-clockwise direction), and the actual body tilt (e.g., clockwise direction) all have positive signs during the optokinetic response.

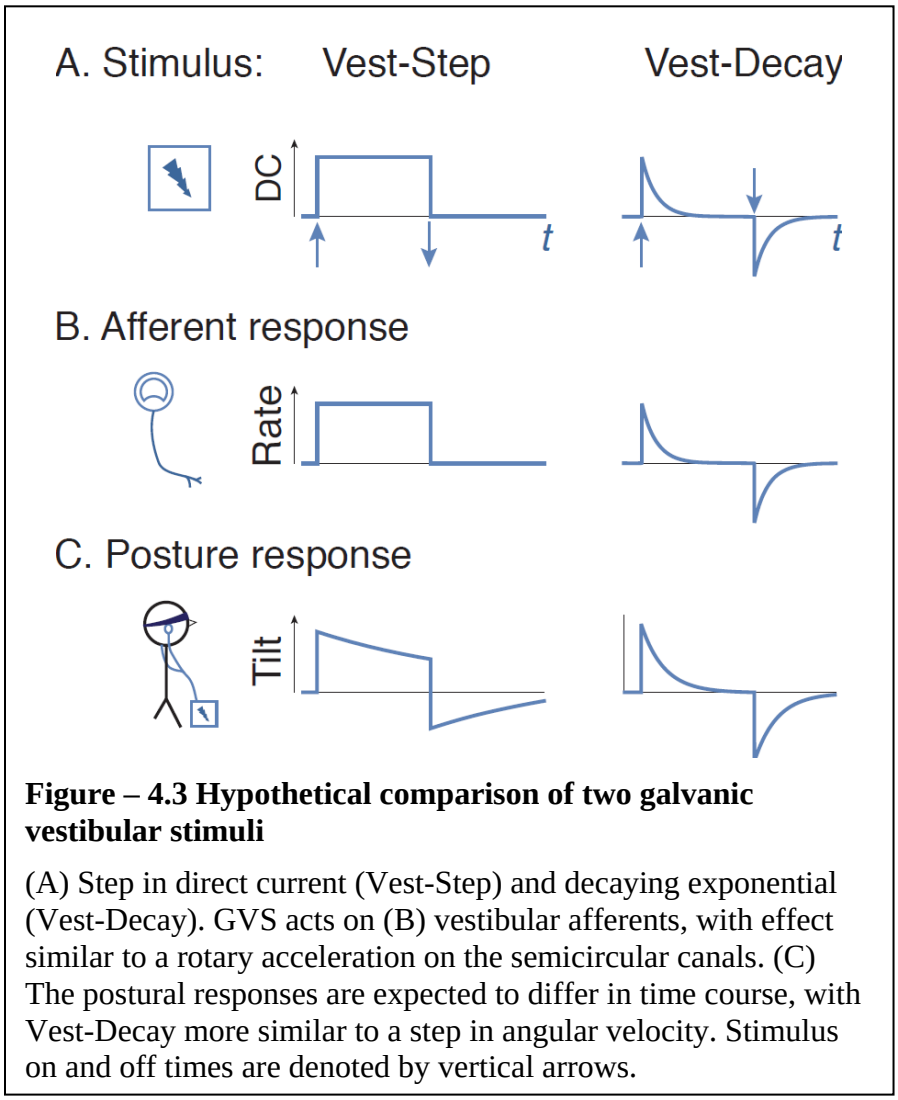

Figure – 4.3 Hypothetical comparison of two galvanic vestibular stimuli

(A) Step in direct current (Vest-Step) and decaying exponential (Vest-Decay). GVS acts on (B) vestibular afferents, with effect similar to a rotary acceleration on the semicircular canals. (C) The postural responses are expected to differ in time course, with Vest-Decay more similar to a step in angular velocity. Stimulus on and off times are denoted by vertical arrows.

We next consider the tilt estimates that arise from the two models. For each model, there are four stimuli of interest: optokinetic step input (Opto-Step), galvanic vestibular stimulation with a step change in current (Vest-Step), galvanic vestibular with an exponential decay (Vest-Decay), and veridical tilt shift. Stimulus Opto-Step refers to a step change in the visual field angular velocity, which results in a gradual (low-pass filter) shift in tilt. Stimulus Vest-Step (Figure 4.3) refers to a step change in direct current applied to the vestibular nerve, which appears to act on the primary afferents, bypassing the canal dynamics (Goldberg et al., 1984). Stimulus Vest-Decay is a variation on the tradition step waveform, where the stimulus is applied with an exponential decay with time constant T_c. The rationale is that the standard constant-current galvanic stimulus might be considered non-physiological, because it corresponds to a physical stimulus of sustained angular acceleration, rarely encountered on earth. Thus, Vest-Decay is intended to crudely model the equivalent of a step change in angular velocity (Cohen et al., 1981), for which the canal afferents would normally produce an exponentially decaying response. Finally, veridical shift refers to a step change in body tilt that affects all three sensory systems together, as might occur with a physical rather than purely sensory perturbation. The present experiment does not apply such a perturbation, but it is expected that humans should rapidly and correctly sense self-tilt in the absence of any sensory conflict.

Application of these stimuli to the models reveals several key features (Table 4.1). The Neural Integrator model only requires indirect pathways for vision and canal inputs to produce tilt responses that roughly approximate the expected experimental responses: An exponentially decaying shape for Opto-Step and Vest-Step inputs (which can each increase or decrease depending on separate weights), an additional exponential (with the time constant T_c) for Vest-

Decay, and a faster, step-like shift for Veridical shift. The corresponding direct weights (w_{DV} and w_{DC}) are therefore treated as zero in the Neural Integrator model henceforth as they only serve to offset responses. In contrast, the Direct Weighting model cannot reproduce the observed optokinetic response dynamics. In response to an Opto-Step stimulus the Direct Weighting model yields a step change in tilt, rather than the low-pass filter response of humans. In addition, the veridical stimulus produces a shift in tilt in the model, but with a relatively slow exponential decay due to the canal time constant, whereas the human veridical response would be expected to be quite fast. The direct pathways for semicircular canals and visual input are particularly problematic, because non-zero weightings would imply an unrealistically impulsive shift. Both models, particularly the Neural Integrator model, produce the expected high-pass filter response for galvanic stimulus. These observations are the case regardless of parameter values, which are also to be determined from experimental data to further test the models.

A. Neural Integrator (NI)

Stimulus	Input	Tilt response
Opto-Step	$\dot{\theta}_{\mathrm{OK}} = 1$	$w_{\mathrm{DV}} + w_{\mathrm{IV}} T_{\mathrm{NI}}(1 - e^{-t/T_{\mathrm{NI}}})$
Vest-Step	$\dot{\theta}_{\mathrm{GV}} = 1$	$w_{\mathrm{DC}} + w_{\mathrm{IC}} T_{\mathrm{NI}}(1 - e^{-t/T_{\mathrm{NI}}})$
Vest-Decay	$\dot{\theta}_{\mathrm{GV}} = 1e^{-t/T_c}$	$w_{\mathrm{DC}} e^{-t/T_c} + \frac{w_{\mathrm{IC}} T_{\mathrm{NI}} T_c}{T_{\mathrm{NI}} - T_c}(e^{-t/T_{\mathrm{NI}}} - e^{-t/T_c})$
Veridical shift	$\theta = 1$	$(w_{\mathrm{DC}} + w_{\mathrm{DV}})\delta(t) + (w_{\mathrm{DT}} + w_{\mathrm{IT}} T_{\mathrm{NI}}) + \frac{w_{\mathrm{IC}} T_{\mathrm{NI}}}{T_{\mathrm{NI}} - T_c} e^{-t/T_c} + \left((w_{\mathrm{IC}} - T_{\mathrm{NI}} w_{\mathrm{IT}}) - \frac{w_{\mathrm{IV}} T_c}{T_{\mathrm{NI}} - T_c}\right) e^{-t/}$

B. Direct Weighting (DW)

Stimulus	Input	Tilt response
Opto-Step	$\dot{\theta}_{\mathrm{OK}} = 1$	w_{DV}
Vest-Step	$\dot{\theta}_{\mathrm{GV}} = 1$	w_{DC}
Vest-Decay	$\dot{\theta}_{\mathrm{GV}} = 1e^{-t/T_c}$	$w_{\mathrm{DC}} e^{-t/T_c}$
Veridical shift	$\theta = 1$	$(w_{\mathrm{DC}} + w_{\mathrm{DV}})\delta(t) + w_{\mathrm{DT}} - \frac{w_{\mathrm{DC}}}{T_c} e^{-t/T_c}$

Table 4.1 Predicted responses from the neural integrator and direct weighting models.

Responses for four possible stimuli: A step in angular velocity of optokinetic field (Opto-Step), a step in galvanic vestibular input (Vest-Step), a decaying galvanic waveform (Vest-Decay) and the equivalent of a veridical positional shift in the body, detected by all sensors.

4.4 Experimental Methods

To test the models, we measured human postural tilt responses in the frontal plane evoked by three types of experimental stimuli. These included an optokinetic stimulus with a step change in visual field roll velocity (Opto-Step), galvanic stimulus with a step change in current (Vest-Step), as well as galvanic stimulus with an exponential decay in current (Vest-Decay) that was meant to mimic the dynamics of the canals (with an assumed time constant $T_c = 7$ s; see Model section for details). The postural responses were quantified in terms of the angular tilt of the trunk laterally from undisturbed quiet stance, as measured by motion capture markers at the base of the neck (near C7 vertebra) and at the pelvis (near L5). As an additional comparison measure, we also recorded lateral excursion of the center of pressure (COP). The time trajectories of trunk tilt were then used to determine best-fit parameter values for the models, with the resulting model trajectories compared against human responses.

Sixteen healthy young adults (22.8 ± 2.8 years old, 4 male, 12 female) were recruited for this study. Informed consent was obtained according to procedures approved by the University of Michigan Institutional Review Board. Subjects were excluded if they reported difficulty with standing, walking or balance, vision problems despite correction, a diagnosed neurological disorder, or if they had used medication or drugs that might impair balance. Subjects stood without shoes with their feet together (Romberg stance) and arms crossed. Kinematic data were recorded at 100 Hz using a passive motion tracking system (MotionAnalysis Corp.). For comparison with body tilt, center of pressure of ground reaction forces was recorded at 1000 Hz from an in-ground force plate (OR6-7, Advanced Mechanical Technology Inc., USA), with signals low-pass filtered with a 5 Hz cut-off frequency.

The optokinetic stimulus consisted of a computer-generated field of random dots displayed on a large projection screen in an otherwise dark room. The screen was curved to wrap around the subjects (O'Connor and Kuo, 2009), who stood about 0.6 m from its front, so that the field of view extended nearly 180 degrees in the horizontal plane, to reduce visual cues regarding vertical. Step changes in angular velocity were applied at speeds of 15 and 30 deg/s and in clockwise or counter-clockwise directions (all randomly selected). Each trial was 80 s long: 20 s pre-stimulus (no rotation, baseline), and 60 s per-stimulus (rotation). Each subject performed three repetitions of each trial type as well as three separate control trials with no stimulus.

Bilateral bipolar galvanic vestibular stimulation was applied to subjects standing with eyes closed in the dark room. Electrodes were placed on the mastoid processes to apply a direct current stimulus (Johansson et al., 1995; St George et al., 2011; Wardman et al., 2003b). Four trial types were defined based on the amplitude (0.25, 0.5 or 1.0mA) and waveform (Vest-Step and Vest-Decay) of the current. However, only two current amplitudes were used for each subject. Default values were 1.0 and 0.5mA, which were briefly applied as a pre-test. If a subject reported discomfort with 1mA, then 0.5 and 0.25mA were applied instead (for 6 of the 16 subjects). Each subject performed three repetitions of each trial type (12 experimental trials) as well as three control trials with no stimulus, for a total of 15 trials. The order of trial presentation and the direction of current (positive or negative) were randomized. These trials were 60 s long: 20 s pre-stimulus (no current), and 40 s per-stimulus (current).

The three repetitions for each trial type were averaged together and fit with exponential curves for comparison with the models. The trunk tilt trajectory of each trial was first normalized for

stimulus direction, by negating the data of the negative-stimulus trials. The mean of the pre-stimulus trunk tilt was also subtracted from the trial data as a baseline.

All model predictions were tested by least squares fitting to generic equations resembling the predicted waveforms $\theta(t)$ (Table 4.1) according to one or more terms of a sum of exponentials

$$\theta(t) = A_1 e^{-(t-\tau_d)/\tau_1} + A_2 e^{-(t-\tau_d)/\tau_2} + c \quad (1)$$

with fitting parameters A_1, A_2, τ_1, τ_2, and c, time delay τ_d relative to stimulus onset at $t = 0$ and upright position $\theta = 0$ (Please note, $\theta(t) = 0$ for $t < \tau_d$). Only the terms relevant to a particular combination of model and stimulus were included. For example, only a constant term *c* was predicted for the Direct Weighting (DW) model's Opto-Step response. A single exponential (one time constant and a constant term) was predicted for Neural Integrator (NI) Opto-Step and Vest-Step, and Direct Weighting Vest-Decay. Only the Neural Integrator Vest-Decay response included all of the terms above. Some fits yielded much longer time constants than the trials themselves, and those exceeding 100 s were considered extraneous and excluded from further statistical tests; 13 of the 192 fits performed (16 subjects x 6 trial types x 2 models) were removed for this reason. In addition, we also observed some cases (9 trials) of a resetting behavior for Opto-Step, similar to a periodic resetting reported previously for long stimulation durations (Dichgans and Brandt, 1978), but too small to warrant modeling its effect. These trials were not removed. The minimum mean-square error and residual sum-squared error were determined by nonlinear optimization (Matlab "fmincon", Mathworks, Natick, MA), and the Bayesian Information Criterion (BIC) was used to quantitatively compare the two models, with a difference of at least 10 considered strong evidence for a superior fit (Schwarz, 1978b).

4.5 Results

Subjects responded to the stimuli with postural responses that generally met expectations (Figure 4.4). Specifically, the Opto-Step response was a slow tilt of the trunk to a steady-state angle, like a low-pass filter. The Vest-Step response was a fast shift (toward the anode) followed by an exponential decay returning toward upright. The Vest-Decay response was similar, except with a somewhat faster decay. Individual curve fits were also performed for each subject's data,

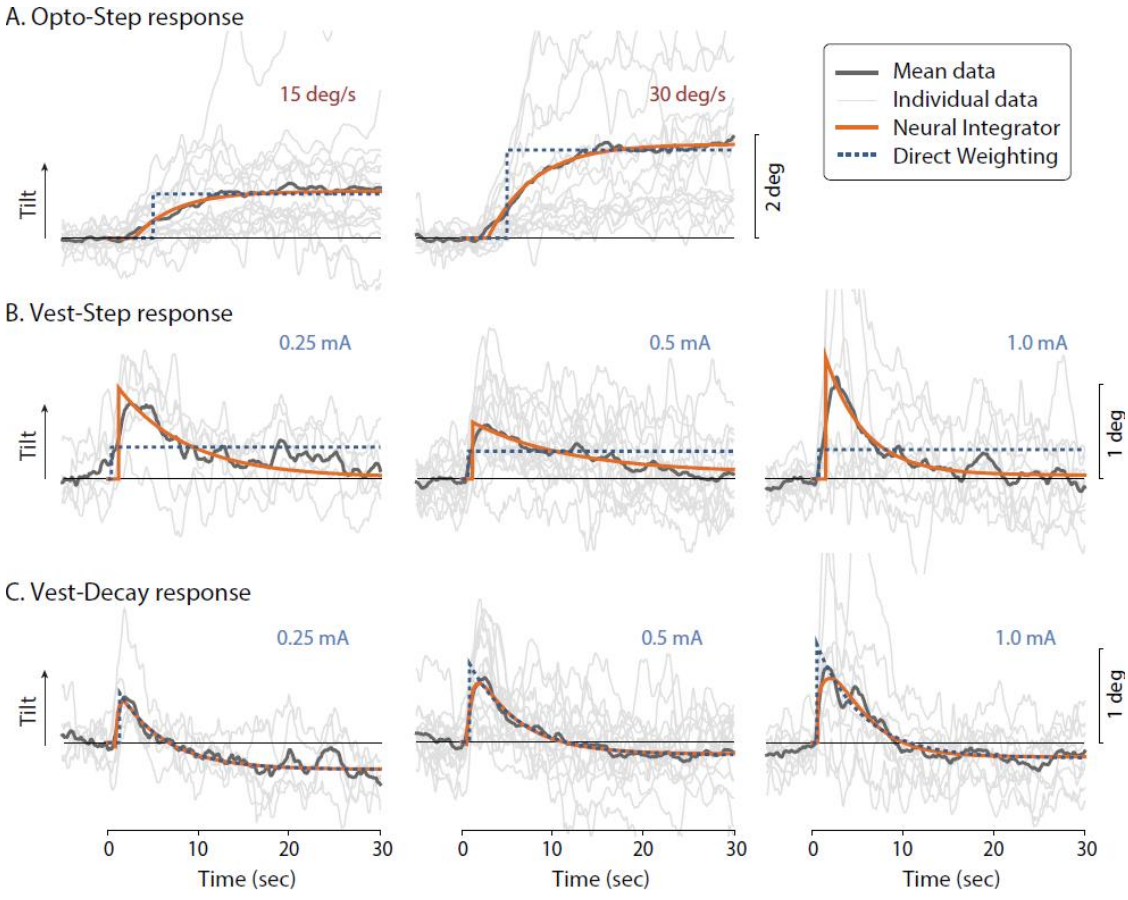

Figure 4.4 – Trunk tilt responses and model fits

(A) Optokinetic step (Opto-Step), (B) galvanic vestibular step (Vest-Step) in current, and (C) galvanic decaying exponential (Vest-Decay). Responses are averaged across all subjects ("Mean data," darker gray); also shown are each individual's responses averaged across trials ("Individual data," lighter gray). Model fits for Neural Integrator (solid lines) and Direct Weighting (dashed lines) are also shown, fitted to mean data.

summarized in Table 4.2. Additionally, we found the COP trajectories, expressed as lateral shift divided by leg length, to correlate well with trunk tilt θ; the correlation coefficient averaged 0.76 across all visual inputs, and 0.74 across all galvanic vestibular inputs. The COP data were not used to test any hypotheses, and therefore subsequent analyses concern only trunk tilt θ.

A. Neural Integrator (NI)

Stimulus	Ampl.	τ_1 (s)		A_1 (deg)		τ_2 (s)		A_2 (deg)		t_d (s)		c (deg)		MSE	BIC
		mean	s.d.	mean	s.d.	mean	s.d.	mean	s.d.	mean	s.d.	mean	s.d.	(x10^3)	
Opto-Step	15°/s	6.79	5.65	-0.99	0.83					2.52	1.85	0.99	0.83	80.78	-8131
	30°/s	9.70	9.01	-2.09	1.58					2.99	1.90	2.09	1.58	185.06	-6965
Vest-Step	0.25 mA	9.63	7.28	1.10	0.55					1.62	1.85	-0.12	0.31	58.72	-5152
	0.50 mA	6.13	6.64	0.73	0.69					0.99	0.65	0.11	0.46	65.49	-5156
	1.00 mA	7.85	7.17	1.51	1.60					2.55	1.63	-0.06	0.34	137.46	-4798
Vest-Decay	0.25 mA	5.78	4.50	1.91	1.14	1.76	2.26	-1.49	1.32	0.51	0.42	-0.34	0.21	36.94	-5773
	0.50 mA	3.75	3.16	2.55	2.07	0.77	0.40	-2.33	2.11	0.59	0.33	-0.10	0.26	36.17	-5960
	1.00 mA	3.55	2.79	3.53	2.20	1.30	1.11	-3.03	2.02	0.67	0.24	-0.26	0.40	85.76	-5403

B. Direct Weighting (DW)

Stimulus	Ampl.	τ_1 (s)		A_1 (deg)		τ_2 (s)		A_2 (deg)		t_d (s)		c (deg)		MSE	BIC
		mean	s.d.	mean	s.d.	mean	s.d.	mean	s.d.	mean	s.d.	mean	s.d.	(x10^3)	
Opto-Step	15°/s									4.32	0.99	0.79	0.65	120.77	-6772
	30°/s									4.84	0.45	1.76	1.20	296.50	-4290
Vest-Step	0.25 mA									0.38	0.33	0.40	0.33	173.41	-3888
	0.50 mA									0.70	0.34	0.35	0.32	115.57	-4512
	1.00 mA									0.67	0.31	0.38	0.49	282.43	-3435
Vest-Decay	0.25 mA	5.80	5.44	1.02	0.43					1.07	0.81	-0.29	0.13	38.86	-5687
	0.50 mA	3.38	1.56	1.20	0.58					1.37	0.71	-0.10	0.27	48.99	-5629
	1.00 mA	5.36	3.58	1.09	0.71					0.94	0.84	-0.18	0.22	65.95	-5429

Table 4.2 – Mean and standard deviation for model parameters across all subjects

Curve fit parameters for (A) Neural Integrator and (B) Direct Weighting models with three stimuli: Opto-Step, Vest-Step, Vest-Decay. Parameters were fit with nonlinear least squares to reveal time constants (τ_1 and τ_2), amplitudes (A_1 and A_2), offset (c), and time delay (t_d). Goodness of fit was measured using mean-square error (MSE; lower is better) and Bayesian Information Criterion (BIC; more negative is better).

The models differed considerably from each other in their ability to reproduce the observed responses (Table 4.2). For optokinetic inputs, the Neural Integrator model's slow time constant

of several seconds was necessary to capture the gradual postural shift exhibited by subjects (compare exponential decaying terms of subject data and NI model for Opto-Step in Fig. 4A; see also estimated values of τ_1 for Opto-Step in Table 4.2A). In contrast, the Direct Weighting model only includes an instantaneous tilt (compare subject data to DW model's step change in tilt in Fig. 4A; see also offset *c* with no exponential terms, Table 4.2B), and therefore could not reproduce the transient dynamics at all. The NI model also yielded considerably lower BIC values than DW (e.g., -8131 vs. -6772 for 15°/s visual stimuli), signifying a better fit while accounting for model parameters.

For galvanic vestibular inputs, the Neural Integrator model also better reproduced observed responses. In particular, its Vest-Step response exhibited an immediate tilt followed by a gradual return to upright with a relatively slow time constant, similar to the experimental findings (Vest-Step exponential decay for both human and NI model, Fig. 4B; see also τ_1 for Vest-Step in Table 4.2A). This response is not reproducible by the Direct Weighting model, which again only produces an instantaneous step change in tilt (DW model in Fig. 4B; offset *c* in Table 4.2B). The Vest-Step input also caused some subjects to exhibit a lingering trunk tilt for the duration of the stimulus (see offset *c* in Table 4.2), as also expected by the Neural Integrator model (constant w_{DC} for Vest-Step in Table 4.1A). For the Vest-Decay input, both models appeared more similar in reproducing the experimental response, because both models include at least one exponential, which was the gross feature dominating the observed human behavior. Some subjects also appeared to exhibit a lingering tilt in the opposite direction (offset *c* in Table 4.2, NI and DW Vest-Decay), which was not expected for either model (Table 4.1, DW and NI Vest-Decay). As

with visual stimuli, the NI model yielded considerably lower BIC values than DW, for five out of the six cases (e.g. -5156 vs -4512 for 0.5 mA Vest-Step).

Our model proposes that a single integrator could explain the responses to both visual and

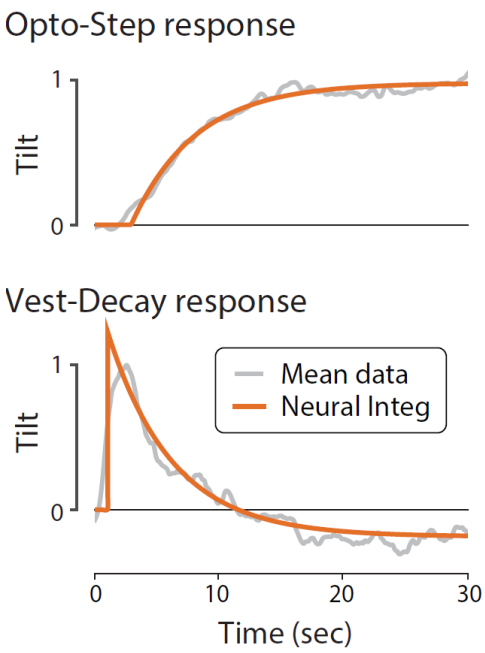

Figure 4.5 –Neural Integrator fit with a shared time constant

Experimental responses to optokinetic and galvanic vestibular decaying exponential inputs (Opto-Step and Vest-Decay) are fit with the proposed Neural Integrator response, constrained with a single time constant ($\tau_1 = 5.2$ s). Tilt data were normalized to unit amplitude

vestibular inputs. To illustrate the consequences of a shared neural integrator and to further test our hypothesis that Vest-Decay would complement Opto-Step, we also conducted an additional fit to the data, where both visual and vestibular responses (Opto-Step and Vest-Decay) were constrained to a single time constant (Figure 4.5). The fit included the same mathematical structure as above, but with the restriction that a single time constant τ_1 was shared across

conditions. A single fit to the mean data—averaged across all subjects and trials for each condition (30 deg/s Opto-Step and 0.5 mA Vest-Decay)—yielded a shared time constant of 5.2 s (mean-square error 0.0082, residual sum-squared error 32.8). We also compared the fitted τ_1 time constants from all subjects for the same Opto-Step and Vest-Decay conditions and found no significant difference (P = 0.13, paired t-test). We chose to fit only a single stimulus amplitude for each condition in order to include all subjects in the analysis (as mentioned previously, all subjects performed both amplitudes of the optokinetic stimulus but the only GVS amplitude used for all subjects was 0.5mA).

4.6 Discussion

The goal of this study was to test how the CNS combines sensory information during standing balance. We characterized human responses to optokinetic and galvanic vestibular stimuli, specifically the exponential rise during Opto-Step stimulus and the exponential decay during both Vest-Step and Vest-Decay stimuli. We found that the Neural Integrator could reproduce all responses (Figure 4.4), as well as the fast hypothetical response expected for a veridical position shift. In contrast, the Direct Weighting model was unable to reproduce the time course of the Opto-Step and Vest-Step responses, as evidenced by substantially poorer fits (differences in BIC greater than 10; Table 4.2). Moreover, there was no significant difference between the separate time constants determined from visual or vestibular stimuli, and forcing the fitted responses to share a single time constant yielded a reasonable match to mean data (Figure 4.5). We interpret our findings to suggest that a neural integrator may play an important role in posture stabilization.

The neural integrator concept was inspired by the velocity storage integrator (Cohen et al., 1981; Robinson, 1981) governing many eye movements. Although long linked to the semicircular canal dynamics, such integration has not similarly been applied to posture control, despite the need to integrate similar sensory information. In our model, the integrator's role is not to store velocity, but instead to filter disparate sensory inputs to estimate the body's angular tilt. Here, gravity contributes to estimation of self-motion, unlike the classic yaw-rotations of visual-vestibular interactions, where gravitational cues do not conflict with the induced sensation. In contrast, roll rotation entails a changing gravitational vector that must be reconciled with graviceptor input such as from the otoliths and somatosensors (Dichgans and Brandt, 1978; Merfeld et al., 1999). The additional input from these sensors inhibits circular vection and instead produces a sensation of tilt, as well as a rotation of subjective visual vertical (Dichgans et al., 1972). The neural integrator for posture could thus be thought of as a position storage integrator.

Accordingly, the neural integrator is important to the general processing of sensory signals for perception and motor control. The dynamics of any sensor would be expected to require some degree of filtering, which implies temporal dynamics within the CNS. Such filtering can be predicted by state estimation theory, which has long been applied to both visual-vestibular interactions (Borah et al., 1988b; Green and Angelaki, 2010; Merfeld et al., 1999) and posture control (Kuo, 1995, 2005). A state estimator uses an internal model of body and sensory dynamics that predicts sensory signals, which are then corrected by comparison with actual afferent information to yield an estimate of spatial orientation. In fact, previously proposed estimators would be expected to generate the responses examined here (Borah et al., 1988b;

Goodworth and Peterka, 2012; Klein et al., 2012; Kuo, 2005). Such models are able to reproduce a variety of responses as well as explain why the observed filtering behavior might be optimal, as a consequence of the high-pass filter dynamics of the semicircular canals. Our intent was to perform an extreme simplification of a filtering behavior, to focus on basic characteristics that could potentially be tied to a neural substrate, analogous to the velocity storage integrator for gaze stabilization. We demonstrate how the same type of integrator may be applied to posture, and by extension how estimator and sensory re-weighting dynamics proposed by others might be physiologically realized.

A secondary aim of this study was to examine the effect of galvanic vestibular stimuli. If it is equivalent to direct stimulation of the vestibular afferents (Goldberg et al., 1984; St George et al., 2011), then the Neural Integrator model predicts that a step in galvanic current should resemble the canal response to angular acceleration, and thus produce an exponentially decaying response, plus a non-zero steady-state offset (Table 4.1). The subjects here appeared to respond with a relatively strong exponential decay and a weaker offset. This model also predicted that the Vest-Decay stimulus would be more similar to a step in head angular velocity, and thus produce a fully decaying exponential, dominated by the relatively slow neural integrator time constant. Some subjects appeared to exhibit a negative steady-state offset not predicted by our model, which was perhaps indicative of yet another, still-slower time constant in the sensory processing dynamics, or even a nonlinear adaptation (discussed below). It is unclear whether subjects produced similar offsets to the model (non-zero for Vest-Step, and zero for Vest-Decay), but both of the galvanic vestibular responses did exhibit evidence of a neural integrator with time constants of several seconds. We also found that the amplitude of the response to the 0.25 mA

stimulus was larger than the response to the 0.5 mA stimulus. However, the observed decrease in amplitude associated with the larger stimulus level may have been a small sample size effect (six out of the 16 subjects performed trials with the 0.25mA stimulus, while all 16 performed trials with the 0.5mA stimulus).

Current practice often treats galvanic vestibular stimulus as a general means to stimulate the vestibular system, but without a specific real-world interpretation. This differs from the rotational (i.e., vestibular) stimuli that are often applied in a controlled manner for assessment and diagnosis of oculomotor and vestibular dysfunction (Dix and Hallpike, 1952; Suzuki and Komatsuzaki, 1962; Zee et al., 1976). It may therefore be helpful for posture assessments to apply interpretable vestibular signals, similar to the visual and support surface perturbations already available (Nashner and Peters, 1990; Woollacott et al., 1986). We posited that the stimulus should ideally be a decaying exponential (Vest-Decay) to model a step in angular velocity of the body (Fitzpatrick et al., 2002b, 2006b). Although we did not prove that possibility, development of vestibular prostheses reveals that a high-pass filter of angular velocity, with a relatively long time constant, yields a galvanic stimulus that partially restores the normal velocity storage behavior (Merfeld et al., 2007). This suggests that head movements might indeed be emulated with a galvanic stimulus that models the dynamics of the semicircular canals, as was intended by our Vest-Decay input. In contrast, the Vest-Step stimulus hypothetically produces an unnatural afferent response of sustained angular acceleration (see Figure 4.3). In the Vest-Step response, we also anecdotally observed that some subjects retained a different steady offset in head tilt than the trunk. It is possible that this is due to different sensory information available to distinct body segments (Goodworth and Peterka, 2012; Kiemel

et al., 2011; Peterka and Benolken, 1995), not considered here. Nevertheless, if galvanic stimulus acts on the vestibular afferents, we would expect a decaying stimulus to better mimic the effects of a physical rotation.

There have been other observations of slow dynamics in posture control. Unperturbed sway exhibits a very slow fluctuation in COP, which could be interpreted as a fluctuation of a reference signal (Dijkstra, 2000; Zatsiorsky and Duarte, 2000). Others have argued that the fluctuation is within the feedback loop, perhaps as a consequence of state estimation noise (Kiemel et al., 2002, 2006). Although we do not preclude the possibility of a fluctuating reference signal, the present results demonstrate slow dynamics specifically associated with sensory processing. We do not explore the origin of the slow time constant here, but would expect that a state estimator would introduce dynamics that are at least qualitatively similar to our observations, although that connection remains to be examined more closely.

There are a number of limitations to this study. We proposed a very simple model with a single neural integrator, whereas more complex models might better reproduce the empirical observations. We also measured trunk tilt as an indicator of the body, and did not consider the multi-segmental kinematics of the entire body, and particularly its interaction with closed-loop, CNS feedback control (Hettich et al., 2014; Kuo, 1995, 2005). Much of this control appears to be relatively fast, as exemplified by the fast rise in tilt at onset of galvanic vestibular stimulus (Fig.4.4; τ_2 in Table 4.2A), far faster than the decaying exponential modeled here. We therefore presume feedback control dynamics to be considerably faster than the neural integrator time constant, which we consider indicative of state estimation. However, even considering state

estimation alone, more sophisticated models typically entail more complex filtering (Goodworth and Peterka, 2012; Kiemel et al., 2011; Kuo, 2005), and therefore multiple, and in some cases, adaptable, neural integrators (Assländer and Peterka, 2014; Borah et al., 1988b; Klein et al., 2012). We also regard most of these as relatively fast, as the slowness of the position storage integrator is a consequence of the uniquely slow dynamics of the semicircular canals.

Our experiment also used extremely simple input functions for both visual and vestibular disturbances. An alternative to step functions and exponentially decaying inputs is to apply broadband input (e.g., Assländer and Peterka, 2014) and perform system identification (e.g., Johansson et al., 1995, 2001). Such approaches are particularly apt for multiple inputs and outputs, and complex models with more degrees of freedom and states. However, our main purpose was to explicitly test a simple model to explain long-recognized responses to step stimuli, analogous to the classic experiments of visual-vestibular interactions (Robinson, 1981). Despite being less sophisticated, simple yet specific models can be more appropriate for hypothesis testing.

Other limitations include our model's ability to characterize longer-term behaviors. The galvanic vestibular responses at times appeared to exhibit a steady-state offset that was more negative than expected, for both the step and decaying exponential stimuli. This could potentially be an indicator of long-term habituation or adaptation to tonic stimuli, included in some models as a very long time constant (Borah et al., 1988b; e.g., Guedry and Lauver, 1961; St George et al., 2011). It might also be reminiscent of a nonlinear, long-term adaptation reported by Johansson et al. (1995) resulting from broadband stimulus. Unfortunately, the present data are insufficient to

confirm whether the lingering effect we observed is either linear or nonlinear; however, they at least superficially agree with the previous reports. For some of our subjects, the optokinetic responses also appeared to exhibit a very slow resetting behavior on the order of tens of seconds, resulting in wide variance in the steady-state offset. This might be interpreted as similar to long-reported periodic resetting of subjective vertical (Mauritz et al., 1977), or to periodic nystagmus of eye movements (Robinson, 1981). We did not model or characterize this behavior, which might be separable as a basic behavior similar to the fast phase of eye movement nystagmus, or might be due to conscious compensations performed by subjects.

Some of these issues might be resolved using more complete kinematic measurements and more sophisticated models. However, despite the simplicity of the present study, there does appear to be evidence in favor of a neural integrator for posture as opposed to direct weighting of sensory inputs. This could potentially inform how these sensory inputs might be tested in the clinic as well as how their functions might be restored using prosthetic devices (e.g., Merfeld et al., 2007).

Chapter 5: Conclusion and Significance

The vestibular system plays a vital role in visual and postural stability, the loss of which have substantial implications for quality of life. Thus, having a comprehensive understanding of the vestibular system's function is critical for accurate diagnoses and effective therapies. This thesis demonstrates that along with known and well-characterized inputs, such as from the visual and vestibular organs, non-traditional inputs, such as efference copy (Chapter 2), noise (Chapter 3), and galvanic vestibular stimulation (Chapter 4), also have a significant effect on the vestibular system's function. And these effects are not without consequence; each input discussed has implications for both laboratory and clinical settings. For example, in Chapter 2, we showed that efference copy driven eye movements (i.e. pre-programmed eye movements (PPEM)) are part of a unique gaze stabilization system, that exists in both healthy and vestibular lesioned animals, and therefore requires independent testing. In Chapter 3, we showed that a single noise exposure can cause significant functional damage to the vestibular system, suggesting that patients with noise-induced hearing loss should be tested for vestibular loss as well. Additionally, we discussed why the VCR, as opposed to the VOR, may be a better metric for noise-induced vestibular loss. Finally, in Chapter 4, we showed that GVS, if properly conditioned, can be integrated like natural vestibular stimulation during postural control. Thus, if GVS is to be used to substitute for lost vestibular input, as it is for vestibular prosthetics, high-pass filtering head velocity would likely produce more natural responses. Finally, though not a primary aim, this thesis demonstrates the value of using simple models to make specific predictions as well as the

usefulness of leveraging models across disciplines. Each point are discussed with respect to each chapter in more detail below.

5.1 Gaze Shifts in Primates & Gaze Stabilization in Rodents

Much of what has been reported on PPEM has focused on their role in replacing the VOR in vestibulopathic subjects. Some even claim that PPEM are solely an adaptive mechanism and not a part of gaze stabilization in healthy subjects (Cullen et al., 2009; Dichgans et al., 1973). In Chapter 2, we add to the building evidence that PPEM are, indeed, used by healthy subjects and propose a model of gaze stabilization which 1) correctly predicts eye movements in healthy and vestibular lesioned animals, 2) provides a mechanism for adaptation after vestibular loss, 3) accounts for why previous reports did not find PPEM in healthy subjects, and 4) offers a possible basis for "linear summation" theory of gaze saccades in primates.

Linear summation theory, first proposed by Bizzi, states that the VOR is selectively cancelled, rather than completely suppressed, during eye-head gaze shifts (Morasso et al., 1973). Although gaze shifts are unique to foveate animals, such as primates, we found a similar phenomenon in an afoveate animal during gaze stabilization. This suggests that PPEM, and the accompanying VOR cancellation, might reflect a much more fundamental system which researchers have only begun to characterize. Further, our finding that PPEM are used by healthy subjects but become more important with decreasing vestibular function suggests that clinicians use both passive and active head movements, to test both the VOR and PPEM respectively, to thoroughly assess ocular stability.

5.2 Noise-induced Vestibular Loss

In Chapter 3, we asked if the semi-circular canals were susceptible to noise damage, and used both the VOR and the vestibulocollic reflex (VCR) to characterize functional damage to both regular and irregular afferents. We found that after a single exposure to intense noise, both the VOR and VCR showed show decreased performance. Further, both pathways exhibited increased variability in responses. Taken together, these two findings (i.e. decreased performance and increased variability) demonstrate that noise-induced vestibular loss is functionally similar to more conventional vestibular lesions and that even a single exposure to high-intensity noise can result in significant decrease in ocular and postural stability.

Given the growing evidence that noise-overstimulation damages the vestibular organs, these results suggest that patients presenting with hearing loss, especially those exposed to high-intensity noise, may need to be examined for vestibular loss as well. Previous research on noise overstimulation in the vestibular system has largely focused on the otoliths (Akdogan et al., 2009; Hsu et al., 2008; Stewart et al., 2016, 2017b, Akin et al., 2012; Hsu et al., 2008; Kumar et al., 2010; Perez et al., 2002; Stewart et al., 2017b). While there have been studies looking at noise overstimulation to the semi-circular canals, they used the vestibular ocular reflex (VOR) as their main metric for functional damage (Fetoni et al., 2009; Golz et al., 2001; Manabe et al., 1995; Oosterveld et al., 1982; Shupak et al., 1994; Stewart et al., 2016; Ylikoski et al., 1988). We found that the VCR also shows significant deficits. Indeed, percent overshoot, a relatively easy metric to calculate, had a little over a 10% increase, similar to the decrease seen the VOR. This is particularly important as the VOR in humans and primates is predominantly driven by regular afferents, while noise effects irregular afferents. Thus, the VOR may not have much diagnostic

value for noise-induced vestibular loss. However, the VCR, as measured by percent overshoot, offers an easy means of assessing irregular afferent function.

5.3 Eye Movement Models in Postural Control

Velocity storage refers to a phenomenon in which the body filters visual and vestibular information such that they become complimentary to each other. In Chapter 4, we tested whether a simple model of velocity storage, originally developed to predict eye movements, could also predict postural responses. We used virtual reality and galvanic vestibular stimulation (GVS) to perturb the visual and vestibular systems respectively in standing subjects. We found that trunk tilt, like eye movements, showed complimentary responses to visual and vestibular perturbations. Our findings demonstrate that velocity storage is not limited to eye movements but shapes postural responses as well, suggesting that it represents a more fundamental mechanism of multisensory integrations used across sensorimotor systems.

While others have proposed more complex models that make similar predictions (Borah et al., 1988b; Merfeld et al., 1999; Ormsby and Young, 1977, Karmali and Merfeld, 2012; Laurens and Droulez, 2007; Paulin, 2005) these predictions have not been explicitly tested and, further, it's not clear if the added complexity is necessary. Additionally, much of the previous literature has used a step waveform of GVS without examining other waveforms (for review: Fitzpatrick and Day, 2004b). Our results show that while additionally complexity might allow models to predict other features of postural control, our model, while simple, was able to accurately predict the gross features of subjects' responses. Further, we showed that while a step in GVS current perturbed posture, the use of an exponential waveform produced responses that were

complimentary to visual perturbations, suggesting that this waveform would be better integrated with other sensory information.

The use of GVS to perturb the vestibular system also introduces possibilities for diagnostics and prosthetic design. Specifically, we found that high-pass filtering the GVS signal appears to be better integrated by the body than the standard step waveform of GVS. This has important implications for vestibular prosthetics which use GVS to replace vestibular information lost through aging and disease. Additionally, current clinical posturography techniques do not directly test the vestibular system's contribution to balance. Rather, they perturb visual and proprioceptive inputs and use a process of elimination to identify vestibular loss. GVS offers a simple and affordable means of perturbing the vestibular system that, as our study shows, can complement the current visual and proprioceptive techniques used.

5.4 Limitations

There were several limitations to each study presented. First, both Chapter 2 and 3 were relatively small and short studies with Chapter 2 having only seven control animals and three lesioned animals, and Chapter 3 only having six animals. Additionally, both studies only collected data from animals for a few months at most. More animals followed for longer amounts of time would have allowed us to better characterize the process of recovery.

We also proposed extremely simple models in Chapters 2 and 4. The Cooperative and Suppression models of Chapter 2 lacked dynamics as well as other known inputs to the vestibular system, such as proprioception. The latter is of particular importance given the role the

COR has been found to play in primates after labyrinthectomy. In Chapter 4, our model did not consider the closed-loop, CNS feedback control (Hettich et al., 2014; Kuo, 1995, 2005). Much of this control appears to be faster than the decaying exponential modeled here, indicative of state estimation. However, even considering state estimation alone, more sophisticated models typically entail more complex filtering (Goodworth and Peterka, 2012; Kiemel et al., 2011; Kuo, 2005), and therefore multiple, and in some cases, adaptable, neural integrators (Assländer and Peterka, 2014; Borah et al., 1988b; Klein et al., 2012).

Finally, in Chapter 3, histology was not performed until after animals had received five noise exposures over the course two months. Although we found no obvious loss of hair cells, it's possible that over the time course of the study, damage to hair cells may have recovered. Additionally, we did not test for synapse loss. Thus, we cannot say with certainty what the mechanism of vestibular loss was in these animals.

Chapter 6: Future Directions

As mentioned in the previous chapter, this thesis demonstrates that non-traditional inputs can have a significant effect on the vestibular system, each of which merits further investigation.

6.1 Adaptation in Pre-Programmed Eye Movements

In Chapter 2, we proposed a model of gaze stabilization that included two internal models, one of the vestibular-ocular reflex (VOR) and another of the head and neck, each of which produces an estimate of eye and head movements respectively. According to our model, the accuracy of PPEM depends on accurate estimates of sensory and body dynamics used by these internal models. However, through development, aging, or even disease, sensory and body dynamics can change. We showed, for example, that the loss and subsequent recovery of PPEM after vestibular lesion can be modeled as a gradual updating of the estimated VOR dynamics. However, an immediate and complete loss of sensor function, like the aforementioned, is rarely encountered in everyday life. This leaves open the question of 1) how the body might adapt to more gradual and subtle changes in sensory or body dynamics and 2) if this motor behavior can be linked to neural behavior.

In a pilot study we altered head dynamics by adding weights and found a modest change in PPEM performance but no evidence of adaptation. However, others have shown that a gradual change in dynamics is more effective at eliciting adaptation, as it more closely reflects the

changes in growth and disease (Kluzik et al., 2008; Torres-Oviedo and Bastian, 2010). In the context of head dynamics, this could be accomplished using a torque motor attached to the head, which would effectively increase head inertia, but would allow for a gradual increase over time. Given our results from using weights, the use of a torque motor would likely yield even more fruitful results and allow the adaptation process to be characterized by tracking PPEM performance.

While the adaptation has been extensively studied in motor systems as well as neural circuits, the vestibular system offers a unique opportunity to link motor behavior to neural behavior, as it is a relatively simple sensorimotor system driven by a three-neuron arc. Our lab and others have already found that a specific subset of vestibular neurons, called vestibular-only (VO) neurons, appear to reflect an estimate of head velocity, as they only encode unexpected head movements. Based on these findings, we suspect that VO neurons would provide a neural correlate to motor adaptation in PPEM.

6.2 Long-Term Effects of Long-Term Noise Exposure

In Chapter 3, we showed that even a single noise exposure can cause significant loss of ocular and postural stability. However, looking at only a single noise exposure and following the animals for only two weeks, leaves open a number of questions: 1) to what extent are subjects able to recover function after noise exposure and 2) what effect would long-term exposure to moderate levels of noise have on the vestibular function.

While we only looked at animals for up to two weeks after noise exposure, others have followed subjects for longer periods of time. Stewart et al. (2017) recorded VsEPs from rats exposed to high-intensity noise and found that after 3 weeks there was evidence of recovery. These authors also noted significant recovery within 3 days after shorter exposures of 15, 30, and 45 minutes (personal communications). Further, Sadeghi et al. (2007) found that after unilateral labyrinthectomy, there was an in increase in the proportion of irregular afferents, which are likely the afferents most affected by noise overstimulation. Thus, there is reason to believe that even after a substantial lesion, ocular and postural stability could recover if given enough time. Histology should also be employed throughout this process to determine a possible mechanism of recovery (e.g. tip-links, hair cell bundles, etc.).

Additionally, a single high-intensity noise exposure is not representative of most people's experience. Instead, most are exposed to moderate noise for hours every day as part of their occupation or through the use of headphones. Tamura et al. (2012) addressed this disparity by exposing mice to 70dB noise for a month and still found significant loss of balance along with evidence of vestibular hair cell loss. However, this study quantified balance using a rotarod test and stride length, which are somewhat crude metrics, and they did not differentiate damage done to the canals versus the otolith, type I versus type II hair cells, or investigate synaptic damage, all of which is relevant to understanding the mechanism by which noise-damage effects the vestibular system and pathways.

6.3 Improving Diagnostics with Optokinetic and Galvanic Vestibular Stimulation

Currently, tests of postural control, such as the Sensory Organization Test, can only eliminate sensory information, and even then, only the visual and somatosensory systems are targeted. Furthermore, the perturbations to balance during testing are the result of natural random variations in the center of pressure and are thus not controlled. Without a known input the interpretation of the output is limited. In Chapter 4, we showed that optokinetic (OK) and galvanic vestibular stimulation (GVS) can be used to perturb the postural stability in a controllable way. Thus, the use of GVS and OK perturbations could provide more comprehensive diagnostics and may be able to detect subtler deficits than tests that are currently available. To answer this question, we suggest testing patient populations with known sensory dysfunction against our model predictions.

In a separate study, we showed that even self-reported healthy older adults respond to GVS and OK stimuli differently than healthy younger adults suggesting that postural responses to GVS and OK may begin to change even before clinically significant symptoms of sensory dysfunction appear. Based on models of eye movements, sensory dysfunction manifests as specific changes to patient responses. For example, patients with vestibulopathy respond to vestibular stimuli with decreased time constants, or have higher gains to visual or proprioceptive perturbations because they weight other inputs to compensate for vestibular loss. Given the similarity we showed in Chapter 4 between gaze and postural stability, we suspect that similar changes to postural responses would also occur.

Bibliography

Agarwal, G.C., and Gottlieb, G.L. (1984). Mathematical modeling and simulation of the postural control loop--Part II. Crit. Rev. Biomed. Eng. *11*, 113–154.

Akdogan, O., Selcuk, A., Take, G., Erdoğan, D., and Dere, H. (2009). Continuous or intermittent noise exposure, does it cause vestibular damage?: An experimental study. Auris. Nasus. Larynx *36*, 2–6.

Akin, F.W., Murnane, O.D., Tampas, J.W., Clinard, C., Byrd, S., and Kelly, J.K. (2012). The effect of noise exposure on the cervical vestibular evoked myogenic potential. Ear Hear. *33*, 458–465.

Assländer, L., and Peterka, R.J. (2014). Sensory reweighting dynamics in human postural control. J. Neurophysiol. *111*, 1852–1864.

Atkin A, and Bender MB (1968). Ocular stabilization during oscillatory head movements: Vestibular system dysfunction and the relation between head and eye velocities. Arch. Neurol. *19*, 559–566.

Baird, R.A., Desmadryl, G., Fernandez, C., and Goldberg, J.M. (1988). The vestibular nerve of the chinchilla. II. Relation between afferent response properties and peripheral innervation patterns in the semicircular canals. J. Neurophysiol. *60*, 182–203.

Beraneck, M., and Cullen, K.E. (2007). Activity of Vestibular Nuclei Neurons During Vestibular and Optokinetic Stimulation in the Alert Mouse. J. Neurophysiol. *98*, 1549–1565.

Bilotto, G., Goldberg, J., Peterson, B.W., and Wilson, V.J. (1982). Dynamic properties of vestibular reflexes in the decerebrate cat. Exp. Brain Res. *47*, 343–352.

Bizzi, E., Kalil, R.E., and Tagliasco, V. (1971). Eye-head coordination in monkeys: evidence for centrally patterned organization. Science *173*, 452–454.

Black RA, Halmagyi G, Thurtell MJ, Todd MJ, and Curthoys IS (2005). The active head-impulse test in unilateral peripheral vestibulopathy. Arch. Neurol. *62*, 290–293.

Blakemore, C., and Donaghy, M. (1980). Co-ordination of head and eyes in the gaze changing behaviour of cats. J. Physiol. *300*, 317–335.

Borah, J., Young, L.R., and Curry, R.E. (1988a). Optimal Estimator Model for Human Spatial Orientationa. Ann. N. Y. Acad. Sci. *545*, 51–73.

Borah, J., Young, L.R., and Curry, R.E. (1988b). Optimal estimator model for human spatial orientation. In Representation of Three-Dimensional Space in the Vestibular, Oculomotor, and Visual Systems, (New York: The New York Academy of Sciences), pp. 51–73.

Boyle, R., Goldberg, J.M., and Highstein, S.M. (1992). Inputs from regularly and irregularly discharging vestibular nerve afferents to secondary neurons in squirrel monkey vestibular nuclei. III. Correlation with vestibulospinal and vestibuloocular output pathways. J. Neurophysiol. *68*, 471–484.

Boyle, R., Belton, T., and McCREA, R.A. (1996). Responses of Identified Vestibulospinal Neurons to Voluntary Eye and Head Movements in the Squirrel Monkeya. Ann. N. Y. Acad. Sci. *781*, 244–263.

Brandt, T., Strupp, M., and Benson, J. (1999). You are better off running than walking with acute vestibulopathy. The Lancet *354*, 746.

Britton, T.C., Day, B.L., Brown, P., Rothwell, J.C., Thompson, P.D., and Marsden, C.D. (1993). Postural electromyographic responses in the arm and leg following galvanic vestibular stimulation in man. Exp. Brain Res. *94*, 143–151.

Bronstein, A.M., and Derrick Hood, J. (1986). The cervico-ocular reflex in normal subjects and patients with absent vestibular function. Brain Res. *373*, 399–408.

Brooks, J.X., and Cullen, K.E. (2013). The Primate Cerebellum Selectively Encodes Unexpected Self-Motion. Curr. Biol. *23*, 947–955.

Brooks, J.X., and Cullen, K.E. (2014). Early vestibular processing does not discriminate active from passive self-motion if there is a discrepancy between predicted and actual proprioceptive feedback. J. Neurophysiol. *111*, 2465–2478.

Burgess, P.R., and Perl, E.R. (1973). Cutaneous mechanoreceptors and nociceptors. In Somatosensory System, A. Iggo, ed. (Springer Berlin Heidelberg), pp. 29–78.

Cannon, S.C., and Robinson, D.A. (1987). Loss of the neural integrator of the oculomotor system from brain stem lesions in monkey. J. Neurophysiol. *57*, 1383–1409.

Chagnaud, B.P., Banchi, R., Simmers, J., and Straka, H. (2015). Spinal corollary discharge modulates motion sensing during vertebrate locomotion. Nat. Commun. *6*.

Chambers, B., Mai, M., and Barber, H. (1985). Bilateral vestibular loss, oscillopsia, and the cervico-ocular reflex. Otolaryngol.--Head Neck Surg. Off. J. Am. Acad. Otolaryngol.-Head Neck Surg. *93*, 403–407.

Cohen, B., Matsuo, V., and Raphan, T. (1977). Quantitative analysis of the velocity characteristics of optokinetic nystagmus and optokinetic after-nystagmus. J. Physiol. *270*, 321–344.

Cohen, B., Henn, V., Raphan, T., and Dennett, D. (1981). Velocity storage, nystagmus, and visual-vestibular interaction in humans. Ann. N. Y. Acad. Sci. *374*, 421–433.

Colebatch, J.G.M., and Halrnagyi, G.M.M. (1992). Vestibular evoked potentials in human neck muscles before and after unilateral vestibular deafferentation. Neurology *42*, 1635–1636.

Colebatch, J.G., Halmagyi, G.M., and Skuse, N.F. (1994). Myogenic potentials generated by a click-evoked vestibulocollic reflex. J. Neurol. Neurosurg. Psychiatry *57*, 190–197.

Collewijn, H., Martins, A.J., and Steinman, R.M. (1983). Compensatory eye movements during active and passive head movements: fast adaptation to changes in visual magnification. J. Physiol. *340*, 259–286.

Cousins, S., Kaski, D., Cutfield, N., Seemungal, B., Golding, J.F., Gresty, M., Glasauer, S., and Bronstein, A.M. (2013). Vestibular Perception following Acute Unilateral Vestibular Lesions. PLOS ONE *8*, e61862.

Crawford, J. (1964). Living without a balance mechanism. Br. J. Ophthalmol. *48*, 357–360.

Cullen, K.E. (2012). The vestibular system: multimodal integration and encoding of self-motion for motor control. Trends Neurosci. *35*, 185–196.

Cullen, K.E. (2014). The neural encoding of self-generated and externally applied movement: implications for the perception of self-motion and spatial memory. Front. Integr. Neurosci. *7*.

Cullen, K.E., and Minor, L.B. (2002). Semicircular Canal Afferents Similarly Encode Active and Passive Head-On-Body Rotations: Implications for the Role of Vestibular Efference. J. Neurosci. *22*, RC226-RC226.

Cullen, K.E., Huterer, M., Braidwood, D.A., and Sylvestre, P.A. (2004). Time Course of Vestibuloocular Reflex Suppression During Gaze Shifts. J. Neurophysiol. *92*, 3408–3422.

Cullen, K.E., Minor, L.B., Beraneck, M., and Sadeghi, S.G. (2009). Neural substrates underlying vestibular compensation: Contribution of peripheral versus central processing. J. Vestib. Res. *19*, 171–182.

Cullen, K.E., Brooks, J.X., Jamali, M., Carriot, J., and Massot, C. (2011). Internal models of self-motion: computations that suppress vestibular reafference in early vestibular processing. Exp. Brain Res. *210*, 377–388.

Curthoys, I.S. (2010). A critical review of the neurophysiological evidence underlying clinical vestibular testing using sound, vibration and galvanic stimuli. Clin. Neurophysiol. *121*, 132–144.

Curthoys, I.S., Betts, G.A., Burgess, A.M., MacDOUGALL, H.G., Cartwright, A.D., and Halmagyi, G.M. (1999). The Planes of the Utricular and Saccular Maculae of the Guinea Pig. Ann. N. Y. Acad. Sci. *871*, 27–34.

Curthoys, I.S., Kim, J., McPhedran, S.K., and Camp, A.J. (2006). Bone conducted vibration selectively activates irregular primary otolithic vestibular neurons in the guinea pig. Exp. Brain Res. *175*, 256–267.

Della Santina CC, Cremer PD, Carey JP, and Minor LB (2002). Comparison of head thrust test with head autorotation test reveals that the vestibulo-ocular reflex is enhanced during voluntary head movements. Arch. Otolaryngol. Neck Surg. *128*, 1044–1054.

Dichgans, J., and Brandt, T. (1978). Visual-vestibular interaction: Effects on self-motion perception and postural control. In Handbook of Sensory Physiology, R. Held, H. W. Leibowitz, H. L. Teuber, Eds., (Berlin: Springer-Verlag), pp. 775–804.

Dichgans, D.J., Bizzi, E., Morasso, D.P., and Tagliasco, D.V. (1973). Mechanisms underlying recovery of eye-head coordination following bilateral labyrinthectomy in monkeys. Exp. Brain Res. *18*, 548–562.

Dichgans, J., Held, R., Young, L.R., and Brandt, T. (1972). Moving visual scenes influence the apparent direction of gravity. Science *178*, 1217–1219.

Dijkstra, T.M.H. (2000). A gentle introduction to the dynamic set-point model of human postural control during perturbed stance. Hum. Mov. Sci. *19*, 567–595.

Dix, M.R., and Hallpike, C.S. (1952). The pathology, symptomatology and diagnosis of certain common disorders of the vestibular system. Proc. R. Soc. Med. *45*, 341.

Eatock, R.A., and Songer, J.E. (2011). Vestibular hair cells and afferents: two channels for head motion signals. Annu. Rev. Neurosci. *34*, 501–534.

Eatock, R.A., Xue, J., and Kalluri, R. (2008). Ion channels in mammalian vestibular afferents may set regularity of firing. J. Exp. Biol. *211*, 1764–1774.

Escudero, M., Waele, C. de, Vibert, N., Berthoz, A., and Vidal, P.P. (1993). Saccadic eye movements and the horizontal vestibulo-ocular and vestibulo-collic reflexes in the intact guinea-pig. Exp. Brain Res. *97*, 254–262.

Fay, R.R., and Popper, A.N. (2000). Evolution of hearing in vertebrates: the inner ears and processing. Hear. Res. *149*, 1–10.

Fernandez, C., and Goldberg, J.M. (1971). Physiology of peripheral neurons innervating semicircular canals of the squirrel monkey. II. Response to sinusoidal stimulation and dynamics of peripheral vestibular system. J Neurophysiol *34*, 661–675.

Fernandez, C., Goldberg, J.M., and Baird, R.A. (1990). The vestibular nerve of the chinchilla. III. Peripheral innervation patterns in the utricular macula. J. Neurophysiol. *63*, 767–780.

Fetoni, A.R., Ferraresi, A., Picciotti, P., Gaetani, E., Paludetti, G., and Troiani, D. (2009). Noise induced hearing loss and vestibular dysfunction in the guinea pig. Int. J. Audiol. *48*, 804–810.

Fitzpatrick, R.C., and Day, B.L. (2004a). Probing the human vestibular system with galvanic stimulation. J. Appl. Physiol. *96*, 2301–2316.

Fitzpatrick, R.C., and Day, B.L. (2004b). Probing the human vestibular system with galvanic stimulation. J. Appl. Physiol. *96*, 2301–2316.

Fitzpatrick, R., Burke, D., and Gandevia, S.C. (1994). Task-dependent reflex responses and movement illusions evoked by galvanic vestibular stimulation in standing humans. J. Physiol. *478*, 363–372.

Fitzpatrick, R.C., Marsden, J., Lord, S.R., and Day, B.L. (2002a). Galvanic vestibular stimulation evokes sensations of body rotation. Neuroreport *13*, 2379–2383.

Fitzpatrick, R.C., Marsden, J., Lord, S.R., and Day, B.L. (2002b). Galvanic vestibular stimulation evokes sensations of body rotation. Neuroreport *13*, 2379–2383.

Fitzpatrick, R.C., Butler, J.E., and Day, B.L. (2006a). Resolving head rotation for human bipedalism. Curr. Biol. CB *16*, 1509–1514.

Fitzpatrick, R.C., Butler, J.E., and Day, B.L. (2006b). Resolving head rotation for human bipedalism. Curr. Biol. CB *16*, 1509–1514.

Foster, C.A., Demer, J.L., Morrow, M.J., and Baloh, R.W. (1997). Deficits of gaze stability in multiple axes following unilateral vestibular lesions. Exp. Brain Res. *116*, 501–509.

Fransson, P.-A., Hafstrom, A., Karlberg, M., Magnusson, M., Tjader, A., and Johansson, R. (2003). Postural control adaptation during galvanic vestibular and vibratory proprioceptive stimulation. IEEE Trans. Biomed. Eng. *50*, 1310–1319.

Freedman, E.G., Ling, L., and Fuchs, A.F. (1998). Perturbing the head: re-assessing the gain of reflex interactions during orienting eye-head movements. In Soc Neurosci Abstr, pp. 557–518.

Girard, S.A., Leroux, T., Verreault, R., Courteau, M., Picard, M., Turcotte, F., and Baril, J. (2014). Falls Risk and Hospitalization among Retired Workers with Occupational Noise-Induced Hearing Loss. Can. J. Aging Rev. Can. Vieil. *33*, 84–91.

Goldberg, J.M., and Cullen, K.E. (2011). Vestibular control of the head: possible functions of the vestibulocollic reflex. Exp. Brain Res. *210*, 331–345.

Goldberg, J.M., and Fernandez, C. (1971a). Physiology of Peripheral Neurons Innervating Semicircular Canals of the Squirrel Monkey. J. Neurophysiol. *34*, 676–684.

Goldberg, J.M., and Fernandez, C. (1971b). Physiology of peripheral neurons innervating semicircular canals of the squirrel monkey. I. Resting discharge and response to constant angular accelerations. J. Neurophysiol. *34*, 635–660.

Goldberg, J.M., Smith, C.E., and Fernandez, C. (1984). Relation between discharge regularity and responses to externally applied galvanic currents in vestibular nerve afferents of the squirrel monkey. J. Neurophysiol. *51*, 1236–1256.

Golz, A., Westerman, S.T., Westerman, L.M., Goldenberg, D., Netzer, A., Wiedmyer, T., Fradis, M., and Joachims, H.Z. (2001). The effects of noise on the vestibular system. Am. J. Otolaryngol. *22*, 190–196.

Goodworth, A.D., and Peterka, R.J. (2012). Sensorimotor integration for multisegmental frontal plane balance control in humans. J. Neurophysiol. *107*, 12–28.

Green, A.M., and Angelaki, D.E. (2010). Internal models and neural computation in the vestibular system. Exp. Brain Res. Exp. Hirnforsch. Exp. Cerebrale *200*, 197–222.

Guedry, F., and Lauver, L. (1961). Vestibular Reactions During Prolonged Constant Angular Acceleration. J. Appl. Physiol. *16*, 215-.

Guitton, D., and Volle, M. (1987). Gaze control in humans: eye-head coordination during orienting movements to targets within and beyond the oculomotor range. J. Neurophysiol. *58*, 427–459.

Guitton, D., Douglas, R.M., and Volle, M. (1984). Eye-head coordination in cats. J. Neurophysiol. *52*, 1030–1050.

Guitton, D., Kearney, R.E., Wereley, N., and Peterson, B.W. (1986). Visual, vestibular and voluntary contributions to human head stabilization. Exp. Brain Res. *64*, 59–69.

Habermann, J. (1890). Ueber die Schwerhörigkeit der Kesselschmiede. Arch. Für Ohrenheilkd. *30*, 1–25.

Halmagyi, G.M., Black, R.A., ThurTEL l, M.J., and Curthoys, I.S. (2003). The Human Horizontal Vestibulo-Ocular Reflex in Response to Active and Passive Head Impulses after Unilateral Vestibular Deafferentation. Ann. N. Y. Acad. Sci. *1004*, 325–336.

Helmholtz, H. von, and Southall, J.P.C. (2005). Treatise on Physiological Optics (Courier Corporation).

Herdman SJ, Schubert MC, and Tusa RJ (2001). ROle of central preprogramming in dynamic visual acuity with vestibular loss. Arch. Otolaryngol. Neck Surg. *127*, 1205–1210.

Hettich, G., Assländer, L., Gollhofer, A., and Mergner, T. (2014). Human hip-ankle coordination emerging from multisensory feedback control. Hum. Mov. Sci. *37*, 123–146.

Holmgren, P.G., and Orembowsky, D.M.N.S. (1927). Die otiatrische Untersuchung der Kesselschmiede in den Hauptwerkstätten der Transkaukasischen Eisenbahn. Acta Otolaryngol. (Stockh.) *10*, 197–208.

Holst, E. von, and Mittelstaedt, H. (1950). Das Reafferenzprinzip. Naturwissenschaften *37*, 464–476.

Hoshowsky, B., Tomlinson, D., and Nedzelski, J. (1994). The horizontal vestibulo-ocular reflex gain during active and passive high-frequency head movements. The Laryngoscope *104*, 140–145.

Hsu, W.-C., Wang, J.-D., Lue, J.-H., Day, A.-S., and Young, Y.-H. (2008). Physiological and Morphological Assessment of the Saccule in Guinea Pigs After Noise Exposure. Arch. Otolaryngol. Neck Surg. *134*, 1099–1106.

Huterer, M., and Cullen, K.E. (2002). Vestibuloocular Reflex Dynamics During High-Frequency and High-Acceleration Rotations of the Head on Body in Rhesus Monkey. J. Neurophysiol. *88*, 13–28.

Jahn, K., Strupp, M., Schneider, E., Dieterich, M., and Brandt, T. (2000). Differential effects of vestibular stimulation on walking and running. Neuroreport *11*, 1745–1748.

Jamali, M., Mitchell, D.E., Dale, A., Carriot, J., Sadeghi, S.G., and Cullen, K.E. (2014). Neuronal detection thresholds during vestibular compensation: contributions of response variability and sensory substitution. J. Physiol. *592*, 1565–1580.

Jell, R.M., Stockwell, C.W., Turnipseed, G.T., and Guedry, F.E., Jr (1988). The influence of active versus passive head oscillation, and mental set on the human vestibulo-ocular reflex. Aviat. Space Environ. Med. *59*, 1061–1065.

Johansson, R., Magnusson, M., and Fransson, P.A. (1995). Galvanic vestibular stimulation for analysis of postural adaptation and stability. IEEE Trans. Biomed. Eng. *42*, 282–292.

Johansson, R., Magnusson, M., Fransson, P.A., and Karlberg, M. (2001). Multi-stimulus multi-response posturography. Math. Biosci. *174*, 41–59.

Jombík, P., and Bahýl, V. (2005). Short latency responses in the averaged electro-oculogram elicited by vibrational impulse stimuli applied to the skull: could they reflect vestibulo-ocular reflex function? J. Neurol. Neurosurg. Psychiatry *76*, 222–228.

Karmali, F., and Merfeld, D.M. (2012). A distributed, dynamic, parallel computational model: the role of noise in velocity storage. J. Neurophysiol. *108*, 390–405.

Kasahara, M., and Uchino, Y. (1974). Bilateral semicircular canal inputs to neurons in cat vestibular nuclei. Exp. Brain Res. *20*, 285–296.

Kasai, T., and Zee, D.S. (1978). Eye-head coordination in labyrinthine-defective human beings. Brain Res. *144*, 123–141.

Kavounoudias, A., Roll, R., and Roll, J.-P. (2001). Foot sole and ankle muscle inputs contribute jointly to human erect posture regulation. J. Physiol. *532*, 869–878.

Keshner, E.A., and Kenyon, R.V. (2000). The influence of an immersive virtual environment on the segmental organization of postural stabilizing responses. J. Vestib. Res. Equilib. Orientat. *10*, 207–219.

Keshner, F.A., and Peterson, B.W. (1995). Mechanisms controlling human head stabilization. I. Head-neck dynamics during random rotations in the horizontal plane. J. Neurophysiol. *73*, 2293–2301.

Kiemel, T., Oie, K.S., and Jeka, J.J. (2002). Multisensory fusion and the stochastic structure of postural sway. Biol. Cybern. *87*, 262–277.

Kiemel, T., Oie, K.S., and Jeka, J.J. (2006). Slow Dynamics of Postural Sway Are in the Feedback Loop. J. Neurophysiol. *95*, 1410–1418.

Kiemel, T., Zhang, Y., and Jeka, J.J. (2011). Visual flow is interpreted relative to multisegment postural control. J. Mot. Behav. *43*, 237–246.

Kim, J., and Curthoys, I.S. (2004). Responses of primary vestibular neurons to galvanic vestibular stimulation (GVS) in the anaesthetised guinea pig. Brain Res. Bull. *64*, 265–271.

Klein, T.J., Jeka, J., Kiemel, T., and Lewis, M.A. (2012). Navigating sensory conflict in dynamic environments using adaptive state estimation. Biol. Cybern.

Kluzik, J., Diedrichsen, J., Shadmehr, R., and Bastian, A.J. (2008). Reach Adaptation: What Determines Whether We Learn an Internal Model of the Tool or Adapt the Model of Our Arm? J. Neurophysiol. *100*, 1455–1464.

Kumar, K., Vivarthini, C.J., and Bhat, J.S. (2010). Vestibular evoked myogenic potential in noise-induced hearing loss. Noise Health *12*, 191.

Kuo, A.D. (1995). An optimal control model for analyzing human postural balance. IEEE Trans Biomed Eng *42*, 87–101.

Kuo, A.D. (2005). An optimal state estimation model of sensory integration in human postural balance. J. Neural Eng. *2*, S235-249.

Lambert, F.M., Combes, D., Simmers, J., and Straka, H. (2012). Gaze Stabilization by Efference Copy Signaling without Sensory Feedback during Vertebrate Locomotion. Curr. Biol. *22*, 1649–1658.

Lasker, D.M., Hullar, T.E., and Minor, L.B. (2000). Horizontal Vestibuloocular Reflex Evoked by High-Acceleration Rotations in the Squirrel Monkey. III. Responses After Labyrinthectomy. J. Neurophysiol. *83*, 2482–2496.

Laurens, J., and Droulez, J. (2007). Bayesian processing of vestibular information. Biol. Cybern. *96*, 389–404.

Laurutis, V.P., and Robinson, D.A. (1986). The vestibulo-ocular reflex during human saccadic eye movements. J. Physiol. *373*, 209–233.

Lee, B.-C., Martin, B.J., and Sienko, K.H. (2012). Directional postural responses induced by vibrotactile stimulations applied to the torso. Exp. Brain Res. *222*, 471–482.

Lee, B.-C., Martin, B.J., Ho, A., and Sienko, K.H. (2013a). Postural Reorganization Induced by Torso Cutaneous Covibration. J. Neurosci. *33*, 7870–7876.

Lee, B.-C., Martin, B.J., and Sienko, K.H. (2013b). The effects of actuator selection on non-volitional postural responses to torso-based vibrotactile stimulation. J. NeuroEngineering Rehabil. *10*, 21.

Lund, S., and Broberg, C. (1983). Effects of different head positions on postural sway in man induced by a reproducible vestibular error signal. Acta Physiol. Scand. *117*, 307–309.

MacDougall, H.G., and Moore, S.T. (2005). Marching to the beat of the same drummer: the spontaneous tempo of human locomotion. J. Appl. Physiol. *99*, 1164–1173.

MacDougall, H.G., Brizuela, A.E., and Curthoys, I.S. (2003). Linearity, symmetry and additivity of the human eye-movement response to maintained unilateral and bilateral surface galvanic (DC) vestibular stimulation. Exp. Brain Res. *148*, 166–175.

MacDougall, H.G., Brizuela, A.E., Burgess, A.M., Curthoys, I.S., and Halmagyi, G.M. (2005). Patient and Normal Three-dimensional Eye-Movement Responses to Maintained (DC) Surface Galvanic Vestibular Stimulation. [Miscellaneous Article]. Otol. Neurotol. May 2005 *26*, 500–511.

Manabe, Y., Kurokawa, T., Saito, T., and Saito, H. (1995). Vestibular Dysfunction in Noise Induced Hearing Loss. Acta Otolaryngol. (Stockh.) *115*, 262–264.

Mauritz, K., Dichgans, J., and Hufschmidt, A. (1977). The angle of visual roll motion determines displacement of subjective visual vertical. Atten. Percept. Psychophys. *22*, 557–562.

McCrea, R.A., Strassman, A., May, E., and Highstein, S.M. (1987). Anatomical and physiological characteristics of vestibular neurons mediating the horizontal vestibulo-ocular reflex of the squirrel monkey. J. Comp. Neurol. *264*, 547–570.

Mccrea, R.A., Chen-Huang, C., Belton, T., and Gdowski, G.T. (1996). Behavior Contingent Processing of Vestibular Sensory Signals in the Vestibular Nucleia. Ann. N. Y. Acad. Sci. *781*, 292–303.

McCrea, R.A., Gdowski, G.T., Boyle, R., and Belton, T. (1999). Firing Behavior of Vestibular Neurons During Active and Passive Head Movements: Vestibulo-Spinal and Other Non-Eye-Movement Related Neurons. J. Neurophysiol. *82*, 416–428.

Mcfarland, B.L., and Fuchs, A.F. (1992). Discharge patterns in nucleus prepositus hypoglossi and adjacent medial vestibular nucleus during horizontal eye movement in behaving macaques. J. Neurophysiol. *68*, 319–332.

Merfeld, D.M., Zupan, L., and Peterka, R.J. (1999). Humans use internal models to estimate gravity and linear acceleration. Nature *398*, 615–618.

Merfeld, D.M., Haburcakova, C., Gong, W., and Lewis, R.F. (2007). Chronic Vestibulo-Ocular Reflexes Evoked by a Vestibular Prosthesis. IEEE Trans. Biomed. Eng. *54*, 1005–1015.

Minor, L.B., and Goldberg, J.M. (1991). Vestibular-nerve inputs to the vestibulo-ocular reflex: a functional- ablation study in the squirrel monkey. J. Neurosci. *11*, 1636–1648.

Minor, L.B., and Lasker, D.M. (2009). Tonic and phasic contributions to the pathways mediating compensation and adaptation of the vestibulo-ocular reflex. J. Vestib. Res. *19*, 159–170.

Morasso, P., Bizzi, E., and Dichgans, J. (1973). Adjustment of saccade characteristics during head movements. Exp. Brain Res. *16*, 492–500.

Nashner, L.M., and Peters, J.F. (1990). Dynamic posturography in the diagnosis and management of dizziness and balance disorders. Neurol. Clin.

Nashner, L.M., and Wolfson, P. (1974). Influence of head position and proprioceptive cues on short latency postural reflexes evoked by galvanic stimulation of the human labyrinth. Brain Res. *67*, 255–268.

Nashner, L.M., Black, F.O., and Wall, C. (1982). Adaptation to altered support and visual conditions during stance: patients with vestibular deficits. J. Neurosci. *2*, 536–544.

Nashner, L.M., Shupert, C.L., Horak, F.B., and Black, F.O. (1989a). Chapter 33 Organization of posture controls: an analysis of sensory and mechanical constraints. In Progress in Brain Research, J.H.J. Allum and M. Hulliger, ed. (Elsevier), pp. 411–418.

Nashner, L.M., Shupert, C.L., Horak, F.B., and Black, F.O. (1989b). Organization of posture controls: an analysis of sensory and mechanical constraints. Prog. Brain Res. *80*, 411-418; discussion 395-397.

Newlands, S.D., Ling, L., Phillips, J.O., Siebold, C., Duckert, L., and Fuchs, A.F. (1999). Short- and Long-Term Consequences of Canal Plugging on Gaze Shifts in the Rhesus Monkey. I. Effects on Gaze Stabilization. J. Neurophysiol. *81*, 2119–2130.

Newlands, S.D., Hesse, S.V., Haque, A., and Angelaki, D.E. (2001). Head unrestrained horizontal gaze shifts after unilateral labyrinthectomy in the rhesus monkey. Exp. Brain Res. *140*, 25–33.

O'Connor, S.M., and Kuo, A.D. (2009). Direction-Dependent Control of Balance During Walking and Standing. J. Neurophysiol. *102*, 1411–1419.

Oman, C.M., Marcus, E.N., and Curthoys, I.S. (1987). The Influence of Semicircular Canal Morphology on Endolymph Flow Dynamics: An Anatomically Descriptive Mathematical Model. Acta Otolaryngol. (Stockh.) *103*, 1–13.

Oosterveld, W.J., Polman, A.R., and Schoonheyt, J. (1982). Vestibular Implications of Noise-Induced Hearing Loss. Br. J. Audiol. *16*, 227–232.

Ormsby, C.C., and Young, L.R. (1977). Integration of semicircular canal and otolith information for multisensory orientation stimuli. Math. Biosci. *34*, 1–21.

Paulin, M.G. (2005). Evolution of the cerebellum as a neuronal machine for Bayesian state estimation. J. Neural Eng. *2*, S219.

Peng, G.C.Y., Hain, T.C., and Peterson, B.W. (1996). A dynamical model for reflex activated head movements in the horizontal plane. Biol. Cybern. *75*, 309–319.

Peng, G.C.Y., Hain, T.C., and Peterson, B.W. (1999). Predicting vestibular, proprioceptive, and biomechanical control strategies in normal and pathological head movements. IEEE Trans. Biomed. Eng. *46*, 1269–1280.

Perez, R., Freeman, S., Cohen, D., and Sohmer, H. (2002). Functional Impairment of the Vestibular End Organ Resulting From Impulse Noise Exposure. The Laryngoscope *112*, 1110–1114.

Peterka, R.J. (2002). Sensorimotor Integration in Human Postural Control. J. Neurophysiol. *88*, 1097–1118.

Peterka, R.J., and Benolken, M.S. (1995). Role of somatosensory and vestibular cues in attenuating visually induced human postural sway. Exp. Brain Res. *105*, 101–110.

Peterson, B.W., Choi, H., Hain, T., Keshner, E., and Peng, G.C. y. (2001). Dynamic and Kinematic Strategies for Head Movement Control. Ann. N. Y. Acad. Sci. *942*, 381–393.

Phillips, J.O., Ling, L., Siebold, C., and Fuchs, A.F. (1996). Behavior of Primate Vestibulo-Ocular Reflex Neurons and Vestibular Neurons during Head-free Gaze Shiftsa. Ann. N. Y. Acad. Sci. *781*, 276–291.

Picard, M., Girard, S.A., Simard, M., Larocque, R., Leroux, T., and Turcotte, F. (2008). Association of work-related accidents with noise exposure in the workplace and noise-induced hearing loss based on the experience of some 240,000 person-years of observation. Accid. Anal. Prev. *40*, 1644–1652.

Pickles, J.O., Comis, S.D., and Osborne, M.P. (1984). Cross-links between stereocilia in the guinea pig organ of Corti, and their possible relation to sensory transduction. Hear. Res. *15*, 103–112.

Posada, D., Buckley, T.R., and Thorne, J. (2004). Model Selection and Model Averaging in Phylogenetics: Advantages of Akaike Information Criterion and Bayesian Approaches Over Likelihood Ratio Tests. Syst. Biol. *53*, 793–808.

Precht, W., and Shimazu, H. (1965). Functional Connections of Tonic and Kinetic Vestibular Neurons with Primary Vestibular Afferents. J. Neurophysiol. *28*, 1014–1028.

Raphan, D.T., Matsuo, V., and Cohen, B. (1979). Velocity storage in the vestibulo-ocular reflex arc (VOR). Exp. Brain Res. *35*, 229–248.

Ris, L., Waele, C. de, Serafin, M., Vidal, P.P., and Godaux, E. (1995a). Neuronal activity in the ipsilateral vestibular nucleus following unilateral labyrinthectomy in the alert guinea pig. J. Neurophysiol. *74*, 2087–2099.

Ris, L., Waele, C. de, Serafin, M., Vidal, P.P., and Godaux, E. (1995b). Neuronal activity in the ipsilateral vestibular nucleus following unilateral labyrinthectomy in the alert guinea pig. J. Neurophysiol. *74*, 2087–2099.

Robinson, D.A. (1981). Control of eye movements. In Handbook of Physiology: The Nervous System, (Bethesda, MD: American Physiological Society), pp. 1275–1320.

Roy, J.E., and Cullen, K.E. (1998). A neural correlate for vestibulo-ocular reflex suppression during voluntary eye–head gaze shifts. Nat. Neurosci. *1*, 404–410.

Roy, J.E., and Cullen, K.E. (2001). Selective Processing of Vestibular Reafference during Self-Generated Head Motion. J. Neurosci. *21*, 2131–2142.

Sadeghi, S.G., Minor, L.B., and Cullen, K.E. (2007). Response of Vestibular-Nerve Afferents to Active and Passive Rotations Under Normal Conditions and After Unilateral Labyrinthectomy. J. Neurophysiol. *97*, 1503–1514.

Sadeghi, S.G., Minor, L.B., and Cullen, K.E. (2012). Neural Correlates of Sensory Substitution in Vestibular Pathways following Complete Vestibular Loss. J. Neurosci. *32*, 14685–14695.

Schubert, M.C., Santina, C.C.D., and Shelhamer, M. (2008). Incremental angular vestibulo-ocular reflex adaptation to active head rotation. Exp. Brain Res. *191*, 435–446.

Schwarz, G. (1978a). Estimating the Dimension of a Model. Ann. Stat. *6*, 461–464.

Schwarz, G. (1978b). Estimating the dimension of a model. Ann. Stat. *6*, 461–464.

Scudder, C.A., and Fuchs, A.F. (1992). Physiological and behavioral identification of vestibular nucleus neurons mediating the horizontal vestibuloocular reflex in trained rhesus monkeys. J. Neurophysiol. *68*, 244–264.

Serafin, M., Ris, L., Bernard, P., Muhlethaler, M., Godaux, E., and Vidal, P.-P. (1999). Neuronal correlates of vestibulo-ocular reflex adaptation in the alert guinea-pig. Eur. J. Neurosci. *11*, 1827–1830.

Séverac Cauquil, A., Gervet, M.F., and Ouaknine, M. (1998). Body response to binaural monopolar galvanic vestibular stimulation in humans. Neurosci. Lett. *245*, 37–40.

Shanidze, N., Kim, A.H., Raphael, Y., and King, W.M. (2010a). Eye–head coordination in the guinea pig I. Responses to passive whole-body rotations. Exp. Brain Res. *205*, 395–404.

Shanidze, N., Kim, A.H., Loewenstein, S., Raphael, Y., and King, W.M. (2010b). Eye-head coordination in the guinea pig II. Responses to self-generated (voluntary) head movements. Exp. Brain Res. *205*, 445–454.

Shanidze, N., Lim, K., Dye, J., and King, W.M. (2012). Galvanic stimulation of the vestibular periphery in guinea pigs during passive whole body rotation and self-generated head movement. J. Neurophysiol. *107*, 2260–2270.

Shinoda, Y., Sugiuchi, Y., Futami, T., Ando, N., Kawasaki, T., and Yagi, J. (1993). Chapter 19 Synaptic organization of the vestibulo-collic pathways from six semicircular canals to motoneurons of different neck muscles. In Progress in Brain Research, J.H.J. Allum, D.J. Allum-Mecklenburg, F.P. Harris, and R. Probst, eds. (Elsevier), pp. 201–209.

Shupak, A., Bar-el, E., Podoshin, L., Spitzer, O., Gordon, C.R., and Ben-david, J. (1994). Vestibular Findings Associated with Chronic Noise Induced Hearing Impairment. Acta Otolaryngol. (Stockh.) *114*, 579–585.

Smith, P.F., and Curthoys, I.S. (1989). Mechanisms of recovery following unilateral labyrinthectomy: a review. Brain Res. Rev. *14*, 155–180.

Sprenger, A., Zils, E., Stritzke, G., Krüger, A., Rambold, H., and Helmchen, C. (2006). Do Predictive Mechanisms Improve the Angular Vestibulo-Ocular Reflex in Vestibular Neuritis? Audiol. Neurotol. *11*, 53–58.

St George, R.J., and Fitzpatrick, R.C. (2011). The sense of self-motion, orientation and balance explored by vestibular stimulation. J. Physiol. *589*, 807–813.

St George, R.J., Day, B.L., and Fitzpatrick, R.C. (2011). Adaptation of vestibular signals for self-motion perception. J. Physiol. *589*, 843–853.

Steen, J.V. der, and Collewijn, H. (1984). Ocular stability in the horizontal, frontal and sagittal planes in the rabbit. Exp. Brain Res. *56*, 263–274.

Stewart, C., Yu, Y., Huang, J., Maklad, A., Tang, X., Allison, J., Mustain, W., Zhou, W., and Zhu, H. (2016). Effects of high intensity noise on the vestibular system in rats. Hear. Res. *335*, 118–127.

Stewart, C., Kanicki, A.C.., Joshi, T., Martin, C., Wang, G., Raphael, Y., Corfas, G., Altschuler, R.A., and King, W.M. (2017a). Noise-induced peripheral vestibular injury is associated with decreased head postural control in freely locomoting rodents. (Baltimore, MD), p.

Stewart, C.E., Kanicki, A.C.., Altschuler, R.A., and King, W.M. (2017b). Vestibular short latency evoked potential (VsEP) is abolished by low frequency noise exposure in rats. J. Neurophysiol. jn.00668.2017.

Sultemeier, D.R., and Hoffman, L.F. (2017). Partial Aminoglycoside Lesions in Vestibular Epithelia Reveal Broad Sensory Dysfunction Associated with Modest Hair Cell Loss and Afferent Calyx Retraction. Front. Cell. Neurosci. *11*.

Suzuki, J.-I., and Komatsuzaki, A. (1962). Clinical Application of Optokinetic Nystagmus: Optokinetic Pattern Test. Acta Otolaryngol. (Stockh.) *54*, 49–55.

Tabak, S., Smeets, J.B., and Collewijn, H. (1996). Modulation of the human vestibuloocular reflex during saccades: probing by high-frequency oscillation and torque pulses of the head. J. Neurophysiol. *76*, 3249–3263.

Tamura, H., Ohgami, N., Yajima, I., Iida, M., Ohgami, K., Fujii, N., Itabe, H., Kusudo, T., Yamashita, H., and Kato, M. (2012). Chronic Exposure to Low Frequency Noise at Moderate Levels Causes Impaired Balance in Mice. PLOS ONE *7*, e39807.

Tanahashi, S., Ujike, H., Kozawa, R., and Ukai, K. (2007). Effects of visually simulated roll motion on vection and postural stabilization. J. NeuroEngineering Rehabil. *4*, 39.

Tarr, M.J., and Warren, W.H. (2002). Virtual reality in behavioral neuroscience and beyond. Nat. Neurosci. *5*, 1089–1092.

Ter Braak, J.W.G. (1936). Untersuchungen über optokinetischen Nystagmus. Arch Neerl Physiol *21*, 309–376.

Tian, J., Shubayev, I., and Demer, J.L. (2002). Dynamic visual acuity during passive and self-generated transient head rotation in normal and unilaterally vestibulopathic humans. Exp. Brain Res. *142*, 486–495.

Tomlinson, R.D., Saunders, G.E., and Schwarz, D.W.F. (2009). Analysis of Human Vestibulo-Ocular Reflex During Active Head Movements.

Torres-Oviedo, G., and Bastian, A.J. (2010). Seeing Is Believing: Effects of Visual Contextual Cues on Learning and Transfer of Locomotor Adaptation. J. Neurosci. *30*, 17015–17022.

Tullio, P. (1929). Some experiments and considerations on experimental otology and phonetics: a lecture delivered at the meeting of the Società dei cultore delle scienze mediche e naturale of Cagliari, on 1st. july 1929 by prof. Pietro Tullio, director of the Laboratory of experimental physiology-Bologna: Cappelli, 1929.

Vidal, P.P., Graf, W., and Berthoz, A. (1986). The orientation of the cervical vertebral column in unrestrained awake animals. Exp. Brain Res. *61*, 549–559.

Wardman, D.L., Day, B.L., and Fitzpatrick, R.C. (2003a). Position and velocity responses to galvanic vestibular stimulation in human subjects during standing. J. Physiol. *547*, 293–299.

Wardman, D.L., Day, B.L., and Fitzpatrick, R.C. (2003b). Position and velocity responses to galvanic vestibular stimulation in human subjects during standing. J. Physiol. *547*, 293–299.

Wilson, V.J., and Maeda, M. (1974). Connections between semicircular canals and neck motorneurons in the cat. J. Neurophysiol. *37*, 346–357.

Wilson, V.J., and Schor, R.H. (1999). The neural substrate of the vestibulocollic reflex. Exp. Brain Res. *129*, 483–493.

Wilson, V.J., and Yoshida, M. (1969). Monosynaptic inhibition of neck motoneurons by the medial vestibular nucleus. Exp. Brain Res. *9*, 365–380.

Wilson, V.J., Peterson, B.W., Fukushima, K., Hirai, N., and Uchino, Y. (1979). Analysis of vestibulocollic reflexes by sinusoidal polarization of vestibular afferent fibers. J. Neurophysiol. *42*, 331–346.

Winter, J., Allen, T., and Proske, U. (2005). Muscle spindle signals combine with the sense of effort to indicate limb position. J. Physiol. *568*, 1035–1046.

Woollacott, M.H., Shumway-Cook, A., and Nashner, L.M. (1986). Aging and Posture Control: Changes in Sensory Organization and Muscular Coordination. Int. J. Aging Hum. Dev. *23*, 97–114.

Xu, Y., Simpson, I., Tang, X., and Zhou, W. (2009). Acoustic Clicks Activate both the Canal and Otolith Vestibulo-Ocular Reflex Pathways in Behaving Monkeys. J. Assoc. Res. Otolaryngol. *10*, 569.

Ylikoski, J., Juntunen, J., Matikainen, E., Ylikoski, M., and Ojala, M. (1988). Subclinical Vestibular Pathology in Patients with Noise-induced Hearing Loss from Intense Impulse Noise. Acta Otolaryngol. (Stockh.) *105*, 558–563.

Yokota, J.-I., Reisine, H., and Cohen, B. (1992). Nystagmus induced by electrical stimulation of the vestibular and prepositus hypoglossi nuclei in the monkey: evidence for site of induction of velocity storage. Exp. Brain Res. *92*, 123–138.

Young, L.R. (1981). Visual and vestibular influences in human self-motion perception. In The Vestibular System: Function and Morphology, T. Gualtierotti, ed. (Springer New York), pp. 393–424.

Young, L.R. (2011a). Perception of the Body in Space: Mechanisms. In Comprehensive Physiology, (John Wiley & Sons, Inc.), p.

Young, L.R. (2011b). Perception of the Body in Space: Mechanisms. In Comprehensive Physiology, (John Wiley & Sons, Inc.), p.

Young, L.R., and Meiry, J.L. (1968). A revised dynamic otolith model. Aerosp. Med. *39*, 606–608.

Zatsiorsky, V.M., and Duarte, M. (2000). Rambling and trembling in quiet standing. Motor Control *4*, 185–200.

Zee, D.S., Yee, R.D., and Robinson, D.A. (1976). Optokinetic responses in labyrinthine-defective human beings. Brain Res. *113*, 423–428.

Zhou, W., Mustain, W., and Simpson, I. (2004). Sound-evoked vestibulo-ocular reflexes (VOR) in trained monkeys. Exp. Brain Res. *156*, 129–134.

Zuniga, M.G., Dinkes, R.E., Davalos-Bichara, M., Carey, J.P., Schubert, M.C., King, W.M., Walston, J., and Agrawal, Y. (2012). Association between Hearing Loss and Saccular Dysfunction in Older Individuals. Otol. Neurotol. Off. Publ. Am. Otol. Soc. Am. Neurotol. Soc. Eur. Acad. Otol. Neurotol. *33*, 1586–1592.